universität wien

MASTERARBEIT / MASTER'S THESIS

Titel der Masterarbeit / Title of the Master's Thesis

„Tripartite multidrug efflux pumps in the human pathogen *Salmonella typhimurium*"

verfasst von / submitted by

Tietscher Sandra, BSc

angestrebter akademischer Grad / in partial fulfilment of the requirements for the degree of

Master of Science (MSc)

Wien, 2017 / Vienna, 2017

Studienkennzahl lt. Studienblatt / degree programme code as it appears on the student record sheet:	A 066 834
Studienrichtung lt. Studienblatt / degree programme as it appears on the student record sheet:	Molekulare Biologie
Betreut von / Supervisor:	Dr. Thomas C. Marlovits

für Oma Anna

I wer di nia vogessn!

ACKNOWLEDGEMENTS

The year of my Master thesis was a rewarding challenge for me and I would like to thank everyone who helped, motivated and assisted me: First of all my thesis supervisor Dr. Thomas Marlovits, for giving me the possibility to work on this exciting project and to learn all the experimental approaches. Without his and the other lab members' input, this work would not have been possible.

Special thanks go to my project supervisor Dr. Oliver Vesper, who helped me with detailed scientific discussions as well as in every-day lab life, and to whom I could always turn with whatever problem I had. Next, I would like to thank Tobias Thöni, a previous Master student in the lab, who started this project from scratch and achieved a great amount before handing it over to me, and who taught me many relevant techniques when I first entered the lab.

Next, I want to thank all my colleagues for creating an atmosphere where I felt welcome. It was them who made it a pleasure to come to the lab every morning. Thanks go to Julia Mayr for her valuable help concerning experimental setups and protocols, to Nikolaus Gössweiner-Mohr for both moral and scientific support, to Jiri Wald and Luciano Ciccarelli for sharing their EM knowledge and skills, to Wolfgang "Lux" Lugmayr for computational expertise, to Vadim Kotov for sharing protocols and experimental advice, to Georgi Nikolov for organizing the best lab outings, to Sean Miletic for help with the minicells, to Jan Zalesak for graciously allowing me the use of his bench and to Antoine Chabloz for the delicious Swiss chocolate and some neighborly advice. In addition, I would like to thank Kristina Handler from the Bell lab for the refreshing coffee breaks and motivational boosts.

Further, I would like to thank all IMP/IMBA services and the VBCF for making our daily life much easier - especially the media kitchen, the washing kitchen, the EM facility, the mass spectrometry and the Sanger sequencing service.

Finally, huge thanks go to my parents for supporting me throughout, for investing and believing in me, and trusting whatever decision I took.

Vienna, March 2017

CONTENT

1 INTRODUCTION

1.1 Tripartite efflux pumps in Gram-negative bacteria

Many Gram-negative bacteria such as *Escherichia coli* and *Salmonella* spp. can infect humans and animals and cause gastrointestinal diseases, leading to severe diarrhea and even death in extreme cases. Usually, such diseases can be prevented by high hygienic standards or cured with the help of antibiotics such as fluoroquinolones or extended-spectrum cephalosporins[1]. However, antibiotic resistance has been on the rise in recent years and, as almost no new antimicrobial substances are being developed, has become a major concern in today's health industry[2]. In addition to resistance mechanisms targeting a specific group of antibiotic agents, the acquisition of simultaneous resistance to multiple substances is a serious threat to antibacterial therapy[3]. This multidrug resistance includes not only antibiotics but also other toxic substances such as dyes, detergents and disinfectants and often correlates with increased ability of the bacterial cell to expel these substances via active membrane transporters[4].

The Gram-negative cell wall has a three-layered structure that consists of an inner membrane (IM), an outer membrane (OM) with its integrated porins and lipopolysaccharides facing the environment, and a layer of peptidoglycan in the around 180 Å wide periplasmic space in between[5]. Multidrug transporters are usually located in the inner membrane; however, they often work in association with a periplasmic adaptor protein and an outer membrane channel, resulting in tripartite efflux pumps that span the whole cell wall. These nanomolecular machines are clustered into two major groups according to their mode of action, as well as phylogenetically classified into five distinct families (Transporter Classification Database[6]; Figure 1.1):

i) Primary-active pumps directly use ATP hydrolysis as a source of energy. Only the ATP-binding cassette (ABC)-type family of drug efflux pumps belongs to this category.

ii) Secondary-active pumps work as proton/drug antiporters and couple their transport to the electrochemical potential difference at the inner membrane by pumping protons or sodium ions into the cell. The four other major families, namely the major facilitator superfamily (MFS), the small multidrug resistance family (SMR), the multi antimicrobial extrusion protein family (MATE) and the resistance-nodulation-cell division superfamily (RND), are part of this group.

MFS-type pumps are often singlet pumps that do not transport their substrates all the way to the outside but only into the periplasm, and are therefore less effective in producing a detectable decrease in susceptibility[7]. One exception to this is the tripartite MFS pump EmrB, which works together with the periplasmic adaptor protein (PAP) EmrA and the multifunctional outer membrane channel TolC. Members of the SMR superfamily are, as the name implies, very small in size and are involved in the efflux of lipophilic drugs[8]. The MATE family of multidrug transporters is the most recent to have been categorized and appears to be wide-spread in many bacteria[9]. RND transporters play a major role in increasing the resistance to a large variety of toxic compounds. The prototype of this superfamily is the constitutively expressed pump AcrB, which exists in the AcrA-AcrB-TolC tripartite complex and is highly efficient in expelling its substrates through both membranes. ABC-type transporters are less wide-spread in Gram-negative bacteria, but are also implicated in multidrug resistance. The best studied member of this family is MacB, which also functions in concert with TolC and the periplasmic adaptor protein MacA to pump out macrolides.

This study focuses on one representative of each of the two main groups: MacAB-TolC as the major primary-type efflux pump in *Salmonella,* and AcrAB-TolC as the best studied representative of the secondary-type efflux pumps. AcrAB-TolC has been the main subject of a previous thesis in our lab (Master thesis by Tobias Thöni), but MacAB-TolC has not been studied in our lab before.

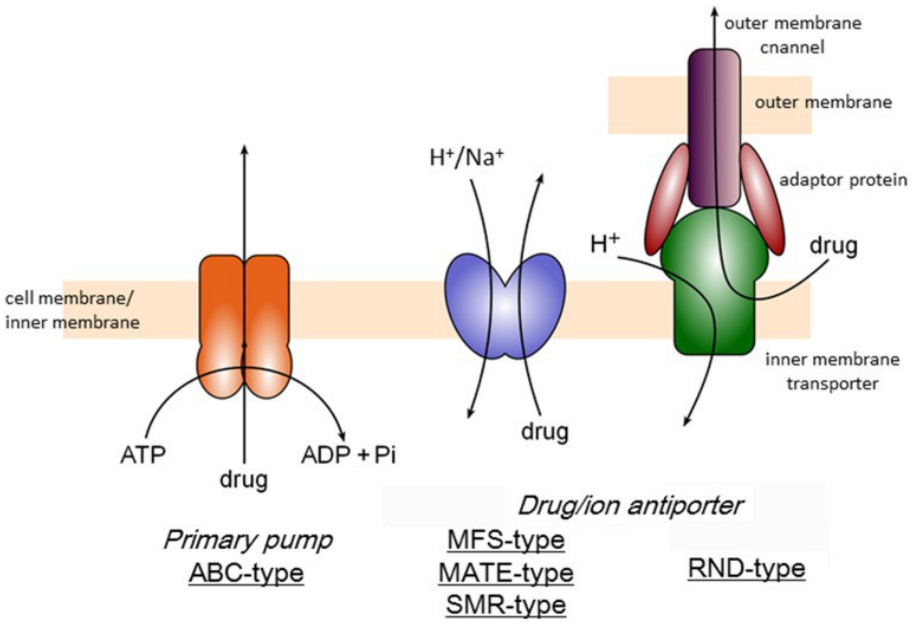

Figure 1.1: Bacterial efflux pump families

Primary-type pumps such as the ABC-type transporters use ATP hydrolysis as a primary energy source. They can be singlet pumps, or triplet pumps such as MacAB-TolC. Drug/ion antiporters, also termed secondary-type pumps, comprise the RND transporter family whose members always exist in a tripartite complex, as well as the MFS, MATE and SMR families.

Figure adapted from Yamaguchi et al.[10]

1.2 The Resistance-Nodulation-Division (RND)-type efflux pump AcrAB-TolC

RND-type exporters are the major multidrug efflux transporter in Gram-negative bacteria and are implicated in most multidrug-resistant infections caused by these pathogens[10]. They have an extraordinarily broad substrate specificity ranging from antibiotics over detergents to ionic compounds[11], which they expel directly into the environment, based on their shared tripartite structure. All RND-type pumps are composed of an inner membrane protein which provides the energy for substrate transport, an intermediate periplasmic component and the outer membrane channel TolC (Figure 1.2). The best studied representative of this family is the acridine resistance complex, where AcrB acts as the proton-driven inner membrane transporter and AcrA as the periplasmic adaptor protein. The AcrAB-TolC pump is considered the most clinically relevant of the RND-pumps and is present in *E. coli*, *S. enterica, Pseudomonas* spp*, Shigella* spp and other Gram-negatives. It has been intensively studied both in terms of mechanism and assembly and has been chosen in this work to study in parallel with the less-explored ABC-type transporter MacAB-TolC.

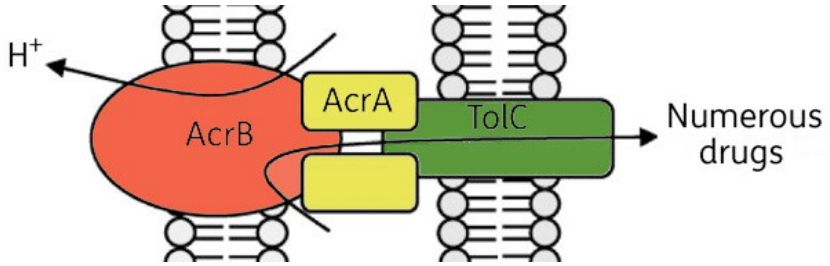

Figure 1.2: Schematic representation of the multidrug efflux pump AcrAB-TolC

AcrB (red) is located in the inner membrane and acts as a proton-substrate antiporter. AcrA (yellow) is a periplasmic protein that couples AcrB to the outer membrane channel TolC and therefore enables direct expulsion of substrates to the environment.

Figure adapted from Horiyama et al. (2010)[25].

1.2.1 Individual components of AcrAB-TolC

Each individual component of AcrAB-TolC has been investigated in depth regarding its structure and its function in the complex. The structure of the inner membrane transporter AcrB from *E. coli* has been resolved to 3.5 Å in 2002 and shows a homotrimeric assembly where each protomer can be divided into a transmembrane domain and a headpiece domain facing the periplasm (Figure 1.3) [12]. A central cavity is located at the bottom of the headpiece, connected by a long pore to a funnel-like opening at the top. Subsequent structural analyses with higher resolution were able to capture the

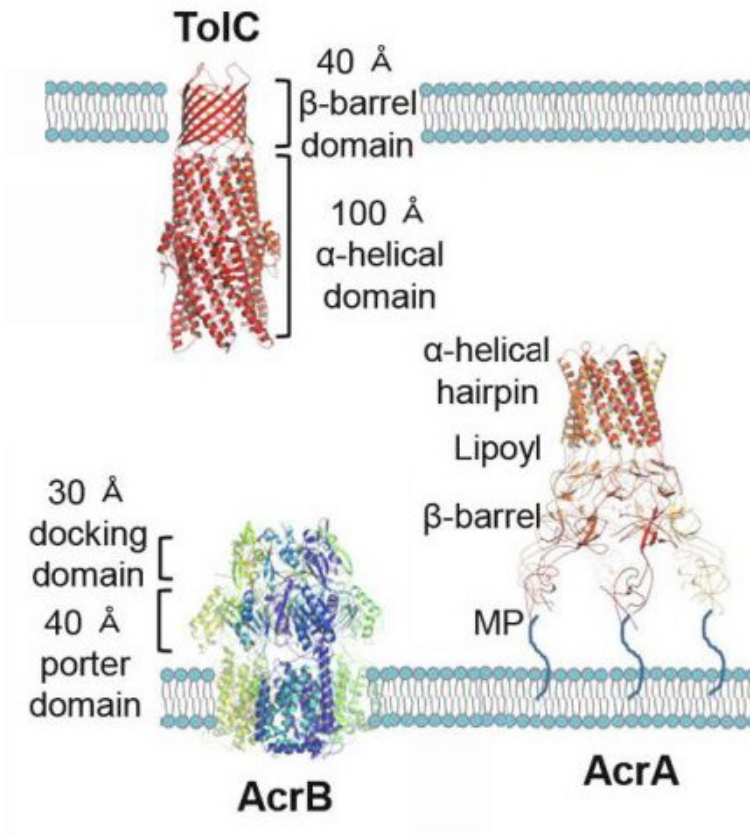

Figure 1.3: Components of the AcrAB-TolC efflux pump

The homotrimeric inner membrane protein AcrB consists of a transmembrane domain and a periplasmic headpiece, divided into a docking and a porter domain. AcrA acts as a periplasmic adaptor protein and comprises four linearly arranged domains. The oligomerization state for AcrA is still under debate; here, a trimer is depicted. In contrast, the homotrimeric nature of TolC with its transmembrane β-barrel and periplasmic α-helical domain has been confirmed.

Figure adapted from Song et al. (2015)[37]

pump extrusion mechanism, which can be described in three steps[13–15]: Each monomer moves sequentially from a loose (L) or access, to a tight (T) or binding and finally to an open (O) or extrusion state, resulting in a functional rotation mechanism of three protomers. During pump operation, a substrate loosely bound to an L state monomer is gripped tightly by transition to the T state and

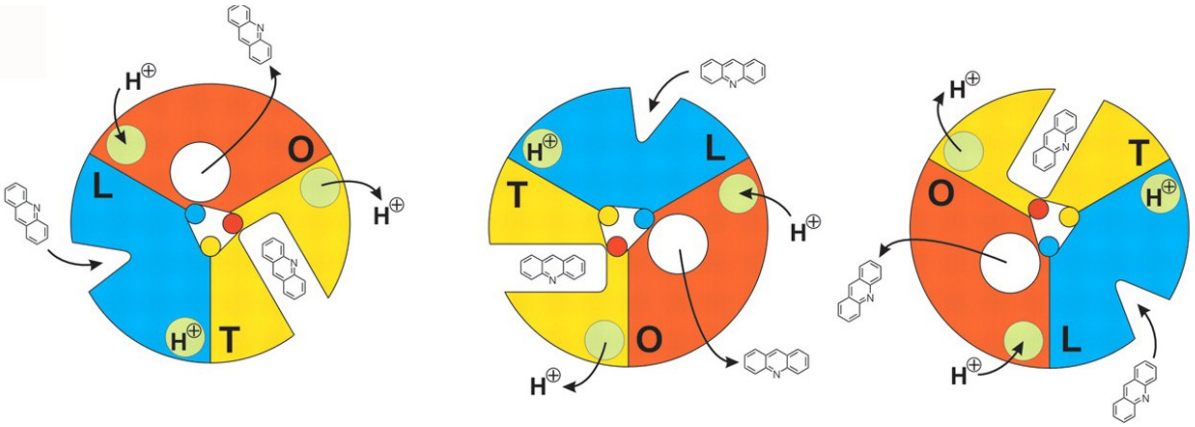

Figure 1.4: Schematic depiction of the AcrB functional state rotation mechanism for substrate transport

The conformational states L (loose), T (tight) and O (open), are colored in blue, yellow and red, respectively. First, a monomer in the loose conformation binds a substrate (here: acridine) in its transmembrane domain. In the next step, the substrate is transported to the hydrophobic binding pocket (T state) and finally released through the funnel opening towards TolC (O state). The state conversions are coupled to proton uptake from the periplasm and subsequent release into the cytoplasm.

Figure adapted from Seeger et al. (2006)[14]

expelled through the periplasmic funnel by a final change to the O state. The conformational changes are coupled to a proton antiport across the inner membrane (Figure 1.4).

Various inhibitors of the AcrB pump mechanism are known and have been shown to increase antibiotic sensitivity, however, none of them are clinically available – the most promising candidates, derivatives of the peptidomimetic PAβN, failed at preclinical stage due to toxicity issues[16,17].

The periplasmic adaptor protein (PAP) AcrA is necessary to facilitate substrate passage from AcrB to the outer membrane channel. The general architecture of PAPs shows an elongated shape with an α-hairpin domain as docking part to the outer membrane channel, followed by a linear arrangement of a lipoyl domain, a β-barrel domain and a membrane proximal domain(MPD)[18]. The crystal structure of AcrA presented in 2006 showed that it shares all of these domains but failed to completely resolve its MPD due to conformational flexibility[19]. However, re-refinement of the structure of a close homolog to AcrA in *P. aeruginosa*, MexA, allowed modeling of the MPD[20,21]. Additionally, all of these PAPs contain an N-terminal signal sequence that allows transport into the periplasmic space and anchors them to the inner membrane[22].

The homotrimeric outer membrane channel TolC is common to all tripartite efflux pumps in *Salmonella* including the MacAB-TolC efflux pump and is therefore discussed in more detail in the following chapter.

1.2.2 The outer membrane channel TolC

The function of the *tolC* gene product as an outer membrane channel and its major impact on outer membrane functions in *E. coli* have been reported more than twenty years ago[23]. Early experiments with TolC mutants have reported growth effects and increased sensitivity to chemical stress in the presence of detergents or other solvents in the environment, leading to the hypothesis that TolC is involved in the efflux of these small molecules. Among the substrates of the TolC exit duct are hydrophobic agents, bile acids, organic solvents, dyes, fatty acids and antibiotics[24]. The vast variety of substrates is rooted in the ability of TolC to function in concert with many different classes of inner membrane transporters, including RND-type pumps (such as AcrB), MFS-pumps (EmrB) and ABC-type transporters (MacB)[25]; the inner transporter protein usually determines the range of substrate specificity. TolC homologues are ubiquitous among Gram-negative bacteria and show similar effects

in drug resistance and virulence for example in *Pseudomonas aeruginosa*[26], *Borrelia burgdorferi*[27], *Vibrio cholera*[28] and the model organism used for this study, *Salmonella typhimurium*[25,29–31].

E. coli TolC is a 51 kDa protein with a cleavable N-terminal signal sequence that is important for passage through the inner membrane, while insertion into the outer membrane is believed to be catalyzed by the β-barrel assembly machinery (Bam) complex[32]. The crystal structure of a C-terminally truncated version of *E. coli* TolC has been solved at high resolution (2.1 Å), revealing a previously unknown, distinctive fold[33]. In this structure, three TolC protomers assemble to form a continuous, solvent-accessible channel of 140 Å length which spans the outer membrane and sticks out into the periplasmic space (Figure 1.5 A). The large interior is mostly solvent-filled with an internal diameter of 35 Å and a total volume of 43000 $Å^3$, thus allowing even small folded polypeptides to pass[33].

Each TolC molecule can be partitioned into a β-domain, an α-helical domain and a mixed α/β domain. In the trimer, the β-strands associate to create a 12-stranded β-barrel within the outer membrane which forms an opening towards the external environment. Contiguous to the β-barrel structure, four α-helices of each protomer assemble to form an α-helical barrel protruding 100 Å long into the periplasmic space, with the proximal end of the tunnel virtually closed by the inwards-folding coiled-coil endings. This constriction with a minimum radius of 1.95Å is lined by a ring of six aspartate residues that determine the highly electronegative environment and the ion selectivity of the tunnel entrance[34].

It is apparent that for a substrate to enter, the width of this “gate” needs to be extended. The open form has been experimentally determined and structures of the open and partially open states are available (Figure 1.5 B)[35,36]. Gate opening is connected to the exposure of three intra-protomer grooves in the TolC trimer where contact points for interaction with a periplasmic component (AcrB) are located. Thus, an induced fit model for opening of the TolC tunnel after binding to the periplasmic adaptor protein has been proposed. *Salmonella* and *E. coli* TolC share a sequence identity of around 90 % (including the aspartate closing ring structure), suggesting conservation of a similar architecture.

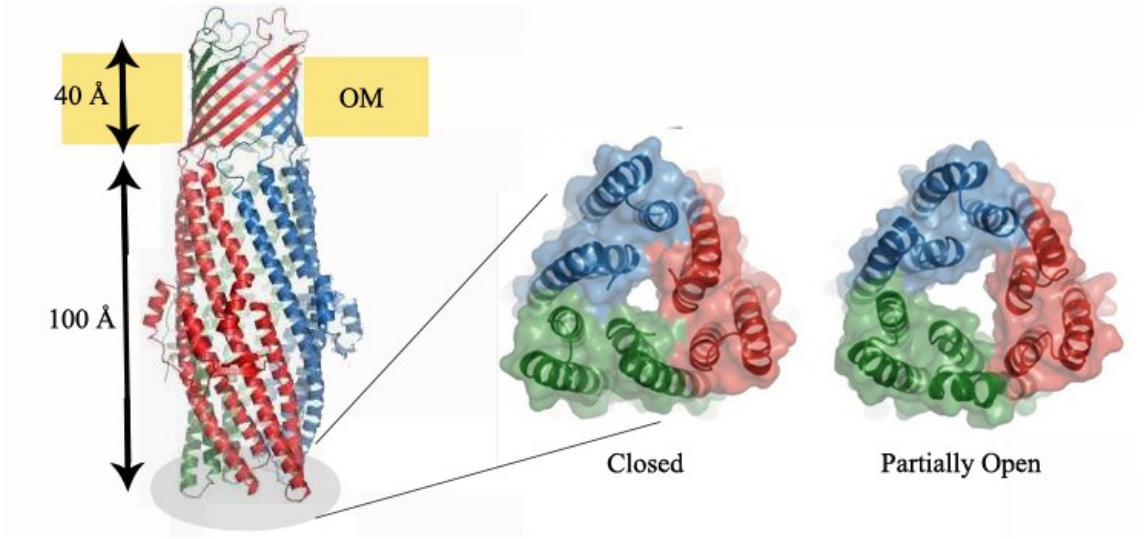

Figure 1.5: Crystal structure of the outer membrane channel TolC from *E. coli*

(A) Three protomers of TolC (in red, blue and green, respectively) assemble to form a solvent-filled channel consisting of a β-barrel structure in the outer membrane and an α-helical barrel that protrudes 100 Å far in the periplasmic space (PDB: 1EK). (B) Crystal structures of the closed and the partially open state (PDB: 2VDE); view along the trifold axis at the periplasmic side of the tunnel.

Figure adapted from Bavro et al. (2008)[36]

1.2.3 AcrAB-TolC assembly models

Even though a lot of structural and biochemical data is available on the single components of the RND efflux pump, its overall organization is controversially discussed. This is mostly due to the lack of a high resolution structure of the whole complex. However, two models have been put forward that could explain the assembly of efflux pumps: the "adaptor wrapping model" and the "adaptor bridging model"[37,38]. The two major differences in the model are the ratio of the involved components and the proposed binding mode (Figure 1.6).

The **adaptor wrapping model** was described first in 2002 after the AcrB structure was solved and assumes direct binding of the outer channel to the docking domain of the inner membrane transporter. The proposed stoichiometry for AcrB:AcrA:TolC in this model is 3:3:3, with the periplasmic adaptor protein stabilizing the interaction by wrapping around the contact site[12]. The model was supported by many studies including *in vivo* cross-linking and cysteine-substitution experiments, resulting in detailed interaction maps of the individual components that proved the close proximity of AcrB and TolC[39–41]. However, physical binding of the two components remains

uncertain, because simple incubation did not result in a binary complex and it was not possible to isolate them together without adding cross-linking reagents. Moreover, pump variants used for cysteine cross-linking experiments showed decreased or abolished efflux activity[42,43], putting the model in question.

In contrast, structural and functional data favoring a 3:6:3 component ratio and no direct contact between AcrB and TolC have accumulated over the past decade, supporting a second proposed model[42,44–46]. The **adaptor bridging model** receives its name from the idea that the inner membrane component and the outer membrane channel are not directly interacting with each other, but that the periplasmic gap between the two is bridged by an AcrA hexamer generating a tunnel large enough for substrate passage. In other tudies on efflux pumps such as the homologous RND-type pumps MexAB-OprM from *P. aeruginosa*[47], MtrCDE from *N. gonorrhea*[48] and the CusBA-heavy metal efflux pump from *E. coli*[49] models with the same ratio of 3:6:3 are preferred.

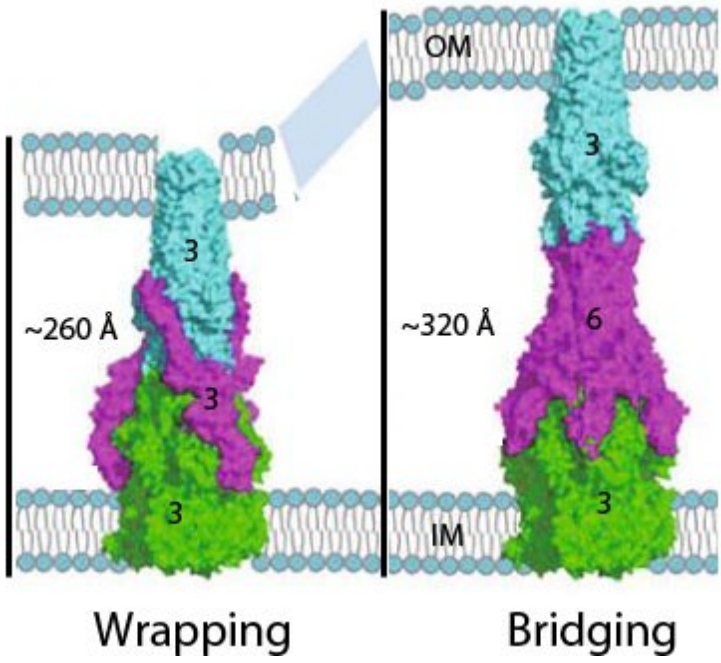

Figure 1.6: Current models for the tripartite AcrAB-TolC assembly

In the adaptor wrapping model (left), AcrB binds directly to TolC, with AcrA wrapping around and stabilizing the interaction. This model proposes a binding ratio of 3:3:3 and results in a length of around 260 Å for the whole efflux pump. The adaptor bridging model claims a stoichiometry of 3:6:3 (AcrB:AcrA:TolC) and no direct contact between AcrB and TolC. Here, AcrA builds a funnel that channels the substrate between the two membrane components. The pump length according to this model is 320 Å, which is in good agreement with the cell wall thickness of Gram-negative bacteria[5].

Figure adapted from Song et al. (2015)[37]

Recently, three EM based structures of assembled AcrAB-TolC from *E. coli* were presented that are in good agreement with the adaptor bridging model[44,45,50]. The most recent model (Jeong et al. 2016) reaches a resolution of 8.1 Å for large parts of the complex and a cogwheel-like interactions between the AcrA hexamer and the TolC trimer is suggested. However, all three models were generated either by cross-linked chimeric fusion proteins[45] or by assemblies of genetic fusion proteins that were

incubated for an extended time to ensure close contact[44,50]. This arrangements force a 3:6:3 stoichiometry simply by the gene copy number present in the fusion constructs and may result in a non-natural assembly. A fourth study employed separate reconstitution of the membrane components into nanodiscs, followed by mixing with native lipidated AcrA to reconstitute the complex *in vitro* without the help of fusion constructs[51]. TEM analysis of this assembly revealed 33 nm long tripartite particles in accordance with the adaptor bridging model, but cryo-EM experiments were performed and no 3D structure was solved.

Preliminary work on the *S. enterica* AcrAB-TolC pump in our lab has resulted in 31 Å electron density map of the near-native pump generated by negative stain electron microscopy (Master thesis of Tobias Thoeni). Although of comparatively lower resolution, this structure further supports the adaptor bridging model, as deduced by comparison to the two available structures and rigid body fitting of the individual components.

1.2.4 Relevant AcrAB homologs in *Salmonella*

In *S. enterica*, two close homologs of the AcrB transporter protein are known[7]. While the homologous AcrD shares 79 % of amino acids with AcrB in *S. enterica*, AcrF is even more similar with an amino acid identity of 90 %. AcrD exhibits low constitutive expression and has a different, but partly overlapping substrate range compared to AcrB[11]. Furthermore, AcrD has been reported to also work together with AcrA and, when overexpressed, to significantly alleviate drug sensitive phenotypes caused by *acrB* deletion in *Salmonella*, suggesting a possible assembly of an AcrAD-TolC complex[52]. In contrast, AcrF is expressed from a bicistronic operon together with AcrE, a close homolog of the periplasmic adaptor protein AcrA. While *acrEF* deletion has only minor effects, its overexpression is able to partly compensate for deletion of *acrAB*[53]. Consistently, in *acrB* mutant strains grown in the presence of fluoroquinolone antibiotics, genomic acrEF was overexpressed by spontaneous changes in its promoter region[54].

1.3 The ATP-binding cassette (ABC)-type efflux pump MacAB-TolC and its components

The first experimental evidence of an ABC-type efflux pump in a Gram-negative bacterium was reported by Kobayashi et al.(2001)[55], who identified an integral membrane protein (MacB) and a periplasmic membrane protein (MacA) that together with TolC conferred resistance to macrolides in *E. coli*. Both proteins are encoded on the *macAB* operon and showed a significant effect only when expressed together and only on the resistance to 14- and 15- membered macrolide antibiotics like erythromycin and oleandomycin, but not to 16- membered ones like rokitamycin. Additionally, the MacAB-TolC efflux pump has since been shown to be involved in a number of other processes: It is required to expel excess Protoporphyrin IX when natural heme homeostasis is disrupted by iron shortage in the cell[56] and plays a crucial role for survival of *S. enterica* in the inflamed intestine and in macrophages where the bacteria are exposed to highly toxic reactive oxygen species (ROS)[57]. Moreover, MacAB has been implicated in the TolC-dependent secretion of heat-stable enterotoxin II in *E. coli*, an extracellular peptide that causes diarrhea in the host[58], as well as in the transport of outer membrane glycolipids[59]. A recent study suggested the potential use of MacAB-TolC in metabolic engineering, as its overproduction in *E. coli* significantly facilitated the export of intracellularly accumulated amorphadiene, the precursor of the antimalarial drug artemisin[60]. In addition to *Salmonella* and *E. coli*, homologs of the *macAB* gene have been identified in a wide range of other Gram-negative pathogens such as *Pseudomonas*, *Yersinia* and *Shigella*.

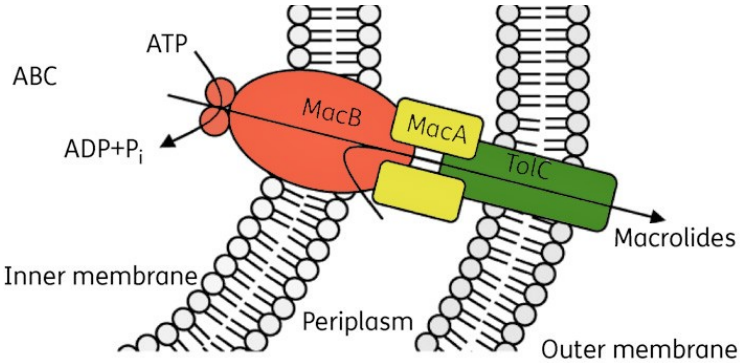

Figure 1.7: Schematic representation of assembled MacAB-TolC

The ABC-transporter MacB (red) sits in the inner membrane and generates energy by cytoplasmic ATP hydrolysis. MacA (yellow) resides in the periplasm and couples MacB with the outer membrane channel TolC (green), enabling active transport of substrates directly from the cytoplasm to the exterior. *Figure adapted from* [25].

Similarly to all tripartite multidrug efflux pumps, MacAB-TolC consists of an inner membrane protein that provides the energy for substrate transport, an outer membrane channel which allows passage of the substrate through the OM and a periplasmic adaptor protein that serves as a bridging element between the two (Figure 1.7). This tripartite architecture allows expulsion of toxic compounds

directly into the external medium, thereby drastically increasing the pump efficiency[25]. In the case of MacAB-TolC, all three pump components have been studied in detail; however, their mode of assembly and exact stoichiometry in the complex are still under debate.

1.3.1 The inner membrane pump MacB

MacB is an ATP-binding cassette (ABC)-type transporter that sits in the inner membrane and provides the driving force for macrolide expulsion by the MacAB-TolC tripartite complex. MacB has a calculated monomeric mass of around 71 kDa and its membrane topology has been determined by site-specific competitive chemical modifications, revealing the presence of 4 transmembrane helices (TM) and a large periplasmic loop of more than 200 amino acids between TM 1 and TM 2 [61]. The single nucleotide binding domain (NBD) is located at the N-terminus at the cytoplasmic side and comprises the Walker A and B and the ABC signature motifs. It is notable that unlike MacB, most canonic half-type ABC transporters have 6 TM helices and a C-terminal NBD. The oligomeric state of MacB in solution has been investigated thoroughly by analytical ultracentrifugation, atomic force microscopy and non-dissociating mass spectrometry and was found to be homodimeric [62].

To date, no crystal structure is available of the full-length MacB; only the large periplasmic core domain (PCD) has been successfully crystallized and its structure solved [63] (Figure 1.8). The PCD has two distinct components: the flexible N- and C-terminal regions directly connected to TM1 and TM2 and a mixed αβ domain which is largely rigid and is divided in an upper and a lower subdomain by a shallow crevice.

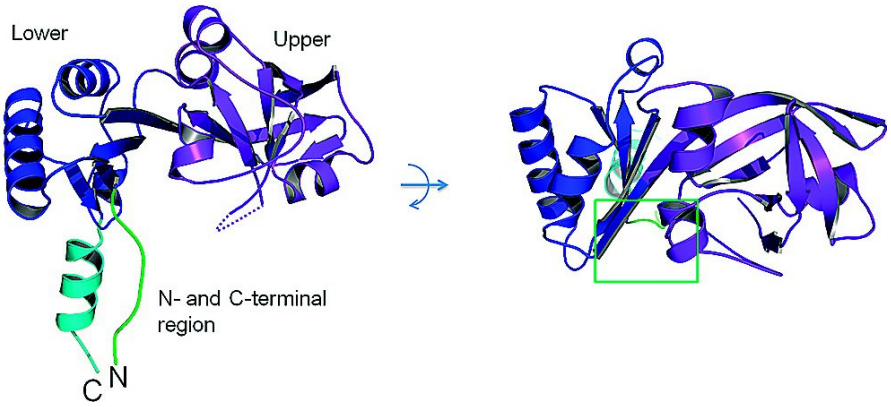

Figure 1.8: Structure of the periplasmic core domain (PCD) of MacB

Ribbon representation of the asymmetric unit of the MacB PCD in top view and side view. The flexible N- and C-terminal regions (depicted in green and cyan, respectively) are connected via flexible linkers to a mixed αβ domain. The green box indicates the shallow crevice that divides the αβ domain into a lower part and an upper part. *(Figure adapted from Xu et al. 2009)*

Motion of the NBD driven by ATP hydrolysis in the cytoplasm could be propagated to the periplasmic domain via TM1 and TM2; the N- and C-terminal regions of the PCD have been suggested to play important roles here. Although the PCDs of individual MacB subunits are probably close together *in vivo*, they do not seem to be in direct contact and do not have a strong affinity towards each other[63].

Although the specific catalytic mechanism of MacB has not been studied in detail, the main conformational cycles of ABC transporters are believed to be highly conserved[64] (Figure 1.9). The four indispensable catalytic steps are (i) binding of substrate and two ATP molecules, (ii) closing of NBD dimer and substrate transport, (iii) ATP hydrolysis and (iv) release of ADP and P_i and return to resting state[65]. The ATPase activity of MacB reconstituted into proteoliposomes has been shown to be very low but is strongly stimulated by the presence of MacA, presumably because MacA increases the affinity of MacB to ATP in the binding step or promotes closing of NBD dimers[66,67].

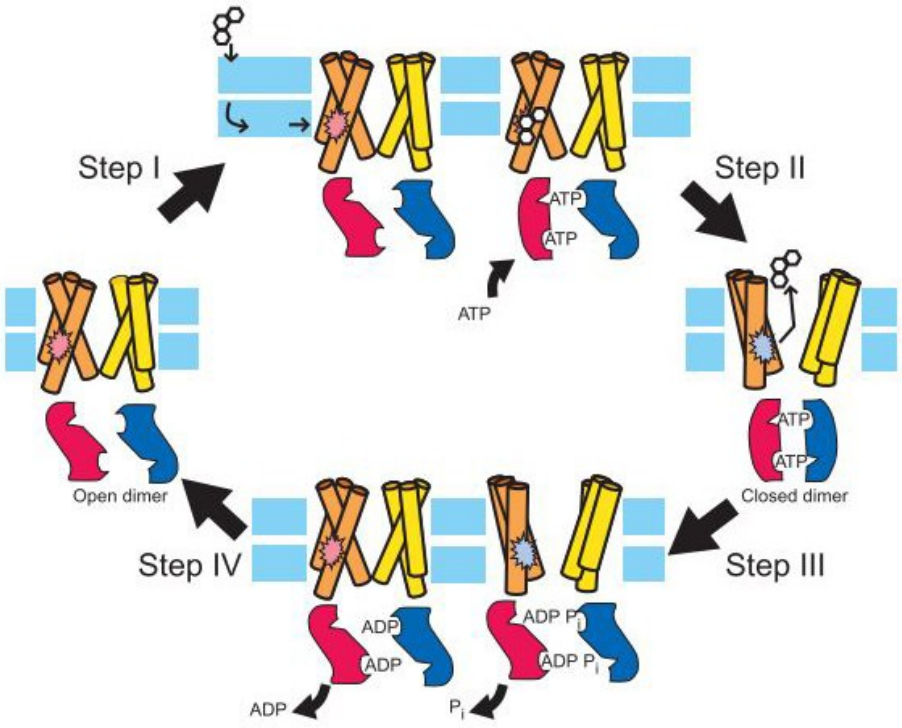

Figure 1.9: ATP switch model for the general ABC transporter cycle

The TM domains are shown as cylinders (viewed in the plane of the membrane) and the NBDs are shown at the cytoplasmic side of the membrane (as if viewed from above). The drug-binding site is shown in red when it is in a high-affinity state and in blue when it is in a low-affinity state. The conserved catalytic steps of ABC transporters include the binding of substrate and ATP (step I), closing of the NBD dimer and substrate release towards the extracellular space (step II), ATP hydrolysis (step III) and release of ADP and P_i and return to basal configuration.

Figure adapted from Higgins et al. 2004

1.3.2 The periplasmic adaptor protein (PAP) MacA

The periplasmic adaptor protein (also called membrane fusion protein, MFP) is an essential component of every tripartite pump as it serves to bridge the inner membrane transporter with the outer membrane factor and allows fast passage of the substrate through the periplasm. The 41 kDa protein MacA is expressed from the same operon as MacB and plays the role of the periplasmic adaptor protein in the MacAB-TolC efflux pump[55]. It has an N-terminal signal-like sequence of 40 amino acids, which is rich in charged residues in its N-terminus and hydrophobic residues in its C-terminus and is predicted to form a transmembrane (TM) helix. Apart from this, the sequence of MacA does not display any large hydrophobic patches. It was shown that MacA does not undergo N-terminal processing and remains tightly associated with membranes even upon treatment with Urea, suggesting that the uncleavable N-terminal signal peptide anchors the protein to the inner membrane[55]. MacA shares a high sequence similarity (44 %) with the best studied PAP AcrA, although recent phylogenetic analysis has shown that the two belong to two different subgroups of the MFP family[68].

Crystal structures of MacA expressed without the N-terminal signal-like sequence were reported from *E. coli* (Ec) and *Actinobacillus actinomycetemcomitans* (Aa)[69,70]. Structure determination revealed the same elongated sickle-like shape as was reported previously for other PAPs such as *E. coli* AcrA and *P. aeruginosa* MexA[19,20], with three distinct linearly arranged domains. These domains include a long α-hairpin domain, followed by a lipoyl domain and a β-barrel domain comprised of six antiparallel β-strands; their overall structure and orientation is similar in Ec MacA and Aa MacA (Figure 1.10). The coiled-coil α-hairpin domain of MacA has six heptad repeats per helix, making it longer than the respective domains of AcrA and MexA with five and four heptad repeats respectively. The N- terminal and C-terminal regions of MacA were disordered in the crystals and could not be modeled; therefore, no structural information is available on a potential membrane-proximal domain such as reported for MexA and the metal-efflux pump PAP ZneB from *Cupriavidus metallidurans*[71].

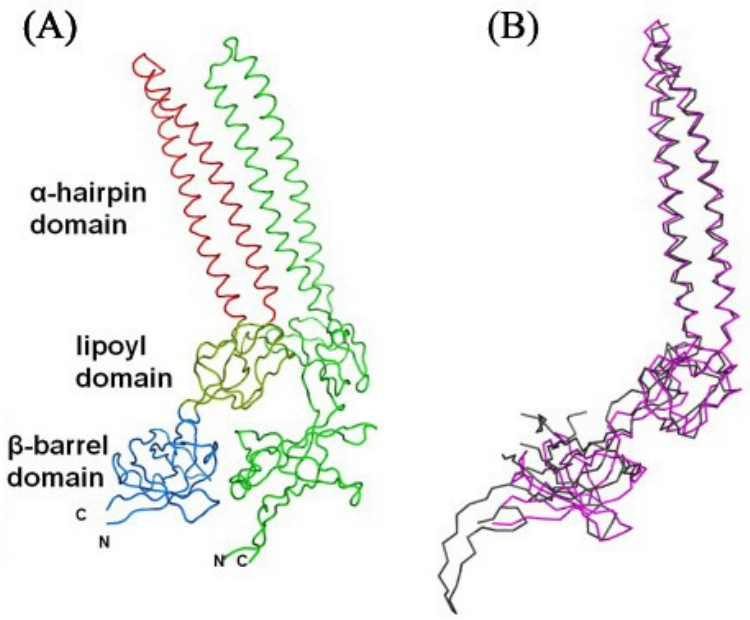

Figure 1.10: Structure of MacA from *E. coli* (PDB: 3FPP) and *A. actinomycetemcomitans* (PDB: 4DK0)

The crystal structure for the periplasmic adaptor protein MacA from both organisms has been resolved except of the flexible N- and C-termini. (A) Asymmetric unit of the Ec MacA crystal which consists of two protomers. In the left protomer, the three domains common to all PAPs are shown; the α-hairpin domain is highlighted in red, the lipoyl domain in yellow and the β-barrel domain in blue. (B) Superposition of the C_α traces of Ec MacA (magenta) and Aa MacA (grey).

Figure adapted from Yum et al. (2009)[69]

In the MacA crystals, a hexameric arrangement of the molecules was commonly found[69]. Side-by-side packing interaction of six protomers generated a funnel-like structure with a central channel around the crystallographic 6-fold axis (Figure 1.11). The funnel has a stem created by juxtaposition of the α-hairpin domains that together form a channel that is 70 Å long and 35 Å wide, with a structure resembling a cogwheel at the top. The conical mouth of the funnel is formed by the lipoyl and β-barrel domains and is suggested to be associated with the inner membrane transporter MacB, while the stem part should be associated with the outer membrane channel TolC. Two conserved Glu and Tyr residues in the β-barrel domain that were involved in hexamer formation in the crystals also played a crucial role in the oligomerization of Aa MacA in solution and in the macrolide resistance of *E. coli* cells *in vivo*. The hexameric assembly is further supported by electron microscopy studies of Aa MacA and is likely to be relevant *in vivo*[69].

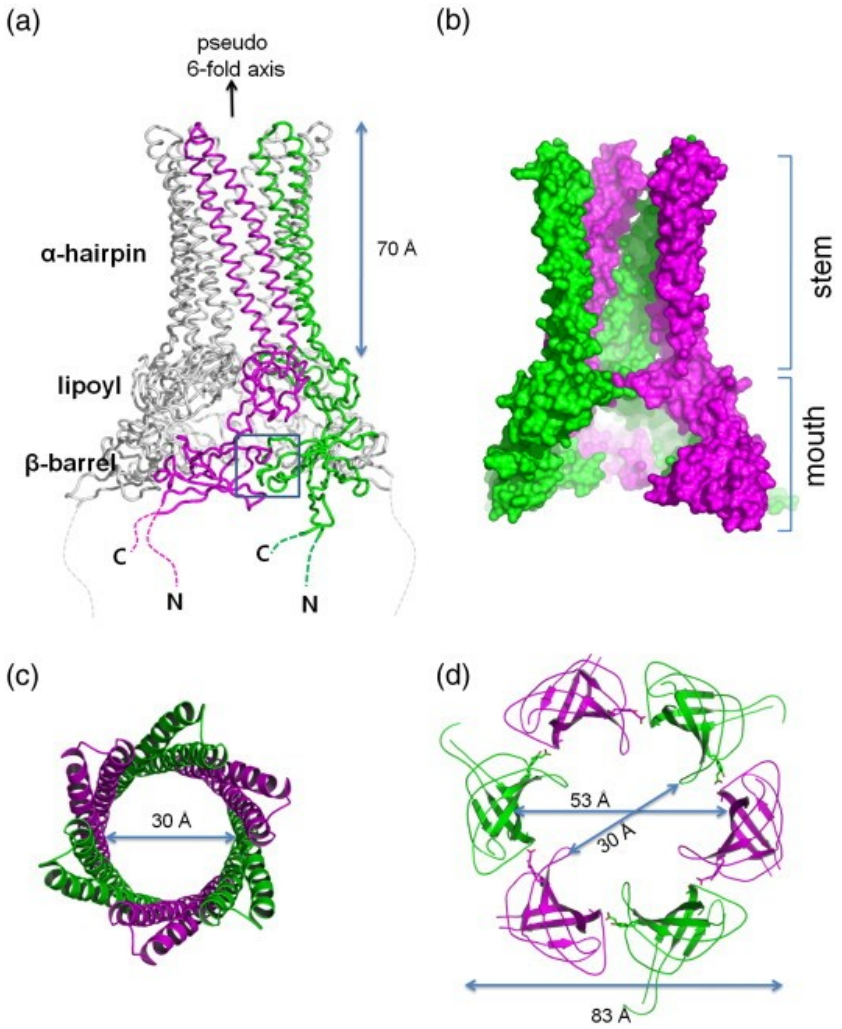

Figure 1.11: Hexameric arrangement of MacA protomers

(A) Ribbon representation of the hexameric assembly of Ec MacA. The pseudo-6-fold symmetry (crystallographic 3-fold symmetry) is indicated and two protomers of the asymmetric unit are colored in magenta and green. Flexible regions at the N- and C-terminus are shown as dotted lines. (B) Surface representation of the MacA hexamer (with two front protomers omitted) clearly shows the central channel of the funnel. (C) Top view on the hexameric MacA assembly reveals a cogwheel-like shape of the upper stem part; only α-hairpin domains are shown for simplicity. (D) Bottom view on the conical mouth of the funnel; only β-barrel domains are shown.

Figure adapted from Yum et al. (2009)[69]

1.4 Assembly of the MacAB-TolC efflux pump

Although all individual components of the ABC-type MacAB-TolC efflux pump have been studied intensively, no detailed structural model is available of the whole efflux pump. Similar to the assembly models of the RND-type efflux pump AcrAB-TolC (see section 1.2), an "adaptor wrapping model" with direct contact between the outer membrane channel and the inner membrane transporter and an "adaptor bridging model" with the PAP bridging the gap between the two membrane components have been proposed for MacAB-TolC[69,72]. However, crystal structures and EM studies of MacA reveal a funnel-like hexameric assembly that was shown to represent the functional state of the protein[69]. This arrangement strongly supports the "MacA bridging model" in which MacA directly contacts TolC in a tip-to-tip manner and thus intervenes between MacB and TolC (Figure 1.12). Evidence for this binding mode comes from mutational analysis of the conserved

residues at the MacA tip region[73] and the use of a chimeric protein containing the α-barrel tip of trimeric TolC that was found to interact with the MacA α-barrel tip in an intermeshing, cogwheel-like fashion[74].

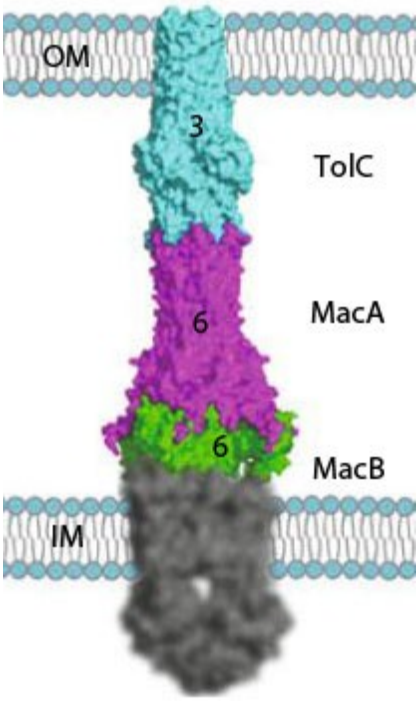

Figure 1.12: Adaptor bridging model of tripartite MacAB-TolC assembly

The current state of knowledge favors a model in which MacB and TolC do not directly bind to each other. MacA interacts with TolC in a tip-to-tip manner and with MacB via its periplasmic core domain, serving as a bridge between the two. The ratio of the individual components in the complex is still unclear, but a binding stoichiometry of 6 MacB : 6 MacA : 3 TolC has been suggested[72]. Because no full-length structure of MacB is available so far, the unknown transmembrane and cytosolic domains are depicted in grey.

Figure adapted from Song et al. (2015)[37]

In contrast, the oligomeric state of MacB in the complex remains unclear. As expected for an ABC transporter in which the NBDs need to interact for catalytic function, biophysical experiments indicate that MacB forms dimers[62]. One potential solution to the question how this could match the symmetry of the other components is the association of MacB subunits as a trimer of dimers[72]. This organization would also be consistent with the hexameric assembly of MacA, resulting in a stoichiometry of 6:6:3 (MacB:MacA:TolC) as depicted on Figure 1.12. An *in vitro* binding assay showed that TolC did not bind to the periplasmic core domain of MacB, giving further evidence for the "adaptor bridging model" of MacAB-TolC. Moreover, a chimeric AcrA protein that contained the α-helical domain of MacA was demonstrated to be fully functional *in vivo*, highlighting the possibility that MacAB-TolC may have a similar architecture to that of the AcrAB-TolC assembly[43]. However, knowledge about how the individual components assemble and interact as a whole remains elusive and a final determination of the MacAB-TolC assembly model is impeded by the lack of an available structure of the whole complex.

1.5 Regulation of AcrAB-TolC and MacAB-TolC expression in *Salmonella*

Expression of many RND-type efflux pumps in Gram-negative bacteria is regulated by transcriptional regulators of the AraC/XylS family, such as MarA and SoxS, that allow sensing of environmental signals[75,76]. In the case of the AcrAB-TolC efflux pump, an additional regulator named RamA is present in some pathogenic Enterobacteriaceae such as *Salmonella* spp., *Enterobacter* spp. and *Klebsiella* spp., but not in *Escherichia coli* or *Shigella* spp[77,78]. RamA, also an AraC family member, acts as a transcriptional activator for all three components of AcrAB-TolC and is itself regulated by its local repressor RamR, encoded upstream of *ramA* in the *S. enterica* genome(Fig. 1.13 A). RamR has been shown to inhibit *ramA* expression by binding to its promoter region[79]. The interruption of RamR by point-mutations, disruption of its binding site upstream of *ramA* as well as expression of RamA from an inducible plasmid have been found to increase expression of AcrAB-TolC but not other efflux pumps in *S. enterica*[79,80].

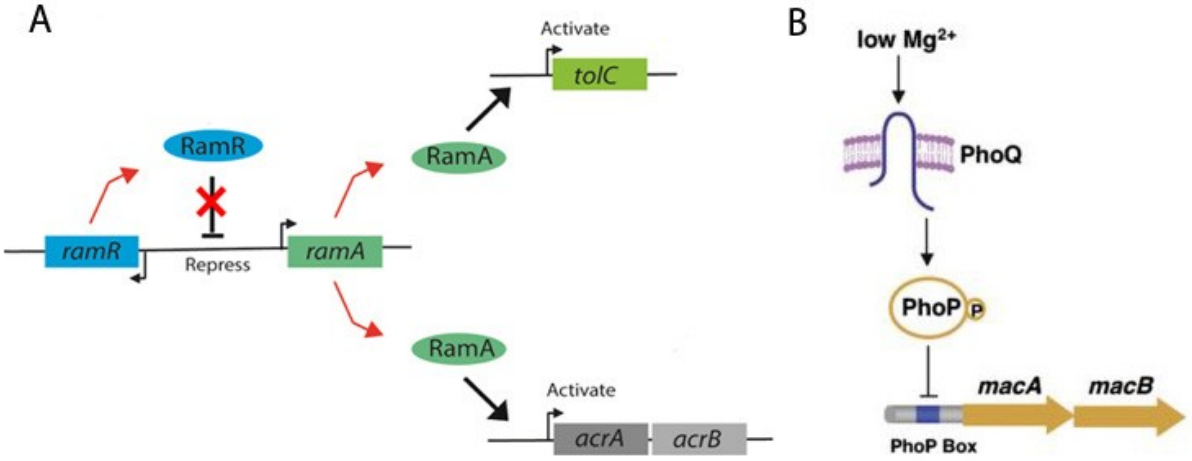

Figure 1.13: Regulation of efflux pump expression in Salmonella

Models of efflux pump gene regulation by the RamA/RamR system and the PhoPQ system. (A) The transcriptional regulator RamA binds upstream of the *acrAB* operon and the *tolC* gene and activates gene expression. RamR is a transcriptional repressor that is encoded upstream of *ramA* and inhibits its expression by binding to the promoter region. Inhibition of RamR by binding of small molecule drugs results in activation of RamA and elevated AcrAB-TolC expression. (B) In low Mg^{2+} conditions, PhoQ activates PhoP, which binds upstream of the *macAB* operon and represses its transcription.

Figure adapted from Nishino et al. (2009)[86]

RamR belongs to the TetR family of transcriptional repressors and contains an N-terminal DNA-binding domain and a C-terminal ligand-binding domain[81]. These regulators usually bind several of

the chemically diverse drugs that are expelled by the same transporters that they regulate and are therefore believed to act as cytoplasmic multidrug sensors. Crystal structures of RamR in complex with different substrates of the AcrAB-TolC pump have been solved[81], revealing significant flexibility in its substrate-binding site. Interaction of these drugs with RamR reduces its DNA-binding affinity, which results in higher expression of RamA, an increase in AcrAB-TolC efflux pumps and enhanced multidrug resistance. It has further been reported that RamA protein levels depend on the Lon protease, which degrades the activator and thus reduces its half-life[82]. The RamA DNA-binding site in *S. enterica* consists of a 19-nucleotide consensus region which has been found in the upstream regions of both the *tolC* gene and the bicistronic *acrAB* operon, reinforcing its role as a global activator for all three pump components[83].

As for MacAB, less is known about the regulation of its expression levels. The only regulatory factor that has been associated with it so far is the two-component system PhoPQ, the master regulator of virulence in *S. enterica*[84,85]. A PhoP binding site has been detected upstream of the *macAB* operon, and PhoP-dependent downregulation of *macAB* under low Mg^{2+} conditions has been suggested[85] (Figure 1.13 B).

A survey of expression levels of *S. enterica* efflux pump genes under laboratory conditions showed that expression of *acrAB* and *tolC* was by far the highest, exceeding *macAB* expression by five-fold[86] (Figure 1.14). Although this is not necessarily reflected in expression levels at infection sites, where multiple additional activating signals could play a role, it is consistent with the high clinical relevance of AcrAB-TolC.

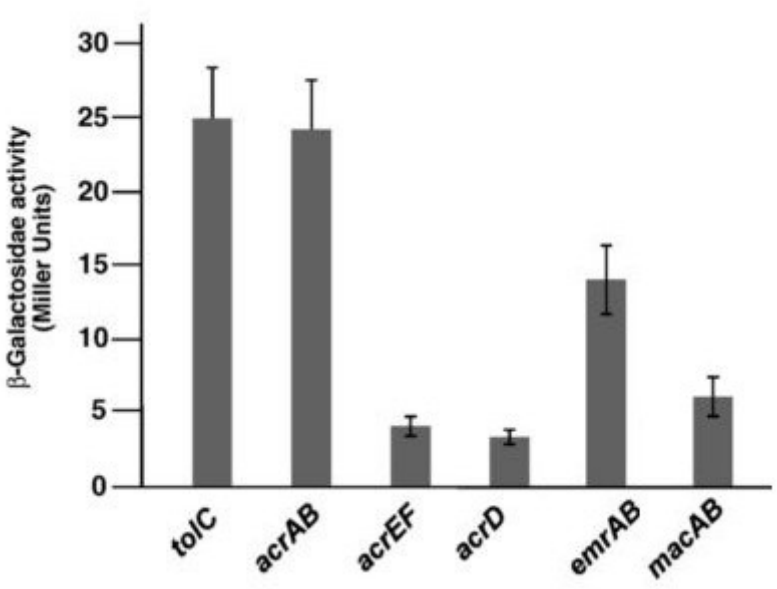

Figure 1.14: Efflux pump expression levels in *Salmonella*

Expression levels under laboratory conditions were determined by measuring β-galactosidase activities in different strains in which the lacZY genes replaced the chromosomal copy of the respective drug efflux gene. Expression of *acrAB* and *tolC* is nearly 5-fold higher than expression of *macAB*.

Figure adapted from Nishino et al. (2009)[86]

In this study, the potency of RamA as a transcriptional activator was exploited for overexpression of both the AcrAB-TolC and the MacAB-TolC efflux pumps, partly by activation of genomic copies of the efflux pump genes and partly by introducing RamA binding sites on plasmid-based expression systems.

1.6 Comparison of the two efflux pumps MacAB-TolC and AcrAB-TolC

S. enterica MacAB-TolC and AcrAB-TolC are similar in composition and assembly of their components: They share their tripartite structure, their outer membrane component TolC, and the nature and basic structural features of their PAPs, MacA/AcrA. However, there are major differences in their mode of action, the substrate specificity as well as expression and regulation. These differences are summarized in Table 1.1.

	MacAB-TolC	AcrAB-TolC
classification/superfamily	primary-active pump; ABC-type	secondary-active pump; RND-type
driving force	direct ATP hydrolysis at the cytoplasmic NBD-domain of MacB	proton/substrate antiport (coupled to electrochemical potential difference at the inner membrane)
inner membrane transporter (IMT)	MacB: 71 kDa cytoplasmic NBD-domain, 4 TM helices, large periplasmic domain	AcrB: 113 kDa transmembrane domain & large periplasmic headpiece
periplasmic adaptor protein (PAP)	MacA: 41 kDa N-terminal signal-like sequence (membrane anchor)	AcrA: 42 kDa N-terminal signal peptide (membrane anchor)
proposed stoichiometry (IMT:PAP:OMC)	6:6:3	3:6:3
Prevalent model	Adaptor bridging	Adaptor bridging
Main regulatory system	PhoPQ (Mg^{2+} dependent) [85]	RamA/RamR [77]
Expression level in laboratory conditions	low [86]	high [86]

Table 1.1: Direct comparison of major characteristics of the two efflux pumps

1.7 Aim of the project

Tripartite multidrug efflux pumps play a major role in antibiotic resistance of Gram-negative bacteria. The RND-type pump AcrAB-TolC is the most clinically relevant and also the currently best characterized of these molecular nanomachines. It is also subject of the best cryo-EM based structures available of any assembled tripartite efflux pump so far, reaching a resolution of up to 8.1 Å for some parts of the complex[45,50]. However, all available structures rely on artificially generated, cross-linked fusion proteins and no native structure of a fully assembled multidrug efflux pump was reported so far.

MacAB-TolC is the major representative of ABC-type multidrug efflux pumps in Gram-negative bacteria. Although (partial) crystal structures of its individual components exist [33,63,69], there is currently no structure available of the full tripartite complex, and little is known about its detailed assembly and the interaction of its components.

Thus, both for primary-type pumps such as MacAB-TolC as well as secondary-type pumps such as AcrAB-TolC, some crucial structural and mechanistic information is still lacking. A high-resolution structure of these nanomachines in a native assembled state could substantially contribute to the understanding of the multidrug efflux process and potentially guide the informed search for a non-toxic inhibitor.

Most of the work on tripartite efflux pumps so far has been done in *E. coli*. In this study, we focused our work on the pathogen *S. enterica* due to its relevance for disease in both humans and livestock and to the highly specific transcriptional regulator of AcrAB-TolC that is not present in *E. coli*.

The aim of the study was to structurally and functionally analyze the two tripartite efflux pumps as natively assembled transporters, and based on previous work in our lab. Therefore, the following main questions and subgoals were defined:

1) Can we handle the single efflux pump components?
    - Determine the degree of conservation between *E. coli* and *S. enterica*
    - Individual purification of MacA and MacB for antibody production

2) What is the best way to overexpress the complete efflux pumps, while allowing assembly in a native environment?

- Generation of a mutant strain lacking the major efflux pump genes *acrAB* and its homologs *acrD* and *acrEF* and complementation with a plasmid carrying the *acrAB* operon
- Overexpression of MacAB-TolC by introducing a plasmid carrying the *macAB* operon into this mutant strain; exploitation and adaptation of the RamA regulatory system for overexpression of MacAB-TolC
- Demonstration of the functionality of the plasmid-born efflux pumps

3) How can we isolate and visualize the efflux pumps in a near-native state?
    - Isolation of the efflux pumps in an assembled, near-native state
    - Visualization of the pumps by negative stain electron microscopy (EM) and by cryo - EM
    - 3D reconstruction of the complex from cryo-EM single particle analysis

2 MATERIALS AND METHODS

2.1 Cloning of genes of interest into expression vectors

2.1.1 Conventional cloning with restriction enzymes (for MacB-PCD)

To express the periplasmic core domain (PCD) of MacB, positions 998-1566 of the *Salmonella* typhimurium gene *macB* were cloned into the two expression vectors pET52b(+)(TEV) and pProEx-Htb (see supplementary material, section 8.5). This was done by conventional restriction enzyme cloning (Figure 2.1): Restriction endonucleases (REases) are enzymes that cleave double stranded DNA in a sequence-specific manner, with their recognition site often being a palindromic sequence of six to eight base pairs length. In this study, only REases where used that generate a 3' or 5' overhang ("sticky ends"). In order to insert a piece of linear DNA into the multiple cloning site (MCS) of a vector plasmid, both have to be treated with restriction enzymes that create compatible ends. To achieve this, the insert is amplified with primers containing specific REase recognition sites next to the insert-homology sites. After restriction digest of the amplified insert and the vector backbone to create compatible overhangs, they are ligated and transformed into *E. coli* competent cells.

Insert preparation

For amplification of the periplasmic core domain of the *macB* gene (nucleotides 998-1566), a pET52b(+) vector carrying the full-length gene (lab collection) was used as a template. Because

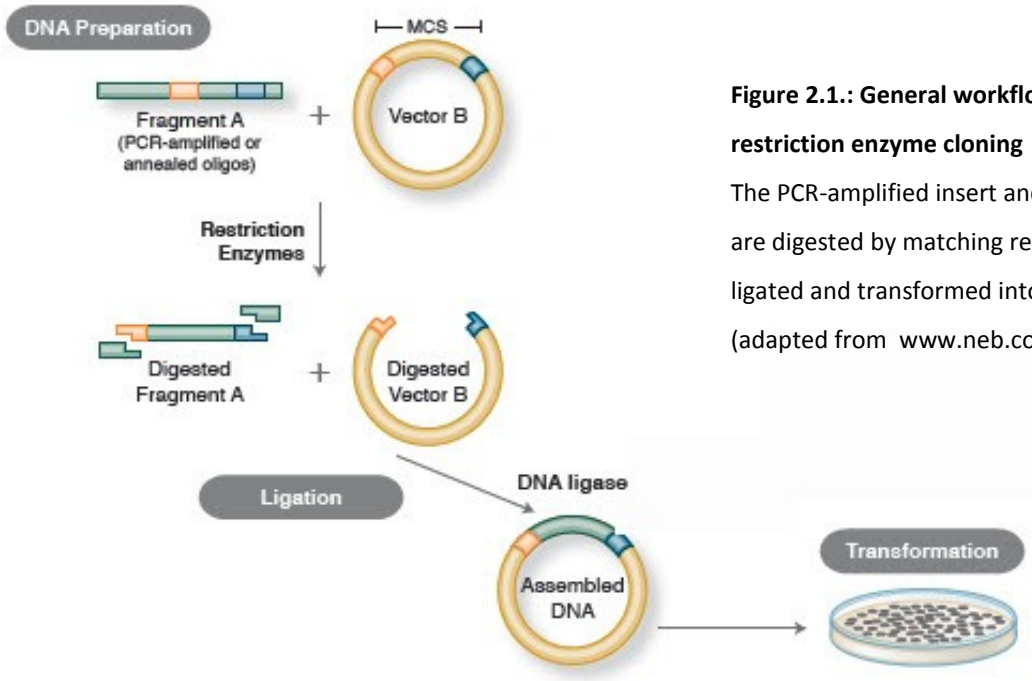

Figure 2.1.: General workflow of conventional restriction enzyme cloning
The PCR-amplified insert and the target vector are digested by matching restriction enzymes, ligated and transformed into *E. coli*.
(adapted from www.neb.com)

cloning into the pET52b(+) and the pProEx-Htb backbone requires different restriction sites, two sets of forward/reverse primers were designed, each containing a 16-19 nucleotides (nt) long sequence complementary to the PCD and the right restriction site at the 5' end (see Section 3.2. for detailed information). The two inserts were amplified by Polymerase Chain Reaction (PCR) using Velocity DNA polymerase (BIOLINE). The annealing temperature and the extension time were selected based on the melting temperature of the primers and the insert length, respectively (based on manufacturer's instructions). The PCR setup and protocol were chosen as follows:

1 x Master Mix		
5 x Buffer Hifi [10 mM Mg^{2+}]	10	µl
DMSO	1.5	µl
dNTPs (10 mM)	1.0	µl
Template DNA (pET52b-MacB)	20	ng
Primer forward [10 µM]	1.0	µl
Primer reverse [10 µM]	1.0	µl
VELOCITY DNA Polymerase [2 U/µl]	0.5	µl
ddH2O	fill up to **50 µl**	

PCR protocol	**temp [°C]**	**t [sec]**	**cycles**
initial denaturation	98	120	
denaturation	98	30	x 5
primer annealing	60	30	
extension	72	20	
final extension	72	150	

The PCR product was then analysed on a 1 % Agarose gel, bands at the corresponding size were cut out and DNA was extracted using the Promega Wizard® Gel and PCR Clean-up system. The concentration was measured using a NanoDrop spectrophotometer from peQlab.

Digest of insert and backbone DNA

REase cleavage of the insert designated for pProEx-Htb and of the corresponding vector was performed in a double digest setup with the restriction enzymes BamHI and PstI (both Thermo Fisher). For each, 500 ng DNA were mixed with 5 µl Fast Digest buffer (Thermo Fisher), 1 µl of both enzymes and double distilled (dd)H_20 to a final volume of 50 µl. The mix was incubated at 37°C for one hour to allow complete digest, followed by DNA cleanup. All DNA purification steps were done using the Wizard® Gel and PCR Clean-up system (Promega).

For the digest of pET52b(+)(TEV) and the corresponding insert, a two-step protocol had to be chosen due to the incompatibility of the restriction enzymes NcoI/PagI (Thermo Fisher, form compatible

overhangs) and SacI-HF (New England Biolabs). Therefore, the vector and the insert were first mixed with 1 µl NcoI or 1 µl PagI, respectively (complete setup as above, except only one enzyme per reaction). After incubation at 37°C for one hour, the DNA was purified and the whole volume (28 µl) was mixed with 1 µl SacI-HF, 5 µl CutSmart buffer (New England Biolabs) and ddH2O to a final volume of 50 µl. The second digest was performed at 37°C for 30 minutes and the DNA was purified again.

Ligation, Transformation and Sequencing

For ligation, 100 ng of the linearized vector backbone were mixed with the corresponding insert in a 1:3 ratio according to the following calculation:

$$ng(insert) = \frac{ng(vector)}{x} \times 3 \qquad x = \frac{vector\,(bp)}{insert\ (bp)}$$

To this mixture, 2 µl T4 ligase buffer, 1 µl T4 ligase (both Thermo scientific) and ddH2O up to a final volume of 20 µl were added. After incubation at room temperature, the mixture was immediately transformed into chemically competent *E. coli* TOP10 cells as described in section 2.3.1. and plated on LB containing ampicillin. The next day, colonies were picked, grown overnight for plasmid Miniprep (section 2.4.) and sent for sequencing to confirm insertion at the right position. The plasmids containing the right insert were frozen at -20°C and used for further experiments.

2.1.2 Site-directed mutagenesis cloning

Site-directed mutagenesis is a method to create site-specific mutations such as deletions, short insertions or substitutions in double stranded DNA[87]. The general workflow is visualized in Figure 2.2: First, primers are designed in a back-to-back orientation. For deletions, the primers are engineered to flank the region that should be deleted, while for substitutions, the forward primer is designed to incorporate the desired nucleotide changes. Insertions were not used in this study.

These primers are used for a PCR on the vector backbone, creating linear double stranded (ds) vector DNA. The remaining circular template vector is removed by DnpI restriction enzyme digest, which targets only methylated DNA. The linear dsDNA carrying the desired mutation is then phosphorylated, ligated and transformed into *E. coli*.

In this study, the deletion method was used to delete the N-terminal region of the *macA* gene on the pET52b(+)-MacA plasmid. The substitution procedure was used to exchange the inefficient thrombin cleavage site to a TEV protease recognition site between the MCS and the C-terminal histidine tag on the pET52b(+)-MacAΔN plasmid (see section 3.2. for detailed cloning list).

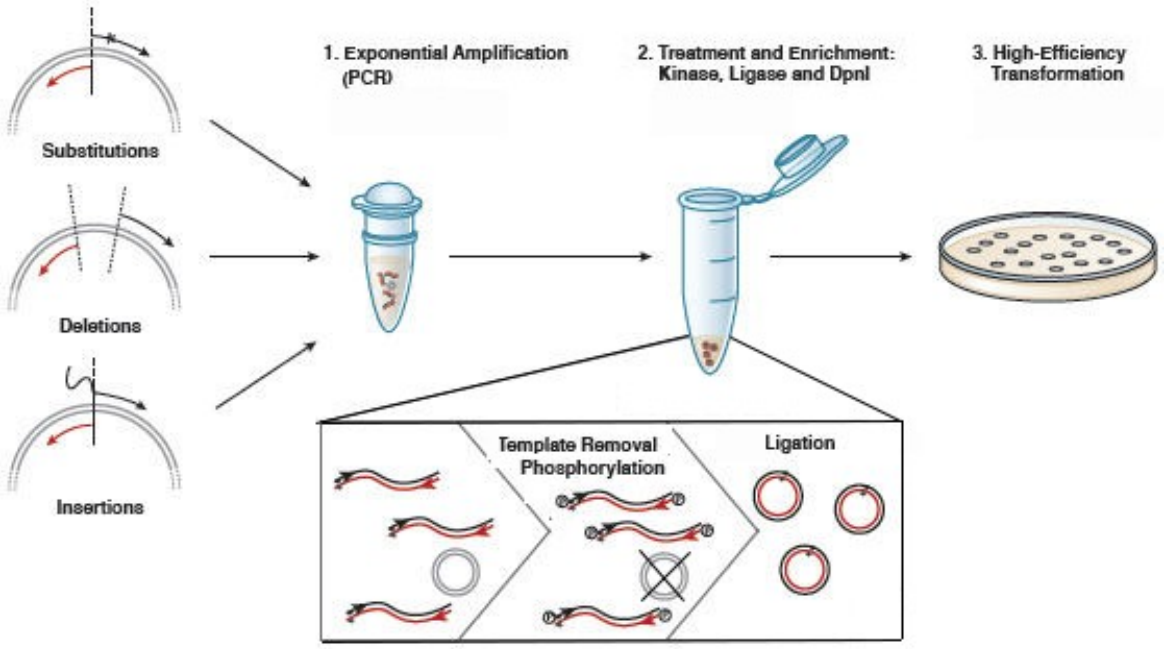

Figure 2.2.: General workflow of site-directed mutagenesis cloning

Mutation-specific primers are designed and used for amplification of the desired vector backbone region. The template is removed by DpnI digest and the remaining linearized DNA is phosphorylated, ligated and transformed into *E. coli.*

(adapted from www.neb.com)

Primer design and linear vector amplification

For MacAΔN cloning, primers were designed that flank the N-terminal region of the gene to be deleted. For thrombin-to-TEV site exchange, the forward primer carried the TEV recognition sequence and 19 complementary nucleotides on the 3' end of the mutation. The PCR setup was in principle the same as in section 2.1.1., except that the annealing temperature was adapted to the primers and the elongation time was significantly longer (usually 4-5 minutes) due to the length of the expected product.

DpnI digest, Phosphorylation and Ligation

To remove the original methylated plasmid, DpnI digest was performed on the unpurified PCR product by adding 1 µl DpnI (10 U/µl, Thermo Fisher) directly to the PCR tube and incubating at 37°C

for one hour. Subsequently, the mixture was loaded on a 1 % Agarose gel, the bands at the right size were cut out and DNA was extracted using the Wizard® Gel and PCR Clean-up system (Promega). In order to phosphorylate the 5' end of the linearized vector DNA to prepare it for ligation, 200 ng DNA were mixed with 1 µl T4 Polynucleotide Kinase (PNK), 1.5 µl T4 ligase buffer (both Thermo Fisher) and ddH2O to a final volume of 20 µl. After incubation at 37°C for 30 minutes, a further 0.5 µl T4 ligase buffer, 2 µl T4 DNA ligase (Thermo Fisher) and 2.5 µl ddH2O were added and ligation took place for one hour at room temperature.

Transformation and sequencing were performed as described for the conventional cloning procedure (section 2.1.1).

2.2 Generation of *Salmonella* competent cells

In the course of this study, different *Salmonella* strains were used to prepare competent cells to allow transformation of plasmid DNA, depending on the experiment. As transformation of *Salmonella* was always done by electroporation, electro-competent cells were prepared by removing surrounding ions in several washing steps, using the following procedure: A colony of the strain of interest was picked and grown in LB and appropriate antibiotic at 37°C overnight. The next day, 1 ml of the culture was inoculated in 50 ml fresh medium, grown to mid-log phase (OD_{600} = 0.4-0.7) and placed on ice for 30 minutes. The culture was then pelleted at 6000 g for 5 minutes at 4°C; the pellet was washed twice with 25 ml double distilled water (ddH2O) and twice with 15 ml 10 % glycerol (centrifuged at 6000 g for 5 min at 4°C in between the wash steps). Finally, the pellet was taken up in 1 ml 10 % glycerol and 80-100 µl aliquots were prepared. Depending on the experiment, electrocompetent cells were used freshly for transformation or frozen in liquid nitrogen and stored at -80°C until usage.

2.3 Transformation of Plasmid Deoxyribonucleic acid (DNA) into competent cells

2.3.1 By heat-shock (*Escherichia coli*)

For amplification and propagation of plasmids the *E. coli* strain TOP10 was used, while for protein expression, the plasmids were transformed either in *Salmonella* or in *E. coli* strain BL21(DE3)

depending on the experiment. Chemically competent *E. coli* cells were obtained from the in-house Molecular Biology Service. For transformation, these cells were thawed on ice and usually 50-200 ng plasmid DNA was added to 150 µl competent cells. The mixture was incubated on ice for one hour, then subjected to a heat-shock at 42°C for 45 seconds and immediately placed on ice for two more minutes. For recovery, 900 µl pre-warmed LB was added without antibiotic and the cells were incubated at 37°C shaking at 850 rpm for at least 30 minutes (for ampicillin resistance) or 60 minutes (for chloramphenicol resistance). Subsequently, the cells were pelleted at 5000 g for 5 minutes, the pellet was resuspended in 100 µl of the medium and plated on LB containing the required antibiotic (concentrations see section 3.1.2). The plates were incubated at 37°C overnight.

2.3.2 By electroporation (*Salmonella*)

For transformation of expression plasmids into *Salmonella*, electro-competent cells were prepared according to section 2.2. and used freshly or thawed on ice. Usually around 100 to 300 ng of plasmid DNA were added to 100 µl of competent cells and incubated for 30 minutes on ice. Electroporation was performed in a Gene Pulser Cuvette (Bio Rad) using an Eppendorf electroporator set at 1800 Volt. Immediately after the pulse, 900 µl SOC medium pre-warmed to 37°C were added to the cuvette, the cell suspension was transferred to an Eppendorf tube and incubated at 37°C and 850 rpm for 1.5 hours. The cells were pelleted by a centrifugation step at 5000 g, resuspended in 100 µl of the medium, plated on LB containing the antibiotic required for selection (usually ampicillin, chloramphenicol or kanamycin) and incubated at 37°C overnight.

For transformation of linear DNA into *Salmonella* during the lambda red-base knockout process (see section 2.7.), the protocol above was used with two changes: Instead of 100 ng of DNA, 1 µg was used, and the recovery time was increased to 3 hours.

2.4 Plasmid Minipreps and Sequencing

For plasmid Miniprep, single colonies of *E. coli* strain TOP10 containing the plasmid of choice were picked and inoculated in 5 ml LB medium with selective antibiotics. The culture was grown overnight at 37°C and 4 ml were used in the morning for plasmid isolation according to the QIAprep Spin Miniprep Kit protocol (Qiagen). The DNA concentration was measured using a NanoDrop spectrophotometer (peQlab).

Sequencing of the plasmid DNA was performed via Sanger sequencing by the in-house Molecular Biology Service. For this purpose, 150-200 ng of plasmid DNA were mixed with 1 µl of 5 µM primer per reaction.

2.5 SDS-Polyacrylamide Gel Electrophoresis and Coomassie Brilliant Blue Staining

Gradient gels were prepared for SDS-PAGE with a 4 % and a 20 % Acrylamide solution (see section 3.1.2) with the help of a gradient mixer. Each of the two vessel chambers was filled with one of the solutions (the 20 % solution being closer to the gradient mixer outlet) and ammonium persulfate (APS) was added to each at a final concentration of 0.1 %. Pre-assembled gel chambers were filled using the gradient mixer, combs were inserted and the gels were left to polymerize for at least one hour. Cast gels were used immediately or stored in a moisture chamber at 4°C for up to two weeks. Before loading the gels, 5x Laemmli buffer was added to the samples at a 1:4 ratio or, for bacterial cell pellets, according to the optical density at 600 nm of the original culture:

$$Laemmli\ buffer\ (\mu l) = \frac{OD_{600}\ units}{0.02\ \frac{units}{\mu l}}$$

The samples were boiled for 5 to 10 minutes at 95°C in order to denature the proteins and loaded onto a gradient gel next to a commercial protein standard ladder (PAGE ruler, Thermo Fisher). Gel Electrophoresis was usually carried out at 45 mA per gel for 50 minutes in 1x SDS buffer. For staining of the gels, they were first rinsed with ddH_2O, followed by two washing steps with ddH2O in the microwave at full heat for 1 minute. The gels were then fully covered with PageBlue® protein staining solution (Thermo Fisher), microwaved for 30 seconds and then incubated for 20 minutes at room temperature while shaking. The gel was then destained with ddH_20 at room temperature until protein bands were clearly visible.

2.6 Western Blotting

For Western Blotting, SDS-Polyacrylamide Gels were run as described above, rinsed with ddH_20 and soaked in 1x Protein Transfer Buffer (PTB) for 10 minutes. Pre-cut Polyvinylidene fluoride (PVDF) membranes were first incubated in methanol for 3 minutes and then in 1x PTB for 5 more minutes. A sandwich consisting of three soaked filter papers, the PVDF membrane, the polyacrylamide gel and

three more filter papers (from bottom to top) was built and semi-dry protein transfer was conducted with a constant voltage of 19 for 45 minutes. After the transfer, the membrane was blocked in 5 % milk powder in Phosphate Buffered Saline with 0.1 % Tween (PBS-T) and then incubated with the primary antibody, diluted in 5 % milk according to its tested dilution (generally 1:5000 for HRP-conjugated penta-His antibody, 1:25000 for anti-TolC, 1:50000 for anti-AcrA and 1:5000 for anti-MacA). Both steps were performed for either one hour at room temperature or overnight at 4°C. After three subsequent washing steps (each 20 minutes) with PBS-T, the blot was either developed (for HRP-coupled anti-His antibody) or incubated with a commercially available secondary antibody (goat anti-rabbit, Sigma), diluted 1:10 000 in 5 % milk. The membrane was then again washed three times for 20 minutes with PBS-T and developed using the ECL Plus Solutions A and B from Pierce. The solutions were mixed according to manufacturer's instruction, applied to the membrane for 3 minutes and imaging was done with a Molecular Imager® (BioRad).

2.7 Multiple genomic knockouts in *Salmonella* using the Lambda Red (λ Red) Recombinase System

2.7.1 General approach

To generate genomic knockouts (KO) in *Salmonella*, the method originally developed by Datsenko & Wanner (2000)[88] was used. In this procedure, the basic principle of homologous recombination by Lambda Red (λ Red) recombinase is exploited to replace entire genes within the bacterial genome with an antibiotic resistance gene. This recombineering process requires a plasmid expressing an inducible Lambda Red recombinase and a linear double stranded DNA strand encoding a bacterial resistance cassette flanked by two FRT (Flippase Recognition Target)-sites as well as two 40 nucleotides long homology regions up- and downstream of the targeted gene. A plasmid-encoded flippase is then utilized to flip out the antibiotic resistance gene, leaving only the priming site and one FRT site (termed the "scar") in the genome (Figure 2.3).

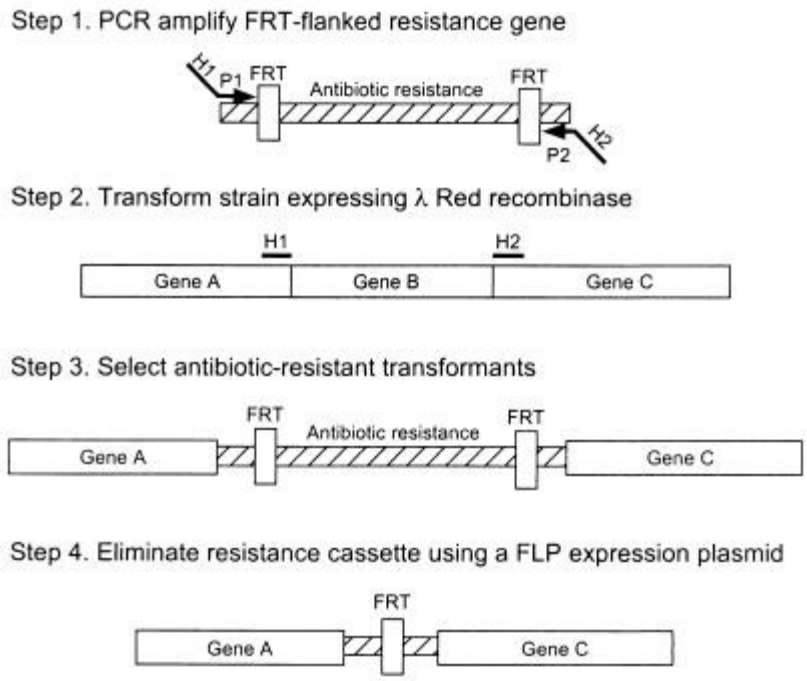

Figure 2.3: Overview of the general steps in genomic recombineering based on λ Red expression, adapted from Datesenko and Wanner (2000).

For this study, knockouts of the *acrD* gene and the *acrEF* operon were generated individually in a clean *Salmonella* strain LT2_pTP223 background and then transferred into a *Salmonella* SB905 wild type strain by phage transduction. To generate the *acrAB/acrD/acrEF* triple KO, the *acrEF* knockout was first transferred into a previously generated SB905*ΔacrAB* strain, followed by transfer of the *acrD* knockout in the resulting SB905*ΔacrABΔacrEF* strain.

2.7.2 Stepwise knockout protocol

Step 1	Primer design and KO-cassette PCR
Step 2	Transformation of competent cells with the KO cassette
Step 3	Knockout verification by PCR
Step 4	Transduction with phage P22
Step 5	Phage removal
Step 6	Removal of the resistance marker via flippase
Step 7	Validation of knockout and cassette removal
Step 8	Repeated transduction to produce the triple knockout

Step 1: Primer design and KO cassette PCR

In this work, the chloramphenicol resistance cassette flanked by two FRT sites that is encoded on the pDK3 plasmid used by Datsenko and Wanner[88] was amplified via Polymerase Chain Reaction (PCR). In order to allow subsequent homologous recombination, primers were designed so that they contained both the priming sites to the pDK3 resistance cassette (19 nt) and the homology region up- or downstream of the gene of interest (40 nt).

Forward primer:

FFFFFFFFFFFFFFFFFFFFFFFFFFFFFFFFFFFFFFFFTGTAGGCTGGAGCTGCTTC (Tm~ 81°C)

Reverse primer:

RRRRRRRRRRRRRRRRRRRRRRRRRRRRRRRRRRRRRRRRCATATGAATATCCTCCTTA (Tm~89°C)

Homology region upstream (F) or downstream (R) to the targeted gene

Priming site ½

For both the *acrD* and the *acrEF* knockout, one primer pair was designed (forward/reverse) where each primer had a total length of 59 nt. All primers were ordered from Sigma Aldrich. To avoid primer dimerization, amplification of the resistance cassette of pDK3 with adjacent homology sites was achieved by a two-step PCR setup: Initially, only the 19 nt long priming regions can bind to the target DNA, thereby lowering the actual melting temperature of the primer. To assure binding at this state, five PCR cycles are carried out at a low annealing temperature (55°C). In a second step, when already some complete PCR product is present that binds the whole primer sequence, the remaining 35 cycles are carried out at a higher annealing temperature (69°C). The length of the resulting product is around 1100 base pairs, therefore an annealing time of 25 seconds per cycle was chosen for VELOCITY DNA polymerase (BIOLINE).

For the PCR reactions, a 50 µl setup was prepared and ran in an Eppendorf Mastercycler as follows:

1 x Master Mix		
5 x Buffer Hifi [10 mM Mg^{2+}]	10	µl
DMSO	1.5	µl
dNTPs	1.0	µl
pDK3 plasmid	100	ng
Primer forward [10 µM]	1.0	µl
Primer reverse [10 µM]	1.0	µl
VELOCITY DNA Polymerase [2 U/µl]	0.5	µl
ddH2O	fill up to **50 ul**	

step	note	temp [°C]	t [sec]	cycles
1	initial denaturation	98	120	
	denaturation	98	30	x 5
	primer annealing	55	30	
	extension	72	25	
	final extension	72	150	
2	denaturation	98	30	x 35
	primer annealing	69	30	
	extension	72	25	
	final extension	72	150	
	cooling	4	∞	

The PCR product was loaded on a 1 % Agarose gel and the band appearing at the right size was cut out. The DNA was extracted from the gel and purified using the Wizard® Gel and PCR Clean-Up System protocol (Promega). The DNA concentration was determined by NanoDrop spectrophotometer (peQlab).

Step 2: Transformation of competent cells with the KO cassette

Electrocompetent cells were prepared from the LT2 strain carrying the pTP233 plasmid (with inducible lambda red gene and a tetracycline resistance, from Addgene) as described in Section 2.2. The competent cells were transformed by electroporation (see Section 2.3.2.) with 1 µg of the respective amplified linear KO cassette (*acrD/acrEF*) and plated on LB containing chloramphenicol for selection.

Step 3: Knockout verification by PCR

As the Lambda Red recombinase can have an offside effect and falsely target other regions in the genome, it is important to check that the chloramphenicol resistance cassette has been inserted in the right position in the selected colonies. Therefore, colonies were picked, grown for several hours

at 37°C in LB with chloramphenicol and 0.5 µl were used as a template for colony PCR. Special primers up- and downstream of the gene of interested were designed for this purpose, generating a product of about 1100 base pairs in case of successful recombination and a product of more than 3000 base pairs if the original gene is still present. For each colony, two 20 µl PCR reactions were set up with extension times of 25 seconds and 2 minutes respectively to ensure possible amplification of either the short or the long product. The annealing temperature was always 61°C. The colonies that demonstrated successful integration of the resistance cassette at the locus of interest were used to proceed further.

Step 4: Transduction with phage P22

Phage P22 is a bacteriophage that specifically infects *Salmonella* typhimurium by binding to the O-antigen lipopolysaccharide on the host surface. In this method, we exploit the phage P22 property to pack parts of their host genome in order to transduce genetic material from the donor strain (LT2_pTP223) into the recipient SB905 strain, where it is inserted by homologous recombination. For phage transduction, phage broth is prepared containing 0.5x E-salt mix (see buffer and reagents), 0.2 % D-Glucose (Sigma) and a final concentration of 108 pfu/ml phage P22 in LB medium. 1 ml of the donor strain containing the new knockout was mixed with 4 ml phage broth and inoculated overnight at 37°C. The next morning, the remaining bacteria and cell debris were spun down at full speed and the supernatant transferred to a new Eppendorf tube. 100 µl of chloroform were added to 1 ml of supernatant to lyse the remaining bacteria, leaving the phage intact. The phage lysate was used as soon as the chloroform has settled or was stored at 4°C until usage (stable for years). 100 µl of fresh culture of the recipient strain (*SB905ΔacrAB*) was mixed with 100 µl phage lysate in different concentrations (1:200, 1:500 or 1:1000), incubated at 37°C for one hour and plated on LB containing chloramphenicol for selection.

Step5: Phage Removal

The next day, the new SB905 colonies with incorporated Cm cassette were streaked onto green plates (see buffer and reagents). On these indicator plates, phage-containing cells lyse and make small, dark green colonies, while uninfected cells produce larger light green colonies. The grown colonies were repeatedly streaked onto new green plates, until most colonies seemed uninfected. To check for pseudolysogeny (stalled development of a bacteriophage in a host cell), 100 µl of phage broth was spread in the middle of a green plate and healthy-looking colonies were streaked from left to right through the phage border. Phage free colonies should be light green on the left, lysed in the phage streak and dark green after it. Colonies passing this test were selected for further use.

Step 6: Removal of the resistance marker via flippase

The pCP 20 plasmid contains an ampicillin resistance gene and an inducible flippase that removes the resistance cassette by homologous recombination of the two FRT sites. It is thermosensitive, meaning that it is lost if incubated at 37°C. The newly generated phage free SB905 knockout clones were made electrocompetent and transformed with 50 ng pCP20 as described in Section 2.3.2. (except the recovery step was performed for 3 hours at 30°C). Cells were then plated on LB containing ampicillin and incubated for 24 hours at 30°C. Single colonies were picked and streaked on LB/tetracycline plates and grown at 37°C for at least 20 hours to remove the pCP20 plasmid.

Step 7: Validation of knockout and cassette removal

To test for loss of the pCP20 plasmid and chloramphenicol cassette removal, colonies grown in step 5 were picked and streaked on index plates (LB containing either ampicillin, chloramphenicol or tetracycline). All SB905 colonies should grow on tetracycline, but only the colonies that did not grow on ampicillin (pCP20 loss) and chloramphenicol (resistance cassette loss) were investigated further by PCR to check for presence of the knockout at the right position. The colony PCR was performed as in Step 3, except that the primers were chosen to lie further up- or downstream the deleted gene, so that the PCR product from successful knockouts with deleted resistance cassettes are 250 base pairs long, whilst the ones still containing the cassette and the wild type are around 1200 and more than 3000 base pairs, respectively.

Step 8: Repeated transduction to produce the triple knockout

To produce the *acrAB/acrEF* double and the *acrAB/acrD/acrEF* triple knockouts, both the *acrD* and the *acrEF* single knockouts were first generated individually in the donor strain LT2_pTP223 and phage lysates were prepared (step 1-3). The *acrEF* knockout was transferred into the existing SB905*ΔacrAB* strain (lab collection) by performing steps 4 to 6, thereby generating the SB905*ΔacrABΔacrEF* strain. Steps 4 to 6 were then repeated with the double knockout as recipient strain and SB905*ΔacrD* as the donor strain for phage P22 transduction, resulting in the final triple knockout strain SB905*ΔacrABΔacrDΔacrEF* (short SB905*ΔABΔDΔEF*).

2.8 *Salmonella* Growth Curves

A growth curve was recorded for wild type SB905, SB905*ΔacrAB* and the SB905*ΔABΔDΔEF* triple knockout carrying the pBAD-ramA plasmid to investigate whether there was a growth effect visible in the deletion strains compared to the wild type strain, with and without *ramA* expression. For this

purpose, the respective cultures were incubated overnight, diluted to an OD_{600} of 0.1 the next morning and kept shaking at 37°C. Every 30 minutes, the optical density at 600 nm was measured. At an OD_{600} of around 0.5, one culture aliquot of each strain was induced by arabinose while the second one was not. All optical density measurements were recorded to follow the bacterial growth characteristics over a period of time.

2.9 Plasmid complementation of the deletion strain and plasmid-expression of MacAB

For future structural and functional experiments, the *acrAB/acrD/acrEF* triple knockout strain was transformed separately with the plasmid-encoded *acrAB* or *macAB* operon. For *acrAB*, this should result in complementation of the knockout, while for *macAB* a strong gene dosage effect is expected to be seen as an increase in protein expression. For both constructs, a 250 nucleotide stretch upstream of the *acrAB* operon containing the RamA binding site was inserted between the ribosome binding site and the efflux pump operon. Additionally, a 6x histidine tag was introduced at the C-terminal ends of *acrB* and *macB*.

The SB905ΔABΔDΔEF triple knockout strain was transformed with the pQE70-MacAB or pQE70-AcrAB plasmid (without T5 promotor and CAM resistance cassette) and additionally a plasmid expressing the transcriptional activator RamA under control of the arabinose-inducible araBAD system[89] . The transformation was carried out as described in Section 2.3.2. and the bacterial cells were plated on LB agar plates containing chloramphenicol and ampicillin.

To check for successful complementation, the transformed strains were inoculated in LB and antibiotics, induced with 0.4 % L-arabinose at an OD_{600} of 0.5 and samples were taken 5 hours after induction. The cells were pelleted, resuspended in Laemmli buffer according to the calculation in Section 2.5. and assessed on Western Blot for expression of the plasmid-encoded proteins. MacB and AcrB were detected by a commercially available Horseradish Peroxidase (HRP)-conjugated penta-His antibody (QIAGEN) from rabbit (dilution 1:5000), AcrA was detected by a specific polyclonal antibody (non-commercial, raised in rabbit) in a 1:50000 dilution and for detection of MacA, the newly produced antibody was used in a 1:5000 dilution (see supplementary material, section 8.3).

2.10 Antibiotic susceptibility testing by Minimum Inhibitory Concentration (MIC) determination

To test the functionality of plasmid-expressed AcrAB and MacAB, the minimum inhibitory concentration (MIC) was determined for the macrolide antibiotic erythromycin in different *Salmonella* SB905 variants. The agar dilution method according to the standard protocol published by Wiegand et al. (2008)[90] was used for MIC determination. In this procedure, serial dilutions of the antibiotic in nutrient agar medium are prepared and a standardized number of cells is applied to the surface of the agar plate. The lowest antibiotic concentration that still inhibits visible growth of the bacterium is considered as the MIC value for this antibiotic.

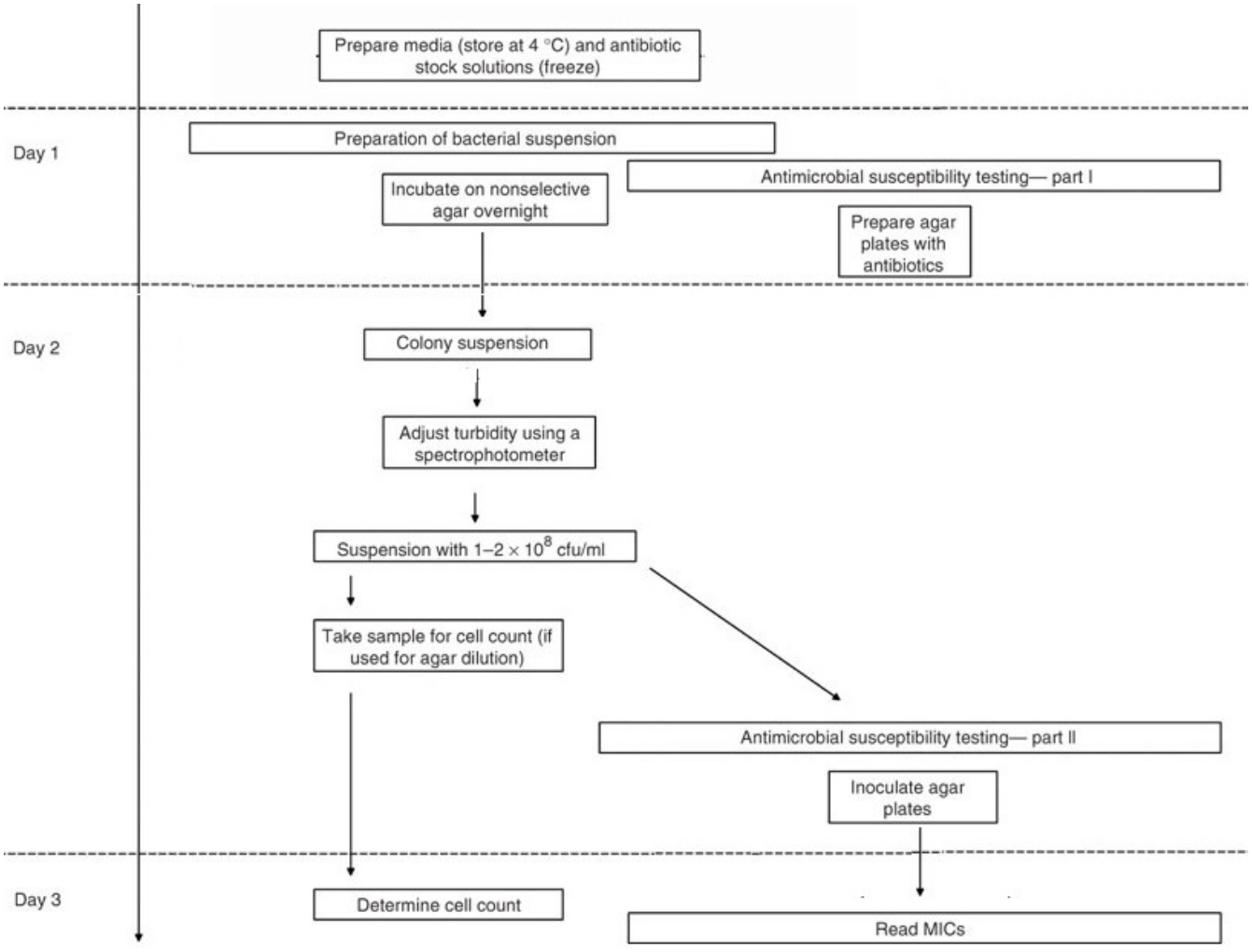

Figure 2.4: Flowchart for antimicrobial susceptibility testing using the agar dilution method, adapted from Wiegand et al. (2008)

Before starting the test, erythromycin in powder form (Sigma-Aldrich) was used to prepare three stock solutions with a concentration of 10, 1 and 0.1 mg/ml respectively. Agar plates with the

following dilutions of the antibiotic were prepared by mixing melted LB/Agar medium with the antibiotic stock solutions:

stock concentration (mg/ml)	volume of stock solution per plate (µl)	**final antibiotic concentration** (µg/ml) when adding 25 ml agar
10	640	**256**
10	320	**128**
10	160	**64**
10	80	**32**
10	40	**16**
1	200	**8**
1	100	**4**
1	50	**2**
0,1	250	**1**
0,1	125	**0,5**
0,1	62,5	**0,25**
0,1	31,25	**0,125**

25 ml medium were poured into a plate and after solidification at room temperature plates were stored at 4°C until further use. For MIC testing, the SB905 wild type strain (strain A), SB905ΔABΔDΔEF triple knockout strain (B) and the triple knockout strains containing either the pQE70-AcrAB (SB905ΔABΔDΔEF_ramA_AcrAB; C) or the pQE70-MacAB (SB905ΔABΔDΔEF_ramA_MacAB ; D) plasmid and pBAD-ramA were used (see Section 2.9). The strains were streaked on non-selective agar plates and incubated at 37°C overnight. The next day, 3-4 colonies of each plate were picked by touching them with a sterile loop and transferred into 3 ml LB medium. The culture was incubated at 37°C in a shaker and the absorbance at 600 nm was measured regularly in a spectrophotometer. After 2-6 hours an optical density of 0.15 for strains A-C and 0.45 for strain D was reached, corresponding to a bacterial concentration of approximately 10^8 cfu colony forming units)/ml (as determined in a previous test). At this point, the bacterial cultures were diluted 1:10 and 1 µl of each culture was applied to a marked spot on each of the erythromycin-dilution-series plates to deliver the desired cell density of around 10^4 cfu per spot. The inoculum spots were left to dry at room temperature before inverting the plates and then incubated at 37°C for 24 hours. To confirm the viable count of the bacterial suspension that was used to prepare the inoculum, a 10^{-4} and a 10^{-5} dilution of the original suspension were made and 100 µl of each was plated onto antibiotic-free LB agar plates. The following day, these plates were checked and if 50-200 colonies were present on the 10^{-5} dilution, this was an indication that the right number of cfu had been used and the MIC test was valid. The MIC for each strain was determined as the lowest

concentration of antibiotic that still inhibited growth of bacterial cells. The growth of one single colony or faint film caused by the inoculum was disregarded as is recommended in the protocol.

2.11 Expression and purification of the individual proteins MacA and MacB

2.11.1 Purification of MacAΔ2-31

In order to produce antibodies against a purified soluble protein whilst avoiding potential cross-reactions, very high purity and a concentration of around 1 mg/ml have to be reached. To allow for such high concentrations, *Salmonella* MacA was overexpressed from a plasmid in *E. coli* and purified in several steps. MacA is a periplasmic protein, but contains an N-terminal signal-peptide like sequence, which is suggested to anchor the protein to the inner membrane. In order to be able to express MacA in a soluble form, a deletion construct lacking the N-terminal sequence was used.

For protein expression, a 1 L culture of bacterial cells carrying the pET52b(+)(TEV)-MacAΔN plasmid (see plasmid list, Section 3.2.) was grown at 37°C to an OD600 value of 0.5 and then induced by adding 200 mM Isopropyl-β-D-thiogalactopyranosid (IPTG). Bacteria were harvested 4 hours after induction by centrifugation at 4000 g for 15 minutes at 4°C. The bacterial cells were resuspended in 30 ml lysis buffer containing 20 mM Tris (pH 8.0) and 150 mM NaCl with one tablet of EDTA-free Protease Inhibitor Cocktail (Roche) added. Upon complete resuspension, cells were disrupted by sonication (2 x 5 minutes) and centrifuged at 45000 g for 30 minutes at 4°C to remove cell debris. The supernatant containing MacAΔ2-31 was loaded on a 5 ml Ni2+ chelation chromatography column (HisTrap HP 5ml, GE Healthcare) and eluted with a gradient of 0-500 mM imidazole. The peak fractions containing the protein were pooled and incubated with TEV protease (20 µl/ml, from MBS) overnight while dialyzing against the original lysis buffer. The sample was again loaded on a Ni^{2+} chelation chromatography column and the flowthrough fraction containing MacAΔ2-31 without HisTag was collected. This sample was concentrated down to 500 µl using an Amicon Ultra Centrifugal Filter (Merck Millipore) with a molecular weight cutoff of 10 kDa and applied to a Superdex 200 size exclusion column (GE). Fractions containing the purified MacAΔ2-31 were pooled, concentrated down to 1 mg/ml and flash frozen in liquid nitrogen.

Antibodies against MacAΔ2-31 were produced in a rabbit in collaboration with Dr. Marcela Hermann from the Max F. Perutz Laboratories (MFPL) at the Vienna Biocenter.

2.11.2 Expression of periplasmic core domain (PCD) of MacB

In an attempt to purify one domain of the MacB protein for antibody purification, the 226 residues long internal periplasmic core domain (PCD) was selected because it is the largest non-membrane domain and has already been crystallized for *E. coli*.[69] The *Salmonella* MacB periplasmic core domain (residues 297-522) was expressed in *E. coli* strain BL21(DE3) from two different plasmids, pProEx-Htb-MacB(PCD) and pET52b(+)(TEV)-MacB(PCD) (see plasmid list, Section 3.2.).

For overexpression, 1 L of bacterial culture carrying one of the plasmids was grown at 37°C in LB medium containing ampicillin. When an OD_{600} value of 0.5 was reached, protein expression was induced by adding IPTG to a final concentration of 200 µM. After growth at 37°C for 4 more hours, bacterial cells were harvested by centrifugation at 4000 g for 15 minutes, taken up in 5 ml lysis buffer containing 20 mM Tris (pH 8.0) and 150 mM NaCl, centrifuged again and the pellet was frozen for up to two weeks.

For purification, the cell pellet was resuspended in 30 ml lysis buffer containing 8 M urea and complemented with one EDTA-free Protease Inhibitor Cocktail tablet (Roche). Cells were lysed by sonication (2x 5 minutes) and the lysate was centrifuged at 45000 g for 30 minutes at 4°C. The supernatant containing all proteins denatured by urea was loaded on a 5 ml Ni2+ chelation chromatography column (HisTrap HP 5 ml, GE Healthcare) pre-equlibrated in lysis buffer and 8 M urea. The column was washed with 25 mM imidazole and eluted with a gradient of 25-500 mM imidazole. The peak fractions were pooled and dialyzed stepwise in a Slide-A-Lyzer® 10K cassette (Thermo Fisher Scientific) with a molecular weight cutoff of 10 kDa. Each step was performed for one hour at room temperature and the concentration of urea in the lysis buffer was reduced by 2 M in each step, except for the last one, where the concentration was only decreased from 2 M to 1 M urea. After 30 minutes of dialysis in 1 M urea, protein precipitation was clearly visible and did not disappear even when dialyzing back to higher urea concentrations. Addition of β-mercaptoethanol as well as dialysis at different temperatures did not help. As protein solubilized in 2 M urea cannot be used for antibody production in a rabbit, the purification trials were stopped at this point.

2.12 Efflux pump isolation

Expression in large culture volumes

Overexpression of the efflux pumps was performed in large volumes to increase the yield. For this purpose, *Salmonella* SB905 wt strain carrying the arabinose-inducible pBAD-ramA plasmid or SB905ΔABΔDΔEF triple knockout strain carrying pBAD-ramA in addition to the plasmid encoding the

efflux pump operon (pQE70-AcrAB or pQE70-MacAB) was used. For the triple knockout strain, a pre-pre-culture was inoculated from the glycerol stock into 5 ml medium and grown overnight at 37°C. Due to the high antibiotic susceptibility of this strain, it was consistently grown in LB medium with only a third of the standard concentrations of ampicillin and chloramphenicol. The following day, a 1L pre-culture was prepared from this, grown overnight at 37°C and diluted 1:10 to give a total culture volume of 10 L (10x 1 L in 2 L flasks). As soon as an OD_{600} of 0.4-0.5 was reached, the culture was induced with 0.4 % L-arabinose and grown for 5 hours at 37°C while shaking at 220 rpm.

Bacterial cells were then harvested by centrifugation at 4250 g for 12 minutes at 4°C. Cell pellets were resuspended in 5 ml 0.15 M Tris (pH 8.0) and the solution was pipetted dropwise directly into liquid nitrogen. The thus formed "cell beans" were immediately collected in Falcon tubes and stored at -80°C until usage.

General Purification Procedure

For the isolation of efflux pumps a protocol previously established in the lab[91] was used and partly adjusted according to the needs of the sample. An overview of the method is depicted in Figure 2.5 and the details for the buffers used are listed in Section 3.1.

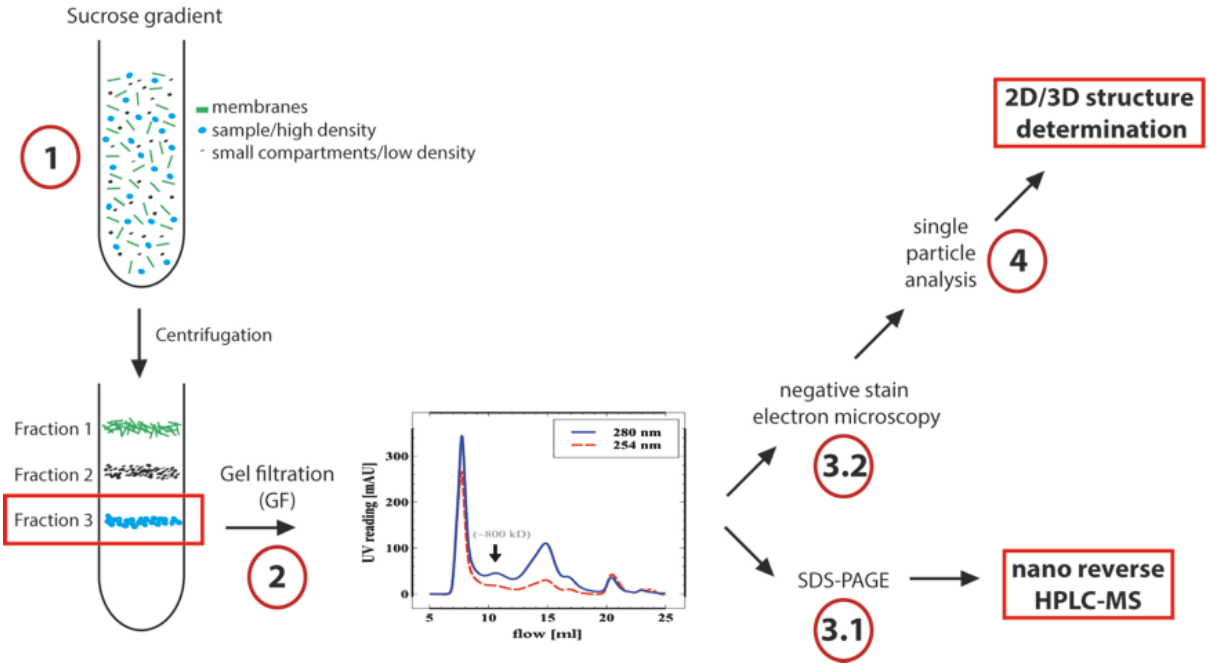

Figure 2.5: A schematic overview of the isolation procedure. The sample is extracted from the membranes, prepared via a differential centrifugation step (1) and subsequently subjected to gel filtration (2). The peak fractions are used for SDS-PAGE and Mass Spectrometry (3.1) or analyzed by electron microscopy (3.1), enabling single particle analysis (4) and finally structure determination.

Previously prepared bacterial cell beans were thawed in 2x 140 ml cold buffer 1 (1x per 5 L original culture) and the sample was stirred at 60-100 rpm on ice in a 1 L bottle. 12 mM EDTA (pH 8.0) and 1.4 mg/ml lysozyme (Sigma) were sequentially added dropwise under stirring and the mixture was incubated on ice for 1 hour for cell lysis. To inactivate all contained proteases, one and a half tablets of EDTA-free Protease Inhibitor Cocktail tablets (Roche) were then added and the mixture was stirred on 37°C for 10 min. For solubilization of membranes, 0.45 % of the detergent Lauryldimethylamine N-oxide (LDAO) were added and the sample was continuously stirred until the solution became viscous. 0.45 M NaCl and, as soon the sample became almost clear, 20 mM $MgCl_2$ were added. When viscosity dropped, the sample was put back on ice, stirred for 25 minutes and the remaining debris was pelleted by centrifuging at 14000 g for 30 minutes at 4°C. The supernatant containing the efflux pumps together with other membrane components was transferred to six new tubes and ultra-centrifuged at 40000 rpm at 4°C for 2:30 hours (Sorvall 90SE, rotor T-647.5, 170 k-factor). The pellets were each resuspended in 2 ml buffer 2 by carefully pipetting up and down and left shaking on ice slowly for 1 hour to allow for proper resuspension. The solutions were then pooled and 12 ml without too many flakes were mixed with 12 ml 52.5 % cesium chloride (CsCl) and 600 ul 10 % LDAO to a final concentration of 27.5 % CsCl and 0.5 % LDAO. A gradient ultracentrifugation was set up overnight at 50000 rpm for 13-15 hours at 4°C (Sorvall 90SE, rotor TH-660, 64 k-factor; deceleration set to 1). 500 ul fractions were taken from the CsCl gradient (normally fractions 1-3 contained the pumps), corresponding fractions were pooled to give a final volume 3 ml per fraction, and filled up to 6 ml with buffer 3. The samples were centrifuged again at 90000 rpm for 35 minutes at 4°C (Sorvall RC M150 GX, rotor: S100-AT4-463), the pellets containing the pumps were resuspended in 200 µl per fraction and incubated under shaking on ice for 30 minutes to 2 hours.

Immediately after, a part of the sample was usually checked with negative-stain transmission electron microscopy (TEM) and the rest was applied to Superose 6 size exclusion column (GE Healthcare) equilibrated with buffer 3. For AcrAB-TolC, peak fractions were pooled and used for further experiments as depicted in figure 2.5.

MacAB-TolC condition screen

The efflux pump MacAB-TolC was found to be aggregated to a large part when purified according to the protocol above and checked in EM before gel filtration. In order to screen for conditions which might prevent aggregation, LDAO was substituted for a range of different detergents when resuspending the pellet after the last ultracentrifugation step. A list of the detergents, their respective critical micelle concentrations (CMC) and the concentrations used can be found below. Usually a 10 % solution of the detergent was prepared initially and then diluted in the buffer accordingly.

Detergent	Full Name	CMC (mM)	0.5% (w/v) corresponds to (mM)	Tested Concentrations (% w/v)
LDAO	N,N-Dimethyldodecylamine N-oxide	1	21,75	0.5 0.1
DDM	n-Dodecyl β-D-maltoside	0.15	9,8	0.5 0.05
Triton X-100		0.2-0.9	8	0.5
Chapso		8	7,95	0.5 3.0
FC-12	Fos-Choline-12	1.5	14,25	0.5
OG	Octyl β-D-glucopyranoside	20-25	17	0.5 1.0 3.0 5.0
DHPC	1,2-diheptanoyl-sn-glycero-3-phosphocholine	1.4	10	0.5
Deoxycholic Acid		2-6	12,75	0.5
Brij-58	Polyoxyethylene (20) cetyl ether	0.08	4,45	0.5
LMNG	Lauryl Maltose Neopentyl Glycol	0.01	5	0.2[92]
OGNG	Octyl Glucose Neopentyl Glycol	1.02	8	1.2[92]

In addition to different detergents, various pH and temperature conditions were tried as listed below:

pH	Additives	Temperature	Incubation Time (Shaking)
8.0 (buffer 2)	10 mM MgCl2	4°C/37°C	overnight
8.0 (buffer 2)	10 mM MgCl2 + 4 mM ß-Mercaptoethanol	4°C/37°C	overnight
6.0 (buffer 2 adjusted)	-	4°C/37°C	overnight
4.0 (20 mM MES buffer)	-	4°C/37°C	overnight
8.0 (buffer 2)	10 mM MgCl2	4°C	3 days
8.0 (buffer 2)	2 mM ATPγS	4°C	overnight
8.0 (buffer 2)	0.01 % SDS	4°C	overnight
8.0 (buffer 2)	5 mM ATP	4°C	overnight
8.0 (buffer 2)	10 mM ATP	4°C	overnight
8.0 (buffer 2)	NaCl omitted in the buffer	4°C	overnight

2.13 Mass Spectrometry

To confirm the protein identity in the purification samples, nano-reverse High Pressure Liquid Chromatography (HPLC) mass spectrometry was performed by the in-house Molecular Biology Service. For this purpose, SDS-PAGE of the sample was performed as described in Section 2.5, gels were stained with Coomassie Brilliant Blue and bands corresponding to the size of the proteins of interest were cut out and analyzed in accordance to the protocols of the Mass Spectrometry Facility. Alternatively, in solution digestion of the sample was performed prior to analysis by mass spectrometry.

2.14 Glow-discharging of carbon grids and negative staining of samples for Electron Microscopy (EM)

In order to improve sample binding on the electron microscopy (EM) grids, carbon coated copper grids were glow-discharged to reduce hydrophobicity. Glow-discharging was performed on continuous carbon electron microscopy grids (Agar Scientific) in a Bal-Tec SCD 005 Glow Discharger for 30 seconds at 25 mV under vacuum and the grids were immediately used for sample adsorption. This was achieved by applying 5 µl of the sample on the grid for 30 seconds, followed by a washing step with 2% phosphotungstic acid (PTA), and a final 45 seconds staining step with 2 % PTA. After each step, the grid was blotted dry by carefully touching its side with filter paper. The grids were stored at room temperature under vacuum conditions or immediately imaged at 100 keV in a FEI Morgani 268D. Efflux pump samples were usually imaged at 71000x magnification, while the magnification for minicell imaging ranged between 2800x and 56000x.

2.15 Sample preparation for cryo-electron microscopy (cryo-EM)

For first cryo-EM trials, sample fractions after SEC were five times concentrated using Amicon Ultra spin columns (Millipore) with a 100 kDa cutoff size. 5 µl of the sample were applied to glow-discharged continuous carbon electron microscopy grids (see above), left for 30 seconds for adsorption and then blotted for 3 seconds from the top using filter paper. The same procedure was also performed with the non-concentrated sample. Plunge freezing was done by hand and grids were imaged on a FEI Tecnai F30 Helium "Polara" (Jiri Wald).

2.16 Production and enrichment of *Salmonella* minicells overexpressing AcrAB-TolC

Due to physical limitations in electron penetration, whole bacterial cells in the size range of *Salmonella* and *E. coli* are usually too large and too thick to be imaged directly by cryo-electron tomography (cryo-ET).[93,94] In order to overcome this issue, anucleated minicells were constructed by knocking out the *minD* gene, thus inactivating the Min system responsible for septum localization prior to cell division. A *Salmonella* SB905*ΔminD* strain (lab collection) was transformed with the pBAD-ramA plasmid as described in Section 2.3.2 to enable transcriptional activation of the AcrAB and TolC locus by expressing ramA. Minicells were prepared and enriched according to a protocol by Nans et al. (2015)[95]: Overnight cultures of SB905*ΔminD* carrying pBAD-ramA were started in 50 ml LB supplemented with chloramphenicol at 37°C. The next morning, the pre-culture was added to 450 ml LB with chloramphenicol and immediately induced by adding 0.4 % L-arabinose. After 5 hours of growth at 37°C, rod-shaped cells and cellular debris were pelleted by centrifugation at 2000 g for 10 minutes at 4°C. Round minicells were isolated from the supernatant by centrifuging at 15500 g for 10 minutes at 4°C. As much as possible of the supernatant was discarded, the minicell pellet was resuspended with the remaining supernatant, transferred to a 1.5 ml Eppendorf tube and centrifuged again at 15400 g for 10 minutes at 4°C in a benchtop centrifuge (Eppendorf). The pellet was resuspended in 100 µl PBS and 5 µl of a 1:2 dilution was used for preparation of electron microscopy grids.

3 LISTS

3.1 Solutions, Reagents and Buffers

3.1.1 Solutions provided by the IMBA/IMP Media Kitchen

LB-Medium

Bacto Tryptone	10.0 g
Yeast Extract	5.0 g
NaCl	5.0 g
Fill up with Mono Q water to 1 L	

Super Optimal Broth (SOB)-Media

Bacto Tryptone	20.0 g
Yeast Extract	5.0 g
NaCl	8.5 mM

PBS pH 7.5

NaCl	137.0 mM
KCl	2.7 mM
Na_2HPO_4	8.2 mM
KH_2HPO_4	1.5 mM
Adjust pH to 7.5 with 6.4 % HCl	

1 x TE

Tris pH 8.0	10 mM
EDTA	1 mM

0.5 M EDTA pH 8.0 (adjusted with NaOH)

1 M Tris pH 7.5 (adjusted with HCl)

1 M Tris pH 8.0 (adjusted with HCl)

1 M $MgCl_2$

5 M NaCl

3.1.2 Solutions prepared in the lab

Chloramphenicol (CM) [25 mg/ml]

25 mg/ml stock solution in EtOH, commonly used 1:1000

Ampicillin (Amp) [100 mg/ml]

100 mg/ml stock solution in Mono Q, commonly used 1:1000

Tetracycline (Tet) [15 mg/ml]

15 mg/ml stock solution in EtOH, commonly used 1:1000

PBS-T

PBS provided by the Media Kitchen with 0.1 % Tween

Blocking Solution for Immunoblotting

5 % milk in PBS-T

20 % L-arabinose

L-arabinose (Sigma) in Mono Q

SOC-Media

36 ml of 20% glucose per 1000 ml SOB Media

E-Salts

1 L distillated water was heated, the salts added (in following order: 300 g Citric Acid monohydrate ($C_6H_8O_7$ x H_2O), 14.1 g Magnesium sulfate ($MgSO_4$), 1965 g Di-potassium hydrogen phosphate ($K_2H_4PO_4$ x $3H_2O$) and 525 g ammonium sodium hydrogen phosphate ($NaNH_4HPO$ x $4H_2O$)) and filled up to a volume of 3 L with distilled water. All salts were supplied by Sigma-Aldrich.

Gradient gels (4-20 %) for SDS-PAGE

	4 % gel	20 % gel
ddH_2O	30.0 ml	3.0 ml
4 x Resolving Gel buffer (1.5 M Tris-HCl pH 8.8)	12.5 ml	12.5 ml
10 % SDS	0.5 ml	0.5 ml
TEMED Tetramethylethylendiamin (PlusOne)	50 µl	20 µl
Acrylamide (Protogel 37.5:1 Acrylam.:Bis-Acrylam.(EC-890))	6.5 ml	33.5 ml

10 x SDS Running buffer

Glycine	288.4 g
Tris base	60.6 g
SDS	20.0 g
Fill up with Mono Q water to 1 L	

5x Laemmli sample buffer

300 mM Tris-Cl pH 6.8
10% SDS
50% glycerol
100 mM DTT
0.05% bromophenol blue

1 x Protein Transfer Buffer

Glycine	2.9 g
Tris base	5.8 g
SDS	0.37 g
ddH_2O	800 ml
Fill up with Methanol to 1 L	

Buffer 1 (pump isolation)

Sucrose	0.5 M
Tris-HCl (pH 8.0)	0.15 mM

Buffer 2 (pump isolation)

Tris-HCl (pH 8.0)	10 mM
NaCl	0.5 M
EDTA	5 mM
LDAO	0.5 % (v/v)

Buffer 3 (pump isolation)

Tris-HCl (pH 8.0)	10 mM
NaCl	0.5 M
EDTA	5 mM
LDAO	0.1 % (v/v)

3.2 Strains, Plasmids, Primers and Cloning List

3.2.1 Strains and Plasmids

Strains	Relevant characteristics	Resistance	Reference
LT2_pTP233	*Salmonella enterica* subsp. *enterica* serovar *Typhimurium* strain LT2 carrying pTP233 plasmid	Tet	lab collection
SB905 (derived from *Salmonella enterica* subsp. *enterica* serovar *Typhimurium* strain LT2)	wild type	Tet (chromo-somal)	[96](and references therein)
SB905_ramA	carrying pBAD33_ramA	Tet, Cam	this study
SB905_ΔAcrAB	acrAB::FRT	Tet	this study
SB905_ΔAcrAB_ramA	acrAB::FRT; pBAD33_ramA	Tet, Cam	this study
SB905_ΔAcrABΔAcrDΔAcrEF	acrAB::FRT; acrD::FRT; acrEF::FRT	Tet	this study
SB905_ΔAcrABΔAcrDΔAcrEF_ramA	acrAB::FRT; acrD::FRT; acrEF::FRT; pBAD33-ramA	Tet, Cam	this study
SB905_ΔAcrABΔAcrDΔAcrEF_ramA_AcrAB	acrAB::FRT; acrD::FRT; acrEF::FRT; pBAD33-ramA; pQE70-AcrAB (-T5-CAM)	Tet, Cam, Amp	this study
SB905_ΔAcrABΔAcrDΔAcrEF_ramA_MacAB	acrAB::FRT; acrD::FRT; acrEF::FRT; pBAD33-ramA; pQE70-MacAB (-T5-CAM)	Tet, Cam, Amp	this study
SB905_ΔMinD	MinD::FRT	Tet	lab collection
SB905_ΔMinD_ramA	MinD::FRT; pBAD33_ramA	Tet, Cam	this study

Plasmids	Characteristics	Reistance	Origin
pPROEX Htb (+)	N-terminal cleavable His-tag; Tac promotor similar to pQE70	Amp	Invitrogen
pET52b (+)	C-terminal cleavable His-Tag (Thrombin cleavage site); strong T7lac promotor	Amp	Novagen
pBAD33	pBAD arabinose inducible promotor	Cam	[97]
pQE70	Plasmid Qiagen Expression vector; C-terminal His-tag	Amp	Qiagen
pTP2223	λ red recombinase	Tet	Poteete et al., 1984
pDK3	bla FRT-cat-FRT pANTSγ oriR6K	Cam	[88]
pCP20	bla cat cl857 IPR flp pSC101 OriTS	Amp	[98]

3.2.2. Primer List

Primers	Sequence (5'-3')	Use
pPROEX_F	CAATTTCACACAGGAAACAG	Sequencing
pPROEX_R	AGCGGTCTGATAAAACAGAA	Sequencing
pBAD33_F	ATCCATAAGATTAGCGGATCC	Sequencing
pBAD33_R	CTGATTTAATCTGTATCAGGCTG	Sequencing
pQE70_F	GTTCTGAGGTCATTACTGG	Sequencing
pQE70_R	CAGGTGGCACTTTTCGGG	Sequencing
AcrABoperon_seq_1	ATGTCGGTGAATTTACAGGC	Sequencing

AcrABoperon_seq_2	AACCGCACGTATCAACCTGG	Sequencing
AcrABoperon_seq_3	TACCGCGGATAACAAACAGC	Sequencing
AcrABoperon_seq_4	GGTCGACGTGATTAACGCGA	Sequencing
AcrABoperon_seq_5	ATGACGGAAGAAGGCCTTCC	Sequencing
AcrABoperon_seq_6	GGTTGAAGCGATTACCCAGC	Sequencing
AcrABoperon_seq_7	CCTGTATGCTATATCGCTGA	Sequencing
KO_A5_AcrA_F	CCACATCCAGGATGTGTTGT	Sequencing
KO_A6_AcrA_F	AGGATACCGTCACGCAGGT	Sequencing
KO_A5_AcrB_F	GACTGACGGATTGAAAGCGG	Sequencing
KO_A6_AcrB_F	CCTGGCTATTTTCTCCTGTCAG	Sequencing
KO_D5_upstream_AcrD_F	CTCACCACGTTCCGTCT	Sequencing
KO_D6_downstream_AcrD_R	CCGCGCGTATTCAGTA	Sequencing
KO_D2 _AcrD_R	TTTTTTGTGCCCGACACCTCGTATCAGGCTGGCCGGGATCCATA TGAATATCCTCCTTA	AcrD KO
KO_D1_ AcrD_F	AAATCTATAACGATATGTAGAAACACGAGGTTTCCCTTTATGTA GGCTGGAGCTGCTTC	AcrD KO
KO_D4_ AcrD_R	ATGCTTCGTAAATAAATGCC	Sequencing
KO_D3_AcrD_F	GCGCATGATAATTTACATTATCT	Sequencing
KO_E1_AcrE_F	TCCGGTGAATAACGAGCTTTCGGTTTTTTAAGGAACAGTATGT AGGCTGGAGCTGCTTC	AcrEF KO
KO_E2_AcrE_R	ATAGGACGTCTAATAAAAAAGTTTGCCATGTACGGTTACCCAT ATGAATATCCTCCTTA	AcrE KO
KO_F2_AcrEF_R	ACCGTTTAAAAAGGCGTCCGAAGACGCCTCTGTTTACCGGCAT ATGAATATCCTCCTTA	AcrEF KO
KO_EF5 _R	GAGAATGCAGAGGTAAGCG	Sequencing
KO_E4 _R	CAGCCATCATCAGGATAATG	Sequencing
KO_E3 _F	AGGATACCCCACTGCTATTC	Sequencing
MacB_F3	TCACCTGGAATATGGACAG	Sequencing
MacB_F2	CACGATTGATATTCATCCAG	Sequencing
MacB_F1	GTCTACGCCGGCATTGAAC	Sequencing
MacB_3_Seq	TCACCTGGAATATGGACAG	Sequencing
MacA_F_2	CGCACAGGTTTATATTCAACTC	Sequencing
MacA_F_1	CTCCATTGGCGATAACGTT	Sequencing
ST1_R	GGATCGATCCCATGGCG	Cloning
ST1F_ST2R	GCCCCGCTGCCAACTTA	Cloning
ST2_F	CATGGTATATCTCCTTCTTAAAGTTA	Cloning
ST3_F	AGCGAGCTCTGGCGTCG	Cloning
ST3_R	GAAAACCTGTATTTTCAGGGCTCCGCTCATCACCACCATC	Cloning
ST4_F	ACAGGTTTTCAGCGAGCTCTGGCGTCG	Cloning
ST4_R	ATTTTCAGGGCTCCGCTCATCACCACCATC	Cloning
ST_5	AGCGAGCTCTGCGGCC	Cloning
ST_6_pQE70_R	ACAGGTTTTCAGCGAGCTCTGCGGCC	Cloning
ST_7_pQE70_F	CGGCAACCGAGCGTTCTGA	Sequencing
ST_8	TGAGCGGATAACAATTATA	Sequencing
ST_11.S	TATATCATGAAACAGATGGTACTGGC	Cloning
ST_12.S	TATAGAGCTCCTGAAGAGTATAGGTGGT	Cloning
ST_13.S	TATAGGATCCAAACAGATGGTACTGG	Cloning
ST_14.S	TATACTGCAGTTACTGAAGAGTATAGGTGG	Cloning

3.2.2 Cloning List

Primer	Sequence	Sequence Features	Vector Backbone	Backbone Features	Resulting Plasmid	Cloning strategy
ST_5_F	AGCGAGCTCTGCGGCC		pET52b(+)	IPTG-inducible, C-terminal His-Tag	pET52b(+) (TEV)	Site directed mutagenesis
ST_3_R	GAAAACCTGTATTTTCAGGG CTCCGCTCATCACCACCATC	TEV site				
ST_2_F	GCCCCGCTGCCAACTTA		pET52b(+)	IPTG-inducible, C-terminal His-Tag, TEV cleavage site	pET52b(+)-MacAΔN	Site directed mutagenesis
ST_2_R	CATGGTATATCTCCTT CTTAAAGTTA	new MacA N-terminus				
ST_3_F	AGCGAGCTCTGGCGTCG		pET52b(+)-MacAΔN	IPTG-inducible, C-terminal His-Tag, Thrombin cleavage site	pET52b(+) (TEV)-MacAΔN	Site directed mutagenesis
ST_3_R	GAAAACCTGTATTTTCAGGG CTCCGCTCATCACCACCATC	TEV site				
ST_11	TATATCATGAAACAG ATGGTACTGGC	PagI site	pET52b(+) (TEV)	IPTG-inducible, C-terminal His-Tag, TEV cleavage site	pET52b(+) (TEV)-MacB(PCD)	Conventional
ST_12	TATAGAGCTCCTGA AGAGTATAGGTGGT	SacI site				
ST_13	TATAGGATCCAAACA GATGGTACTGG	BamHI site	pProEx-Htb	IPTG-inducible, N-terminal His-Tag	pProEx-Htb-MacB(PCD)	Conventional
ST_14	TATACTGCAGTTACTGA AGAGTATAGGTGG	PstI site, Stop codon				

4 RESULTS

4.1 MacAB-TolC efflux pump is strongly conserved in *Salmonella enterica* and other Gram-negative bacteria

The genes for the efflux pump proteins MacA, MacB and TolC that were originally studied in *E. coli* have also been annotated in the genome of *Salmonella enterica* (NCBI reference genome *Salmonella enterica subsp. enterica serovar Typhimurium* str. LT2). To determine the similarity between the proteins in these two Gram-negative bacteria, nucleotide identity and amino acid identity were checked by nucleotide BLAST and protein BLAST, respectively (Table 4.1). For this purpose, the megablast option of the NCBI Basic Local Alignment Search Tool (BLAST; https://blast.ncbi.nlm.nih.gov) was used; except for *macA* gene which gave a significant result only in the discontiguous megablast option, omitting the less conserved N-terminus (nucleotides 1-76).

On genomic as well as on protein level, both *macA*/MacA and *macB*/MacB from *S. enterica* are highly similar to their homologs in *E. coli*, displaying an nucleotide identity of 77 % / 76 % and an amino acid identity of 83 %. The outer membrane channel *tolC*/TolC is even stronger conserved with a nucleotide identity of 83 % and an amino acid identity of 90 %.

Nucleotide Blast (Percentage Nucleotide Identity)

		Salmonella LT2				
		acrA	***acrB***	***macA***	***macB***	***tolC***
E.coli K12 (MG1655)	***acrA***	84	-	-	-	-
	acrB	-	86	-	-	-
	macA	-	-	77*	-	-
	macB	-	-	-	76	
	tolC	-	-	-	-	83

*without N-terminus (nt 1-76)

Protein Blast (Percentage Amino Acid Identity)

		Salmonella LT2				
		AcrA	**AcrB**	**MacA**	**MacB**	**TolC**
E.coli K12 (MG1655)	**AcrA**	92	-	-	-	-
	AcrB	-	95	-	-	-
	MacA	-	-	83	-	-
	MacB	-	-	-	83	-
	TolC	-	-	-	-	90

The efflux pump genes/proteins *acrA*/AcrA and *acrB*/AcrB are also strongly conserved between *E. coli* and *S. enterica.* Their nucleotide and amino acid identities have been determined previously (Master thesis of Tobias Thoeni), but have been confirmed and included in the table for completeness.

Table 4.1

Computed percentages of nucleotide and amino acid identities of pump efflux genes and corresponding proteins in *S. enterica* strain LT2 and *E. coli* strain K12.

The structure of the periplasmic adaptor protein (PAP) MacA has been solved for *E. coli* and *Actinobacillus actinomycetemcomitans*, but not for *S. enterica*. Given the high degree of sequence conservation, it could be expected that this similarity in sequence is mirrored by a similarity in the secondary structure of the folded protein. To confirm this, a three-dimensional structure prediction of *S. enterica* MacA was carried out using the web-server i-Tasser (http://zhanglab.ccmb.med.umich.edu/I-TASSER/)[99,100]. The best model with a C-score of -0.83 is depicted in figure 4.1 and compared to three PAPs with known structure: MexA from an RND efflux pump of *Pseudomonas aeruginosa*[21], ZneB from the heavy metal efflux pump of *Cupriavidus metallidurans*[71] as well as MacA from *A. actinomycetemcomitans*[70]. Four linearly arranged domains similar to those in the related adaptor proteins were found and visualized in the predicted *S. enterica* MacA structure. The most prominent feature is the alpha-hairpin domain depicted in blue, likely responsible for interaction with the exit channel protein TolC. The ensuing three domains (the lipoyl domain in green, the β-barrel domain in yellow and the membrane proximal domain in orange) are representatively termed AcrB-docking[18], as this is where the respective inner membrane transporters will bind. The membrane proximal domain has only been structurally resolved for MexA and ZneB, but can be predicted also for *Salmonella* MacA. Presumably, the attachment to the inner membrane happens via an N-terminal transmembrane helix, although structural information is still missing.

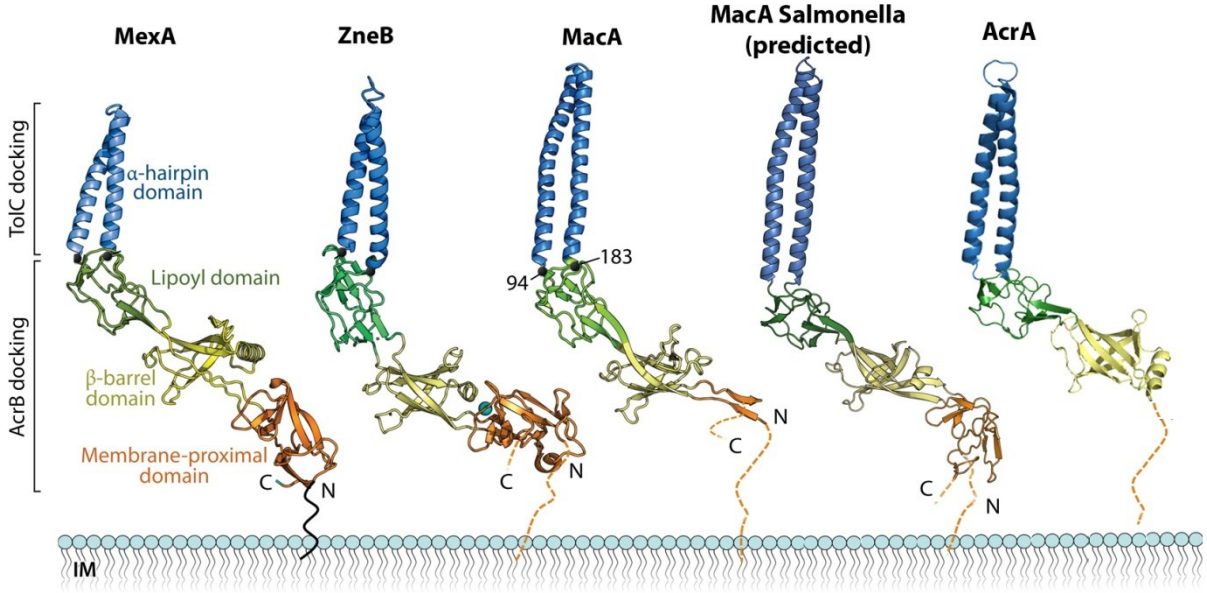

Figure 4.1: Structure comparison of different periplasmic adaptor proteins (PAPs)

Side-by-side comparison of the solved structures of MexA (*Pseudomonas aeruginosa*), ZneB (*Cupriavidus metallidurans*[71]), MacA (*A. Actinomycetemcomitans)*, and AcrA (*E. coli*)[19] as well as the predicted structure of *Salmonella* MacA. Conserved domains are labelled and coloured uniformly (blue: alpha-hairpin domain, green: lipoyl domain, yellow: β-barrel domain, orange: membrane-proximal domain). Dashed lines indicate parts of the structures that have not been solved. Structure prediction was performed using the webserver i-Tasser and PyMol was used for further processing of the model. Image adapted from review [18].

4.2 Generation of a *Salmonella* strain lacking the *acrAB* operon and its homolog pump proteins AcrD and AcrEF results in growth retardation

The efflux system that contributes most to virulence and drug resistance in *Salmonella* typhimurium is AcrAB-TolC[25,85,101]. In order to study this pump via plasmid-derived complementation, a *Salmonella* LT2 *acrAB*-knockout strain was generated in the lab previously (data not shown here, see Master thesis of Tobias Thoeni). However, there exist two paralogs in *Salmonella* whose role is at least partly redundant to AcrAB, namely AcrD and AcrEF. While AcrD is similar in sequence to AcrB and has been suggested to only exert its function in combination with AcrA[52], the *acrEF* operon encodes both the periplasmic adaptor protein AcrE and the inner membrane pump AcrF and has been found to be selectively activated by spontaneous promoter mutations upon AcrB knockout[54]. While expression of acrEF and acrD is more than 6-fold lower than that of acrAB in laboratory conditions in wild-type[86], selective AcrB knockout has been shown to result in elevated levels of AcrEF[54] and might have an effect on AcrD expression as well[52]. Therefore, to individually study AcrAB-TolC and MacAB-TolC without a background of other highly expressed tripartite efflux pumps, a *Salmonella* strain lacking *acrAB*, *acrD* and *acrEF* is needed. This triple efflux pump knockout strain (in the following simply called triple knockout strain) was generated in *Salmonella enterica* strain LT2_pTP233 using the method developed by Datsenko and Wanner[88] and transferred into strain SB905, a less infectious *Salmonella* strain (for strain information, see section 3.2.1), by phage transduction.

As the *acrE* gene is separated from *acrF* by only 11 nucleotides, the entire operon was deleted from the first *acrE* codon to the last *acrF* codon. *AcrD* is not part of a larger operon and was deleted entirely from the first to the last codon. The gene deletions were verified by sequencing of the respective genomic regions. Furthermore, the successful abolition of AcrE could be confirmed additionally by analyzing the strain by Western Bloting using the slightly unspecific antibody raised against AcrA for detection, which cross-reacts with AcrE as determined earlier (Figure 4.2). Whole cell lysate of *Salmonella* strain SB905 and three derivative strains were compared: the isogenic wild type strain (SB905; termed *wt*), the SB905 carrying an arabinose inducible plasmid expressing the transcriptional activator *ramA* (*SB905_ramA*), the *acrAB* knockout strain (*SB905ΔAB_ramA*) and the *acrAB/acrD/acrEF* triple knockout strain (*SB905ΔABΔDΔEF_ramA*), both with the same arabinose inducible plasmid expressing *ramA*.

Clearly, the AcrA antibody gives a strong signal in the wild type, especially upon *ramA* overexpression, and a weaker signal in the *acrAB* knockout strains. However, this signal is completely missing when the genes for the homolog RND-pumps are also deleted in the *acrAB/acrD/acrEF* triple knockout strain. TolC can be detected in all strains, but is a lot more abundant upon *ramA*-

overexpression, nicely showing the importance of this activator not only for the AcrAB-TolC pump but for all efflux pumps relying on TolC as their outer membrane component. Unfortunately, there is no commercial antibody available for AcrB.

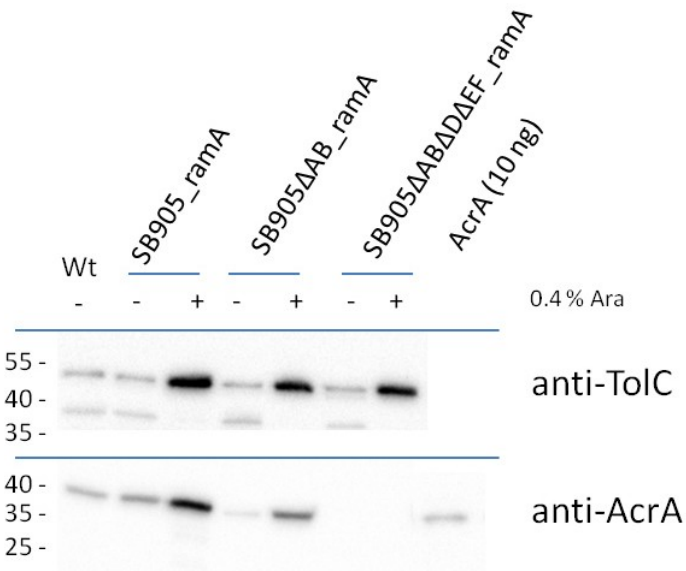

Figure 4.2: TolC and AcrA expression levels

Western Blot analysis of whole cell extracts of Salmonella SB905 strain and three derivatives. Cell extracts from wild type (left), *SB905_ramA* (minus/plus *ramA* induction by Arabinose), *SB905ΔAB_ramA* (minus/plus *ramA* induction by Arabinose), and *acrAB/acrD/acrEF* triple KO *SB905ΔABΔDΔEF_ramA* (minus/plus *ramA* induction by Arabinose; right). The loaded amounts of extracts have been normalized to OD_{600} measurements, each lane containing 0.02 OD units, and 10 ng of purified AcrA have been loaded for comparison The suffix *_ramA* indicates the presence of an arabinose-inducible plasmid expressing the transcriptional activator RamA.. The upper and the lower blot have been incubated with a polyclonal TolC antibody and a polyclonal AcrA antibody, respectively (both raised in rabbit). For clarity, only partial blots are shown; the full blots are depicted in the supplementary material (section 8.8).

The generated triple knockout strain was analyzed for its growth behavior by performing growth curve analysis. Growth curves were recorded for the SB905 wild type (*SB905_ramA), acrAB* single efflux pump knockout (*SB905ΔAB_ramA*) and *acrAB/acrD/acrEF* triple knockout (*SB905ΔABΔDΔEF_ramA)* strains, each with and without induction of plasmid-encoded *ramA* (Figure 4.3). Both knockout strains are showing a combined outgrowth and exponential growth retardation compared to the wild type strain, with the triple knockout growing even slower than the single efflux pump knockout; thus indicating a considerable fitness cost of the efflux pump deletions in growth media with antibiotics. This is not unexpected, given that is has been previously reported that *Salmonella* strains lacking the major efflux pump AcrAB are more susceptible to a range of antibiotics, including the antibiotic chloramphenicol used for plasmid maintenance in this

experiment[85,101]. In contrast, slight deviation in growth between *ramA*-induced and uninduced strains is not consistent and does not allow for conclusions in this analysis.

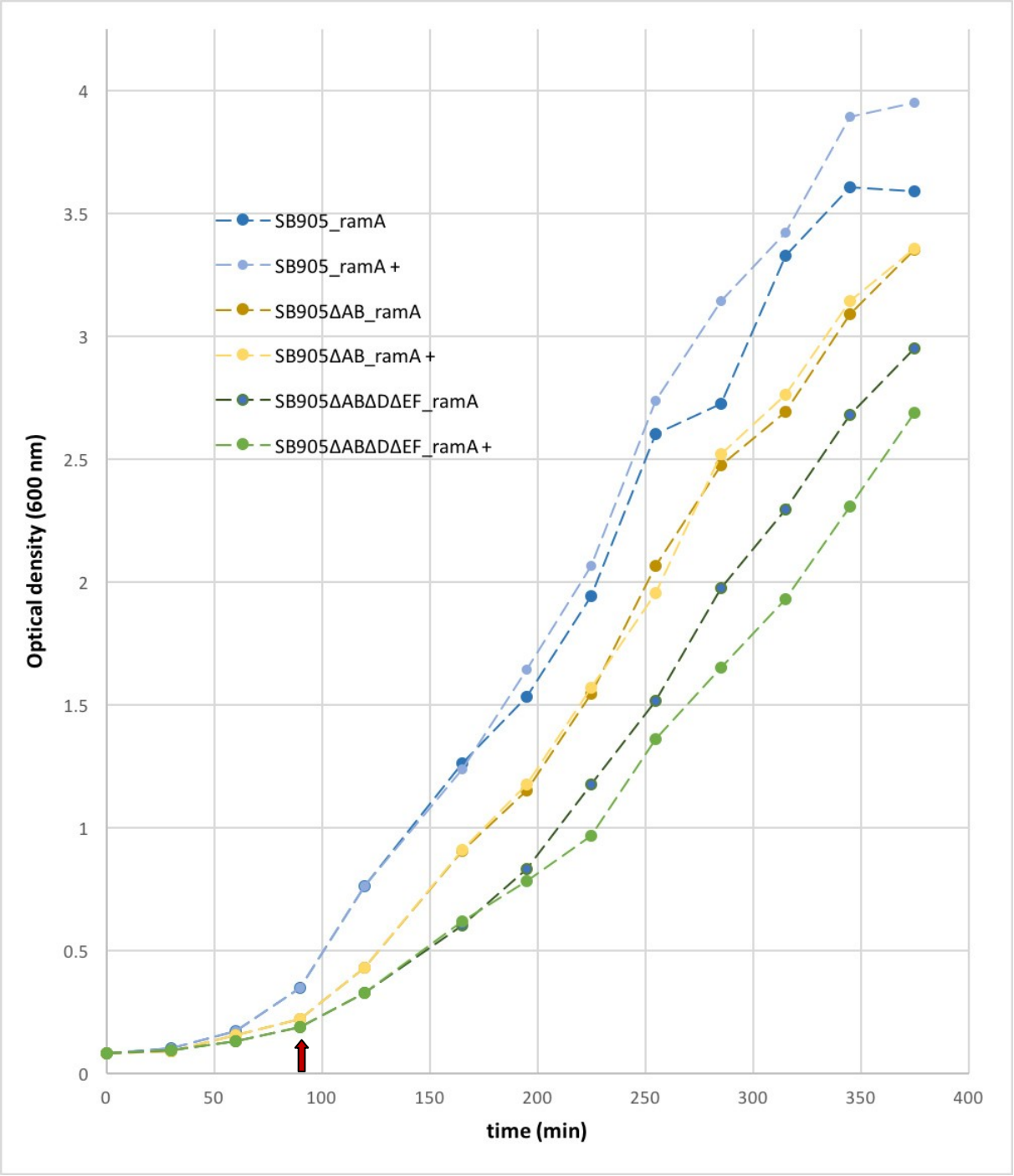

Figure 4.3: Growth comparison of wild type and deletion strains

Growth curves are shown for Salmonella SB905 wild type (blue), *acrAB* knockout (yellow) and *acrAB/acrD/acrEF* knockout strains (green) harboring the arabinose-inducible pBAD-ramA plasmid. The darker colored curve of each pair indicates the non-induced strain and the red arrow points to the time of induction for the induced strains. The deletion strains exhibit a slower growth rate than the wild type strain, with the triple knockout growing even slower than the single knockout.

4.3 The *acrAB* and the *macAB* operon can be overexpressed from a plasmid in the triple efflux pump knockout

It has been demonstrated previously that plasmid-based complementation of an *acrAB* deletion strain results in at least partially restored efflux pump activity in *E. coli*[44] and *S. enterica* (Master thesis of Tobias Thoeni). To be able to study the AcrAB-TolC efflux pump in a clean background, *acrAB* was expressed from a plasmid in the triple knockout strain lacking not only the *acrAB* operon but also its homologs *acrD* and *acrEF.* For overexpression, the high copy number plasmid pQE70 was chosen in order to maximally increase the amount of assembled pumps for future purification and structural studies.

A plasmid (AcrAB-PQE70) containing the acrAB operon together with 250 nt of its upstream sequence, including the ramA binding site, in an adapted pQE70 backbone was available in the laboratory and was used for this purpose (see supplementary material, section 8.5). In this construct, a 6 x C-terminal His-Tag is added to AcrB, making it possible to detect it in whole cell extracts follow its presence during efflux pump purification. The plasmid (AcrAB-PQE70) was transformed into the *Salmonella* SB905 *acrAB/acrD/acrEF* triple knockout strain together with a second plasmid encoding the transcriptional activator *ramA* under control of an arabinose-inducible promoter. A comparison of normalized whole cell extracts of the wild type strains and the non-complemented triple knockout strain to the final *acrAB* complemented strain (*SB905ΔABΔDΔEF_ramA_AcrAB*) is illustrated in figure 4.5. Unfortunately, the promoter exhibits distinct leakiness, resulting in strong expression of *acrA* and *acrB* already prior to induction and only a small increase in protein levels after induction. However, the level of AcrA as detected by the polyclonal antibody available in the lab collection is considerably higher in the complemented than in the wild type strain. Recombinant plasmid-expressed AcrB is visualized using a commercial anti-His antibody.

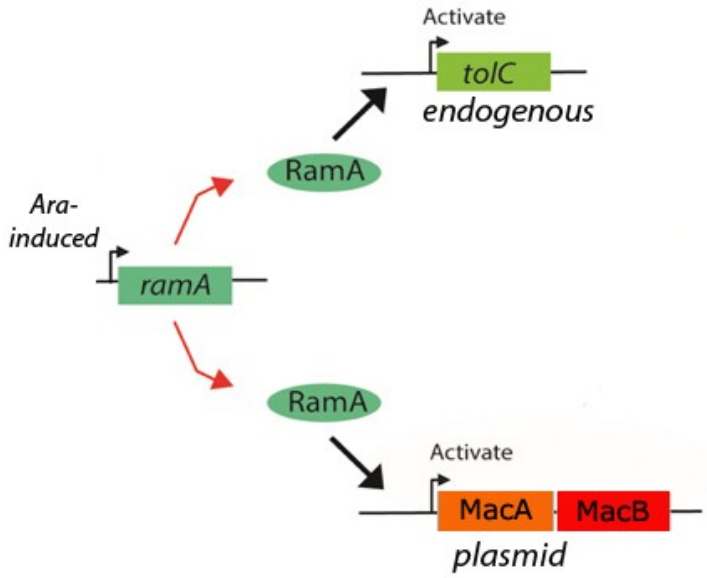

Figure 4.4: Schematic of MacAB-TolC expression strategy

The transcriptional activator RamA is overexpressed from an arabinose-inducible plasmid. It binds to its natural binding site upstream of *tolC* and activates expression of the outer membrane channel gene. Additionally, it binds the RamA binding site introduced upstream of the plasmid-encoded *macAB* operon, inducing also the expression of MacAB proteins.

For overexpression of the ABC-type efflux pump MacAB-TolC, the chromosomal macAB operon was not knocked out as it has already been shown to exhibit significantly lower expression levels in wild type *Salmonella*[86] (see Section 1.5), and knockouts additional to the AcrAB/AcrD/AcrEF triple efflux pump knockout proved to be difficult to achieve. However, to be able to exclude confusion of MacAB-TolC with the much more abundant AcrAB-TolC or its homologs in electron microscopy studies, *macAB* was overexpressed in the above described *acrAB/acrD/acrEF* triple knockout. For this purpose, the pQE70 plasmid mentioned above was used with the difference of exchanging the *acrAB* for the *macAB* operon, thereby keeping the 250 nt upstream region of the *acrAB* gene and retaining the same ramA activation strategy also for the *macAB* plasmid (Figure 4.4). Overproduced recombinant MacB was detected on a Western Blot via its C-terminal 6 x histidine tag (Figure 4.5) and TolC detection was included as a control. MacA was assumed to be overexpressed together with MacB; however, to confirm this, a MacA antibody was generated in a later step.

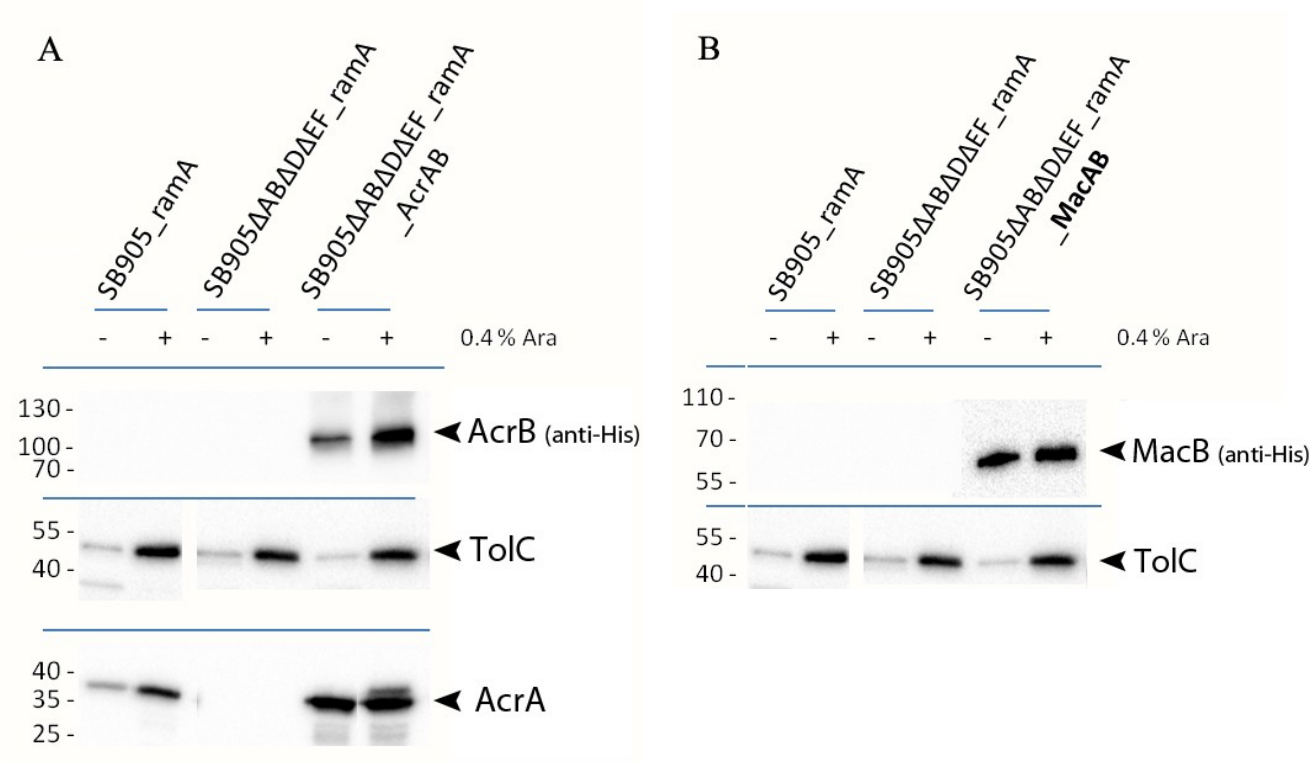

Figure 4.5: Plasmid overexpression of acrAB and macAB in the *Salmonella* triple knockout strain

Western Blot analysis of protein expression in whole cell extracts of Salmonella SB905 carrying the ramA plasmid (SB905_ramA), SB905 triple knockout carrying the ramA-plasmid (SB905ΔABΔDΔEF_ramA) and SB905 triple knockout carrying both ramA- and pump-operon encoding plasmids (SB905ΔABΔDΔEF_ramA_ArAB respectively SB905ΔABΔDΔEF_ramA_MacAB); all minus/plus *ramA* induction by Arabinose . The extracts have been normalized to OD_{600}, each lane containing 0.02 OD units. In (A), the three components of the AcrAB-TolC efflux pump were detected by anti-AcrA, anti-TolC and anti-His antibody for AcrB. TolC levels are significantly higher upon *ramA* induction with arabinose, and both AcrA and AcrB can be readily detected in the complemented strain. For MacAB-TolC (B), two of the components (TolC and his-tagged MacB) can be detected with the available antibodies. However, the anti-His antibody reveals a band at the right size only in the *macAB* expressing strain, indicating that overexpression has indeed been successful.

4.4 Overexpression of the AcrAB-TolC and MacAB-TolC efflux pumps leads to higher resistance to a macrolide antibiotic

In order to assess the functionality of the plasmid-expressed efflux pump proteins AcrAB and MacAB, the resistance of a wild type SB905 strain, the above described *acrAB/acrD/acrEF* triple knockout strain and the knockout strain complemented with plasmid-expressed *acrAB* or *macAB* to the macrolide antibiotic erythromycin was tested. The degree of resistance to antimicrobial substances is usually quantified by determining their minimum inhibitory concentration (MIC), defined as the lowest concentration of a compound that still inhibits visible bacterial growth[90].

It has been reported previously that deletion of *acrB* results in 25-fold lower resistance to a range of compounds, including erythromycin, in *E. coli* and *S. enterica*[85,101]. In these studies, the wild type phenotype was shown to be fully reconstituted by plasmid-based expression of the *acrAB* operon, and overexpression of *macAB* resulted in a two-fold higher resistance compared to the deletion phenotype.

To determine whether this was similar in our strains, lacking more RND efflux pump genes and expressing the efflux pump operons from different plasmids, the MIC of erythromycin for the four strain variants was measured via a standard agar dilution method[90]. The results of the test are listed in table 4.2 and some exemplary agar plate images used for evaluation are shown in figure 4.6. For SB905 wild type strain, a MIC of 128 µg/ml has been determined while the *acrAB/acrD/acrEF* triple knockout had a considerably lower MIC of 4 µg/ml, consistent with the theory that a lack of drug efflux pumps results in higher sensitivity to antimicrobial substances, and in good agreement with data from the literature[85,101]. When complementing the knockout strain with *acrAB* operon on a high-copy plasmid, the MIC did not only go back to, but in fact exceeded wild type levels. This result could be explained by the high copy number of the plasmid, resulting in an AcrAB protein level much higher than in the wild type strain. When *macAB* was overexpressed from the same plasmid, it raised the MIC up to 8 µg/ml, which is two-fold the MIC of the triple knockout. This indicates that MacAB-TolC is indeed assembled and functional when overexpressed, although contributing much less to antibiotic resistance than the major player AcrAB-TolC.

Minimal Inhibitory Concentration for Erythromycin

	strain name	MIC [ug/ml]
A	SB905 wt	128
B	SB905ΔABΔDΔEF	4
C	SB905ΔABΔDΔEF + pBAD-ramA + pQE70-**AcrAB**	256
D	SB905ΔABΔDΔEF + pBAD-ramA + pQE70-**MacAB**	8

Table 4.2: Minimal inhibitory concentrations of erythromycin for the four tested strains, as determined by the standard agar dilution method.

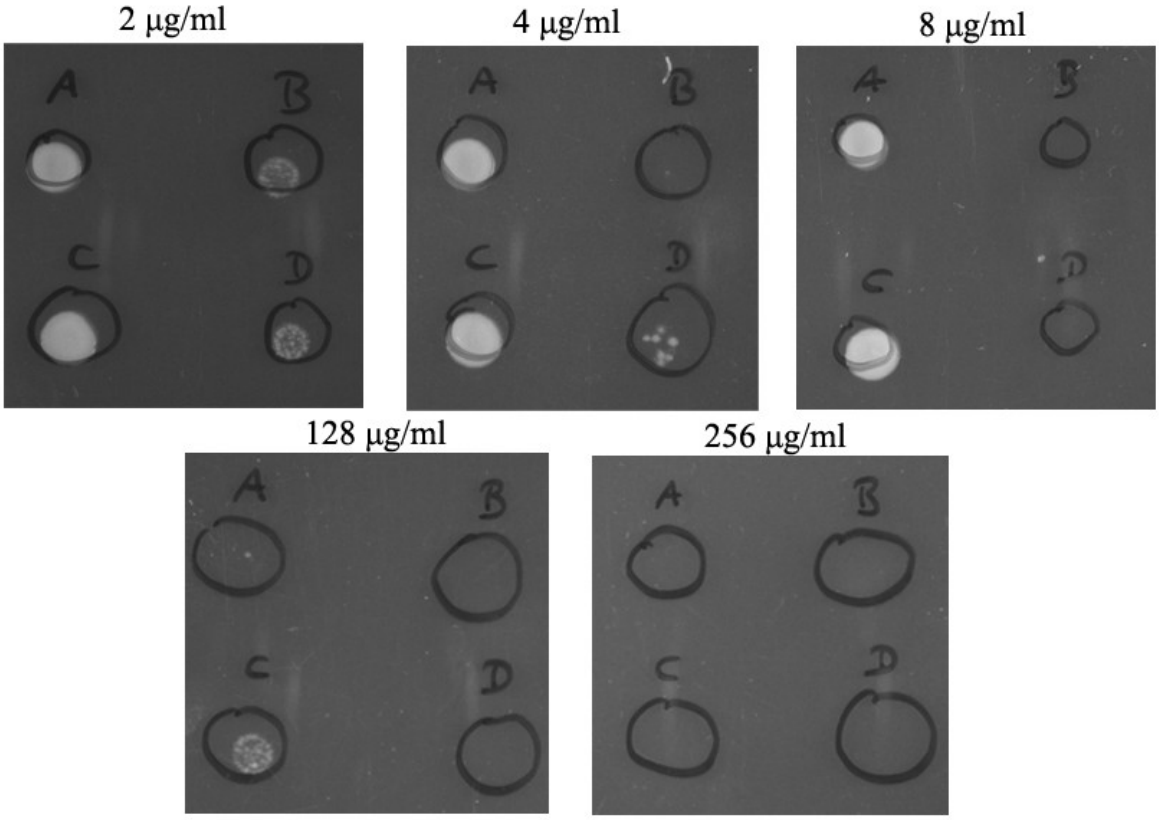

Figure 4.6.: Selected plate images from the agar dilution MIC test

Above each image, the erythromycin concentration of the respective agar plate is given. Encircled are the spots where bacterial cells have been applied, the letters A-B denote the four strain variants as given in h The agar plates were inspected 24 hours after application of the bacterial suspension. Bright spots are bacterial colonies. All images were taken using a Molecular Imager® System (BioRad).

4.5 Purification and Dimerization of N-truncated MacA for antibody production

E. coli MacA is a membrane fusion protein whose protein core is located in the periplasm. However, it contains a signal-like sequence composed of 40 amino acids at its N-terminus which is rich in hydrophobic residues in its C-terminal half and is therefore predicted to be a transmembrane (TM) region[55] that anchors the protein to the inner membrane. In contrast to the full-length protein, a MacA construct lacking the N-terminal TM sequence (MacAΔN) does not stimulate ATPase activity of MacB nor provide an increase in resistance to erythromycin in *E. coli*. However, MacAΔN retains its ability to interact with MacB and the core structure of MacA was shown to be unaffected by the deletion[67]. Both published crystal structures of MacA, one from *E. coli* and one from *A. actinomycetemcomitans,* were obtained from the soluble N-truncated protein lacking the transmembrane sequence[69,70].

In order to generate a polyclonal antibody against *Salmonella* MacA in a rabbit, pure and highly concentrated protein is needed for injection. *Salmonella* MacA shows strong homology to *E. coli* MacA, and although the N-terminus is less conserved (43 % amino acid identity compared to 83 % for the full length protein), basic properties like charge and hydrophobicity are largely identical. Furthermore, transmembrane helix prediction programmes (e.g. TMHMM) predict a TM helix for *Salmonella* MacA from residue 13 to 30 with the N- and C-terminal part in the cytoplasm and periplasm, respectively (figure 4.7).

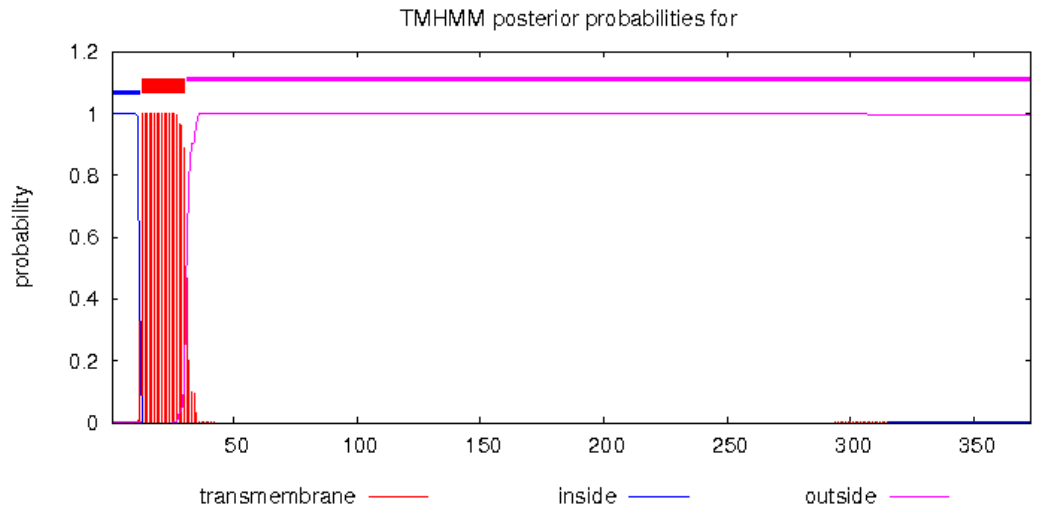

Figure 4.7: The TMHMM webserver predicts a transmembrane helix for residues 13-30 of Salmonella MacA.

Following the same approach as used for the *E. coli* MacAΔN purification, we constructed a plasmid expressing MacAΔ2-31 from *Salmonella enterica* strain *LT2* upon induction. After overexpression in *E. coli*, a 10x C-terminal histidine tag was used to purify the soluble protein on a Ni^{2+} chelation chromatography column (figure 4.8).

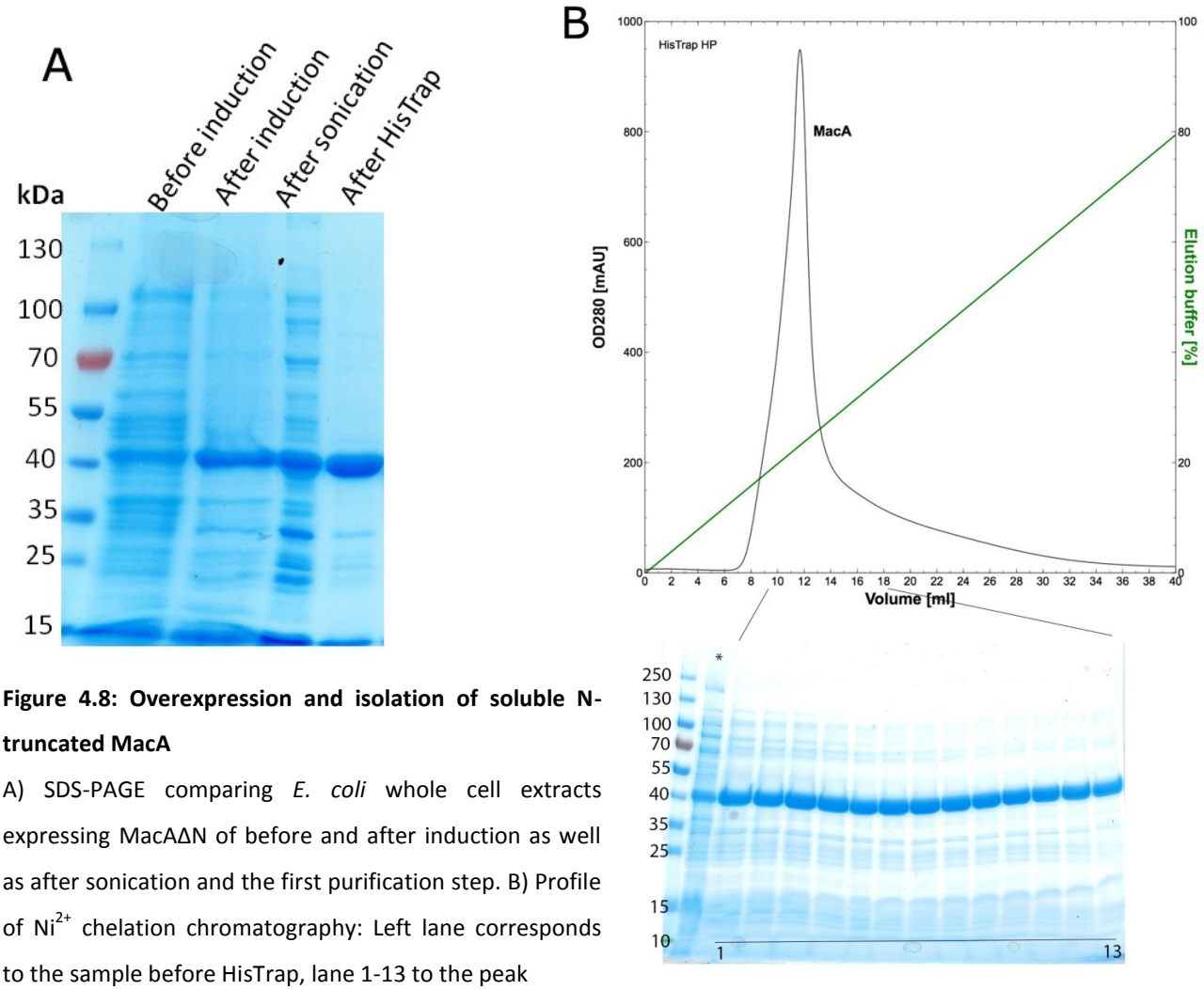

Figure 4.8: Overexpression and isolation of soluble N-truncated MacA

A) SDS-PAGE comparing *E. coli* whole cell extracts expressing MacAΔN of before and after induction as well as after sonication and the first purification step. B) Profile of Ni^{2+} chelation chromatography: Left lane corresponds to the sample before HisTrap, lane 1-13 to the peak fractions.

The histidine tag was cleaved off by TEV protease in an overnight dialysis step and the cleaved protein was separated from uncleaved protein and the TEV protease using an inverse HisTrap step. The purity of the sample was further increased by applying it to a size exclusion chromatography column (figure 4.9). Whilst monomeric MacAΔN has a theoretical molecular mass of 37.5 kDa, our purified MacAΔN elutes at around 71 kDa as calculated from a run of protein standards in the same buffer (standard run and calibration curve: see supplementary materials, section 8.2).This gives a strong indication for a dimeric arrangement of the protein in solution.

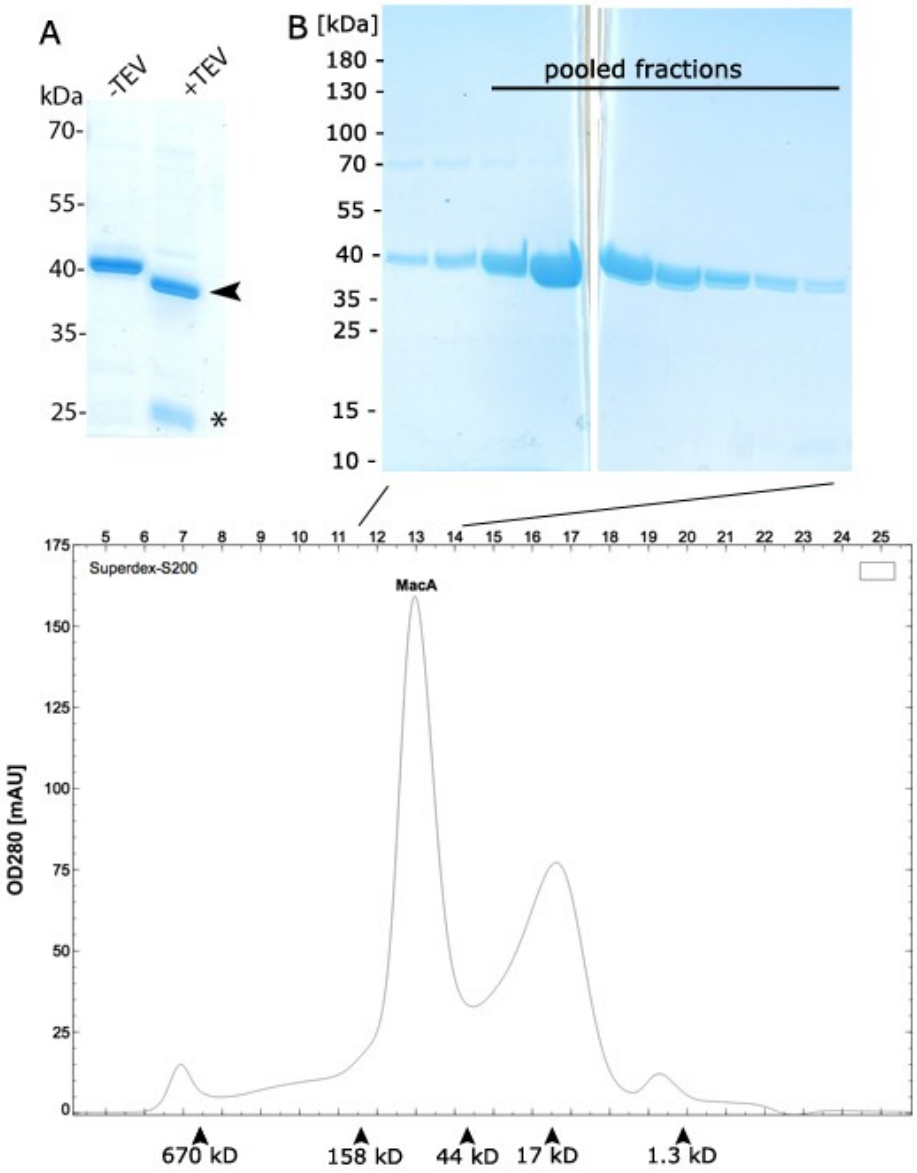

Figure 4.9: TEV cleavage and gel-filtration

A) SDS-PAGE showing the sample before and after cleavage with TEV protease. The arrow indicates cleaved MacAΔN; the star indicates the TEV protease. B) Size exclusion chromatography profile and corresponding SDS-PAGE gel showing peak fractions. Protein sizes from the standard run are indicated with arrows below.

For antibody generation, a rabbit was injected twice with the purified protein, and the blood serum was tested for suitability for MacA detection. An antibody dilution of 1:5000 was found to be sufficient to detect 1 ng of purified MacAΔN and also readily detected full-length MacA protein from a cell lysate of *Salmonella s*train SB905 overexpressing the MacAB operon from a plasmid (see supplementary material, section 8.3).

4.6 Expression of the periplasmic core domain of MacB and purification trials

MacB is an integral inner membrane protein and as such it has large hydrophobic patches and is challenging to purify in large amounts. It comprises, however, a relatively large periplasmic core domain (PCD), which has shown to be soluble in *E. coli* when expressed on its own and could be structurally solved[63]. In order to generate a polyclonal antibody against *Salmonella* MacB which would be beneficial in further experiments, the purification of one accessible domain of the protein is sufficient. Hence, the location of the PCD of *Salmonella* MacB was derived by sequence homology to *E. coli* and confirmed by structural feature predictions using the web tool PredictProtein[102]. MacB residues 297 to 522, which were predicted to build up the PCD in *Salmonella enterica* strain *LT2*, were cloned in two different vector backbones: the pProEx-backbone with an N-terminal 6x histidine tag and the pET52b-backbone with a C-terminal 10x histidine tag. MacB-PCD was overexpressed in E.coli from both plasmids independently, but was found to be insoluble after cell lysis by sonication; this is possibly due to its enclosure into inclusion bodies. Only when 8 M urea was added to the buffer, the protein was soluble after lysis (Figure 4.10) and could be applied to a Ni^{2+} chelation chromatography column (HisTrap) for a first purification step (Figure 4.11). After elution with imidazole, the peak fractions were pooled and dialyzed stepwise against buffers with lower urea concentration in order to allow stepwise refolding of the protein. Despite trying several temperature conditions and additives, it was however not possible to reach a urea concentration lower than 2 M without visible precipitation of the protein. As a solution containing 2M Urea is not suitable for injection into rabbit in order to raise antibodies, the MacB-PCD purification was halted for the moment.

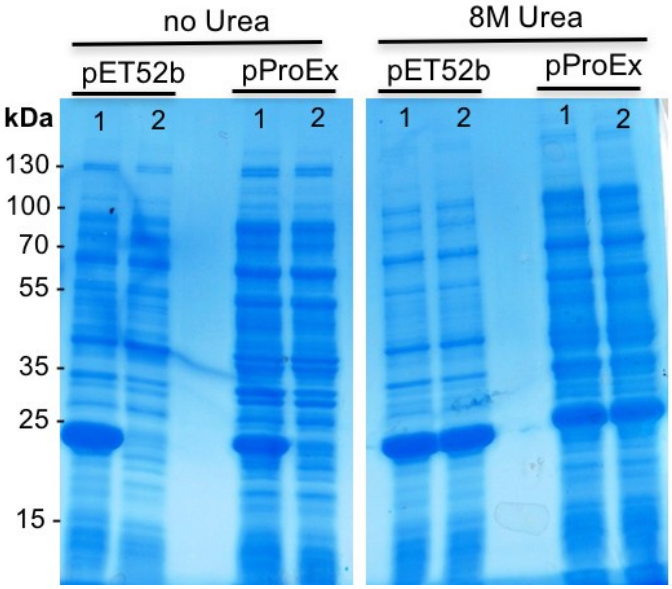

Figure 4.10: Overexpression of the MacB-PCD from two different plasmids

SDS-PAGE showing normalized whole cell extracts from E. coli strains overexpressing the periplasmic core domain of Salmonella MacB from the plasmid pET52b or pProEx. For every pair of lanes, (1) denotes cell lysates before centrifugation and (2) the same lysate after pelleting of insoluble material. Only when 8 M urea is present in the buffer, MacB-PCD remains soluble and can be further processed.

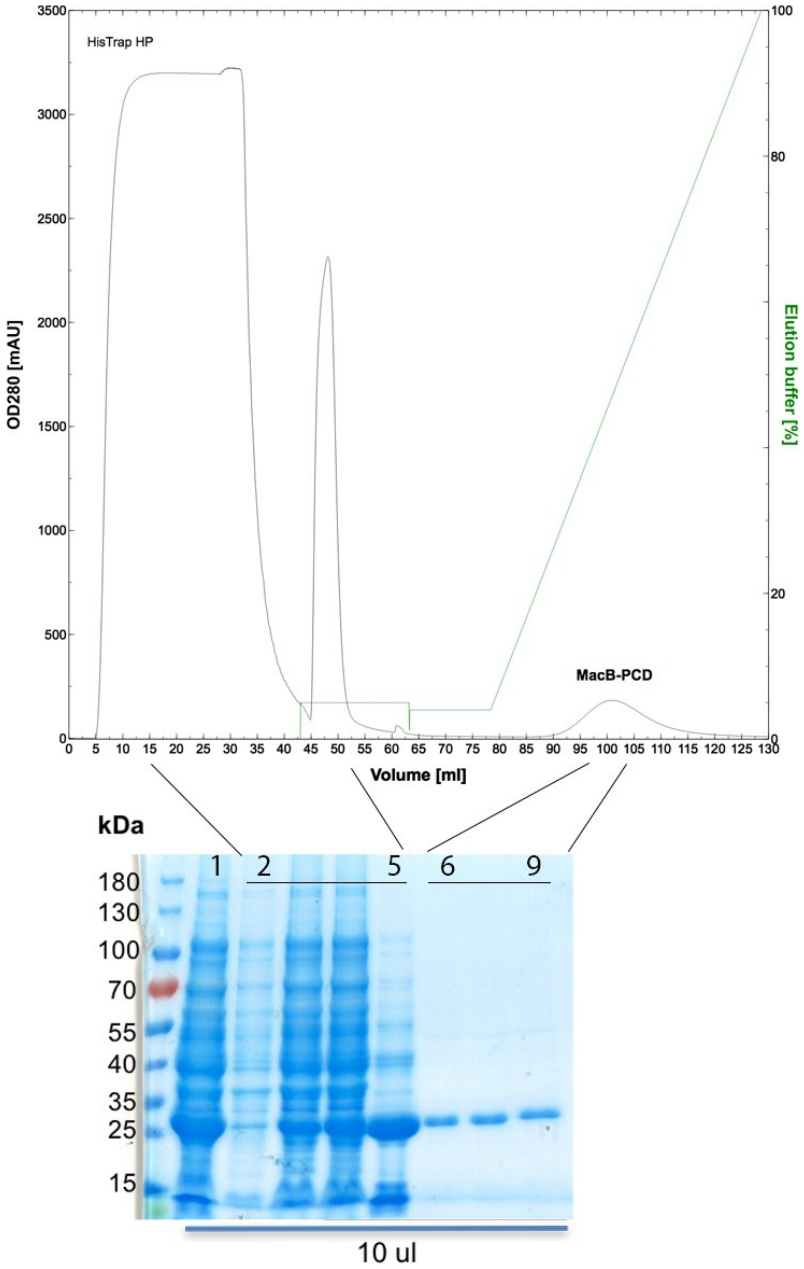

Figure 4.11: Purification of MacB-PCD via a Ni^{2+} chelation chromatography column

Profile of an exemplary Ni2+ chelation chromatography and corresponding SDS-PAGE analysis. Lane 1 denotes the sample before application, lane 2-4 is the flowthrough and lane 5 is the wash fraction, clearly showing that a large part of the protein did not stably bind to the column. However, the peak fractions in lane 6-9 still contain enough protein for our purposes. 10 µl of the sample were applied in each lane.

4.7 Isolation of the near-native AcrAB-TolC efflux pump and visualization in EM

Previous to the first purification efforts in our lab, it had not been possible to isolate a whole native AcrAB-TolC efflux pump from any organism. Instead, different combinations of fusion proteins were used to reconstitute the AcrAB-TolC pump *in vitro* and perform first structural studies[44,45]. However, such cross-linked fusion proteins only allowed restricted insight into the assembly mode and structure of the native pump.

Using a protocol established in our lab, it was possible for the first time to isolate *in vivo* assembled AcrAB-TolC efflux pumps from wild type *S. enterica* strain SB905 (Master thesis of Tobias Thoeni). In my study, I first reproduced the isolation of AcrAB-TolC in the wild type SB905 strain, using an improved protocol for isolation of bacterial membrane fractions overexpressing AcrAB-TolC that included a final size exclusion chromatography (SEC) step (Figure 4.12).The amount of expressed AcrAB-TolC efflux pumps in the *Salmonella* strain used for isolation could be significantly increased by overexpressing the transcriptional activator *ramA*. AcrAB-TolC was shown to elute earlier from the SEC column than the largest standard protein available (670 kDa), consistent with the estimated molecular weight of the assembled pump of around 750 kDa. The peak fractions were concentrated and analyzed on SDS-PAGE (Figure 4.12), giving rise to three bands corresponding to the three pump components AcrA (at around 40 kDa), TolC (under 55 kDa) and AcrB (above 110 kDa). The height of the bands was identical to previous samples where the identity of the components had been verified by mass spectrometry (see Master thesis of Tobias Thoeni), therefore no further mass spectrometry analysis was carried out.

To check the assembly status of the efflux pump, the pooled sample from the peak fraction was negatively stained with 2 % PTA and analyzed by electron microscopy at 71000x magnification (Figure 4.14). Long shaped particles were detected with a length of approximately 320 Å, similar in size and shape to the ones visualized in the fusion protein studies[44,45].

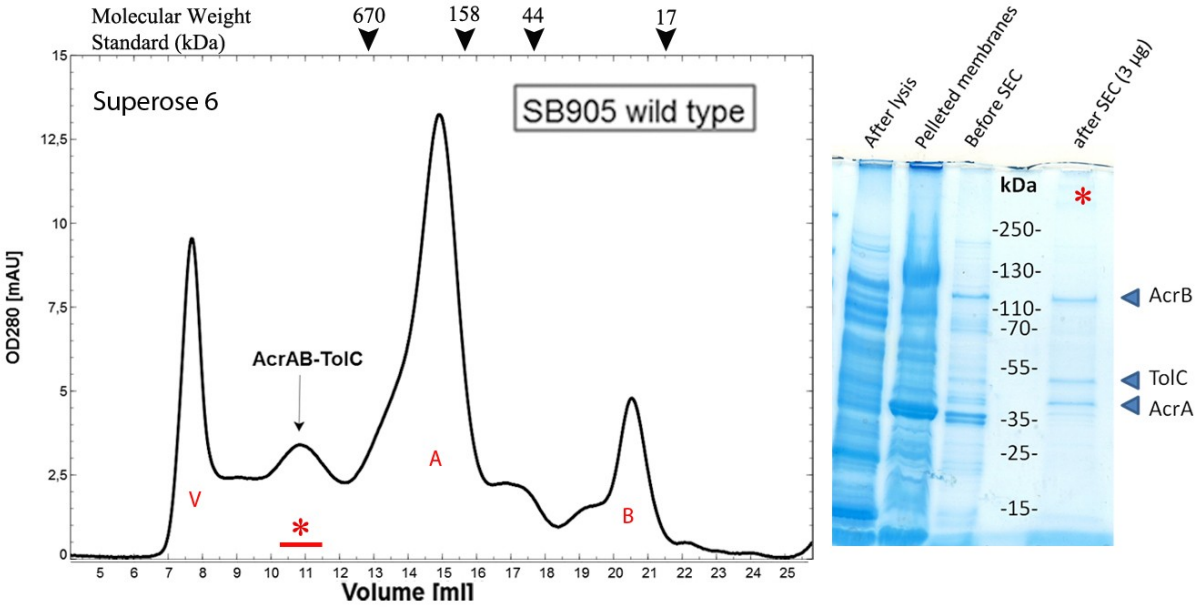

Figure 4.12: Isolation of native AcrAB-TolC from wild type *Salmonella*

Size exclusion chromatography profile of the final isolation step (left). V indicates the void peak. The peak corresponding to the size of the assembled pump is indicated with an arrow.Peaks A and B arise from a variety of smaller proteins, presumably a mixture of disassembled particles and other membrane proteins (see separate SDS-PAGE gel in the Supplementary, section 8.8; detection difficult due to extremely low concentration of individual proteins). The fractions marked with a red star were pooled, concentrated and analyzed on SDS-page (right). Three bands corresponding to the size of the three components are clearly discernible after SEC. The three lanes on the Coomassie stained SDS-PAGE on the left are samples from three breakpoints during the isolation process.

The available protein standard (BioRad Gel Filtration Standard) does not allow precise estimation of the

After successfully isolating AcrAB-TolC from wild type *Salmonella*, I then proceeded to isolate the efflux pump from the *acrAB* complemented *acrAB/acrD/acrEF* triple knockout strain to allow for a minimal background of potentially undesired pump complexes. Given that the plasmid-encoded *acrAB* operon was preceded by a *ramA* binding site, an increase in expression of all efflux pump components could again be achieved by *ramA* overexpression. The same isolation protocol was used as for the wild type; however, output concentrations of the assembled pumps were considerably lower, giving rise to only a modest peak in SEC. Protein yield was not sufficient to allow for both extensive electron microscopy and SDS-PAGE analysis, so the three pump components were individually detected on Western Blot instead (Figure 4.13). The purity of the sample can be judged by negative stain electron microscopy images and is estimated to be similar or slightly inferior compared to the wild type sample (Figure 4.14).

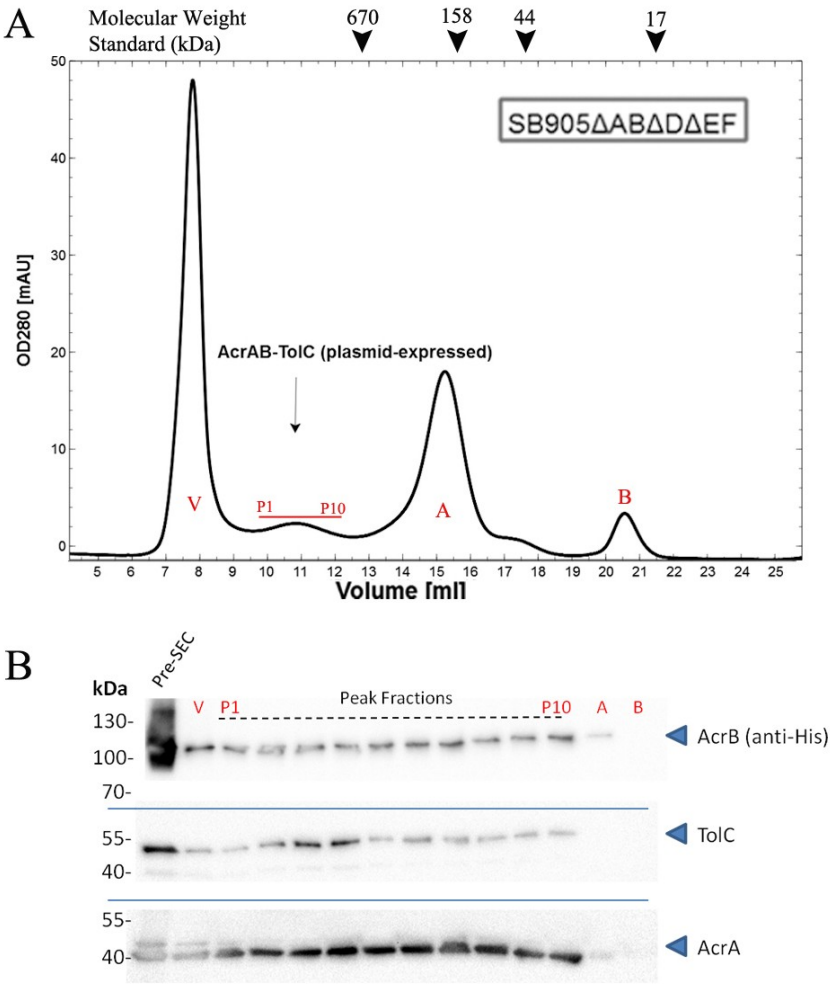

Figure 4.13: Isolation of complemented AcrAB-TolC from *Salmonella* triple knockout strain

(A) Size exclusion chromatography profile of the final isolation step. The peak corresponding to the size of the assembled pump is indicated with an arrow. All fractions labelled in red were analyzed on Western Blot (B), and all three pump components were detected in the peak fractions using specific antibodies. 1 µl was loaded of each fraction.

The isolated near-native AcrAB-TolC particles from the complementation strain as seen in negative stain EM images are identical in size and shape to the particles isolated from wild type *Salmonella*.

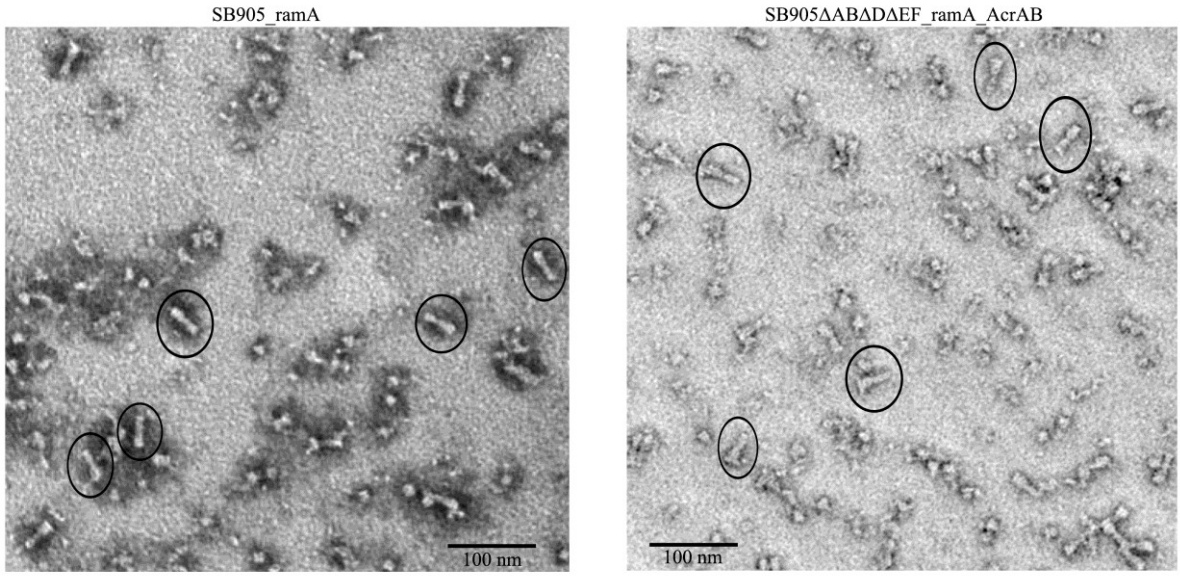

Figure 4.14: Many assembled pump particles were found in isolated membrane fractions of the *Salmonella* SB905 wild type (left) and *acrAB/acrD/acrEF* triple knockout (right). For electron microscopy, undiluted SEC fractions were applied to a continuous carbon grid, stained with 2 % PTA and viewed at a magnification of 71000.

4.8 Isolation of the near-native MacAB-TolC efflux pump

While efforts have been made to elucidate the structure of RND-type pumps such as AcrAB-TolC, for ABC-type tripartite efflux pumps only the structures of single components are available([69,103] among others). The only exception to this is the study of a chimeric MacA-TolCα fusion protein, which indicates tip-to-tip interaction between the two but does not represent the native assembly[74].

By adapting the protocol used for AcrAB-TolC isolation in the previous chapter, it was possible for the first time to isolate near-native MacAB-TolC pump in an assembled state from *Salmonella* and visualize it by electron microscopy (EM). As the endogenous *macAB* operon is expressed in very low levels and no cellular activator is known that would significantly enhance it, *macAB* was expressed from a plasmid under the control of a RamA dependent promoter. This is even more beneficial, as overexpression of *ramA* also increases the expression of the third efflux pump component gene *tolC*, thereby enabling overexpression of all pump components with one single activator protein. First isolation trials of MacAB-TolC were performed in an *acrAB* deletion background only, but mass spectrometry analysis of the final sample revealed relatively high abundance of AcrE and AcrF and slightly lower abundance of AcrD (Figure 4.15). Therefore, to avoid simultaneous overexpression not only of AcrAB but also of its homologs, all following experiments involving MacAB-TolC were carried out in an *acrAB/acrD/acrEF* triple knockout background.

	Score (Normalized Area)	Sequence Coverage [%]
TolC	6,52E+06	88,2
AcrA	n.d.	n.d.
AcrB	n.d.	n.d.
AcrE	1,48E+05	55,1
AcrF	2,99E+05	31,7
AcrD	3,38E+04	2,2
EmrA	1,92E+04	5,9
EmrB	n.d.	n.d.
MacB	1,85E+06	65,0
MacA	4,57E+07	92,5

Figure 4.15: In solution digestion mass spectrometry analysis reveals the abundance of single efflux pump components in the final step of a MacAB-TolC isolation from an *acrAB* deletion background (with plasmid-born MacAB). This gives hints about which components are the most promising candidates for deletion to improve sample homogeneity. n.d. = not detected. Complete data can be found in the Supplementary Material (see section 8.9).

To isolate bacterial membrane fractions containing MacAB-TolC, the same protocol as established previously was used up to the step where detergent-solved membrane proteins are fractionated by density in a cesium chloride gradient. Hereafter, the proceeding of the isolation was analyzed on

Western Blot with antibodies specific for the three components and MacAB-TolC was found to be enriched in the first two fractions of the gradient (Figure 4.16). The identity of the three components was further confirmed by SDS-PAGE and following mass spectrometry analysis of individual bands (Figure 4.17). It is notable that in SDS-PAGE, the MacB protein runs somewhat lower than its calculated molecular weight of 70 kDa would suggest. Although the MacB sequence coverage in MassSpec analysis of the corresponding band was not more than 58.4 %, both the N- and the C-terminus of MacB were covered by the detected peptides. This suggests that MacB is in fact not truncated, but that its unexpected gel running behavior must be caused by other, unknown characteristics of the protein.

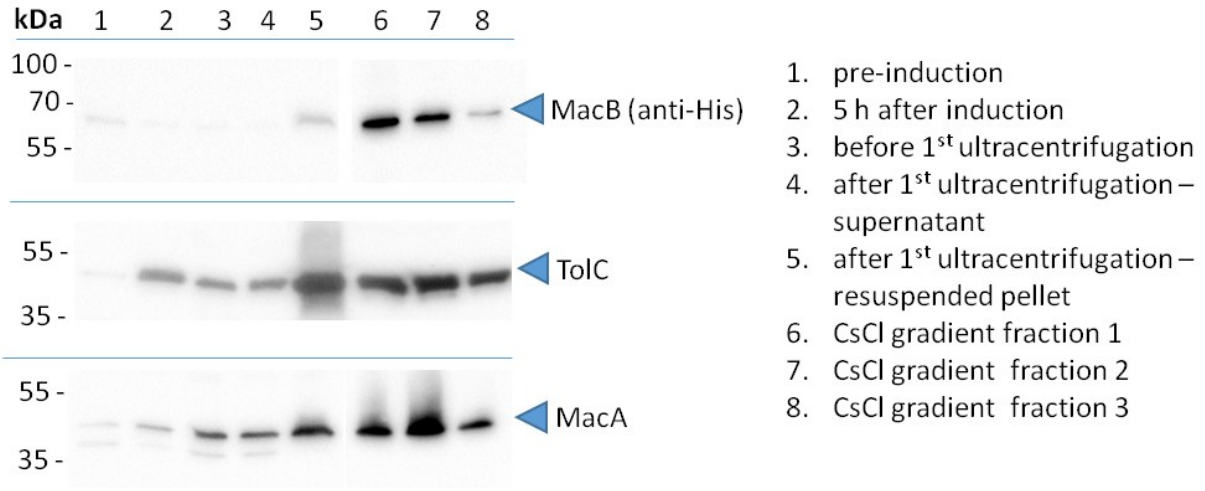

Figure 4.16: Western Blot of MacAB-TolC isolation steps

During overexpression and isolation of membrane fractions, samples for Western Blot analysis were taken at various breakpoints. Lanes 1 to 8 denote the various steps as given in the description on the right. 0.02 OD units were loaded for whole cell lysates (lane 1 and 2) and 1 ul of the sample was loaded in all other lanes. TolC and MacA was detected individually by specific antibodies and MacB was detected via its C-terminal HisTag.

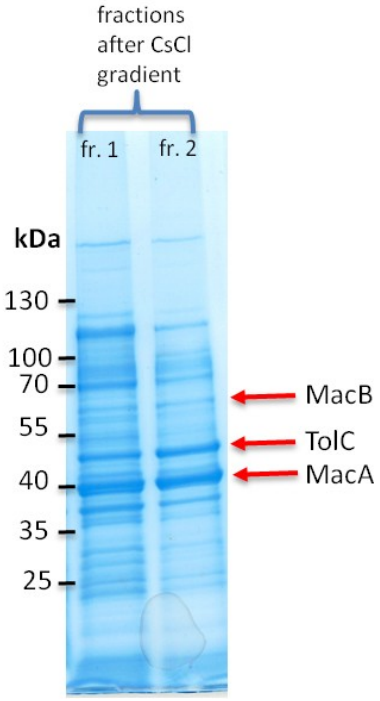

#	identified protein	molecular weight [kDa]	sequence coverage [%]
1	MacB	70,7	58,64
2	TolC	53,7	67,41
3	MacA	40,8	89,25

Figure 4.17: SDS-PAGE and mass spectrometric analysis of MacAB-TolC containing gradient fractions

10 ul of fraction 1 and 2 after the CsCl gradient were loaded on an SDS-PAGE gel and stained with Coomassie (left). Red arrows indicate the bands that were cut out and analysed by mass spectrometry. All three components of the MacAB-TolC efflux pump could be identified with a sequence coverage as given in the table (top). It is notable that for unknown reasons MacB runs lower than its calculated molecular weight would suggest.

To determine whether the detected signals arise only from individual disassembled components in the sample or whether the tripartite pump is still assembled at this step, the sample was stained with 2 % PTA and checked by transmission electron microscopy. In fact, a large part of the particles visible in CsCl fraction 1 and 2 were long and pump-shaped and appeared to be assembled MacAB-TolC. This assumption was further validated by a control experiment, where the exact same isolation procedure carried out without plasmid-expressed *macAB* did not yield any visible long shaped particles in these fractions (see supplementary information, section 8.4).

However, when isolating MacAB-TolC only a small percentage of the pumps were present as individual particles. Instead, the assembled pump particles tended to form aggregates in all shapes and sizes, ranging from two to dozens of pumps sticking together (Figure 4.18, left) and heavily hampering all further purification procedures such as size exclusion chromatography. In an attempt to find an experimental condition that would prevent these aggregates, incubation of the sample in different pH and temperature conditions or with different additives was performed, unfortunately without satisfying results. As an example, MacAB-TolC in a buffer containing 20 mM bivalent magnesium ions is shown in Figure 4.18 (right).

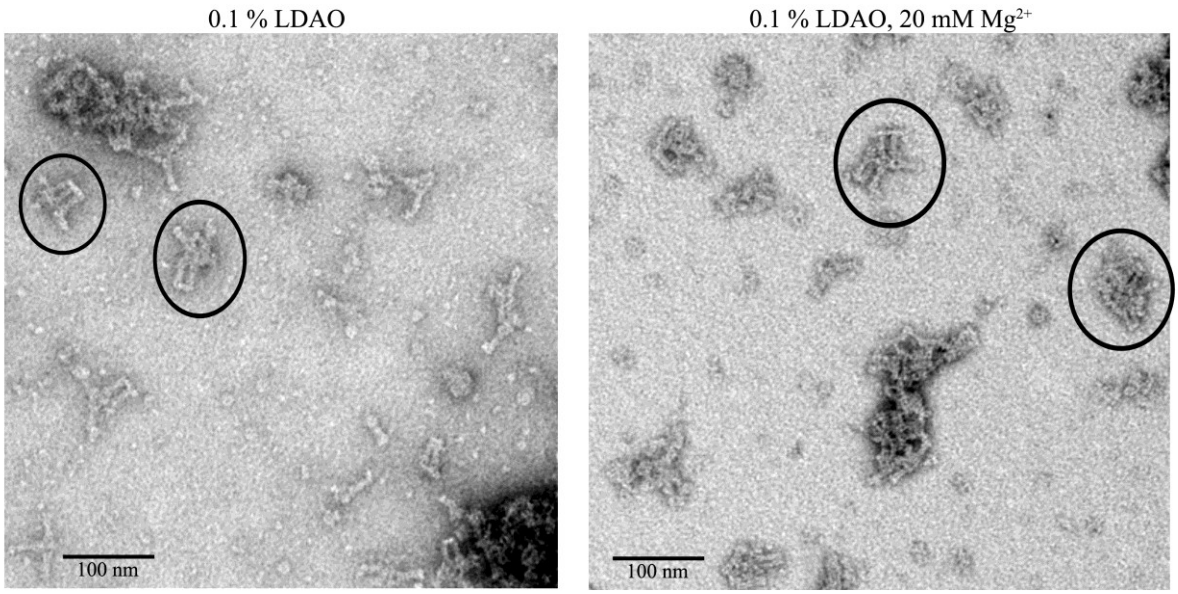

Figure 4.18: Micrographs of MacAB-TolC enriched *Salmonella* membrane fractions in negative stain EM

Plasmid-overexpression of *macAB* in a Salmonella *acrAB/acrD/acrEF* knockout strain yields long pump shaped particles with a strong tendency to stick to each other both head-to-head and site-to-site. This happens in the standard isolation buffer comprising 0.1 % LDAO (left) as well as with all other tested buffers and additives (for example 20 mM $MgCl_2$, right). Both images show a 1:25 dilution of CsCl gradient fraction 2 after ultracentrifugation and pellet resuspension.

Solubilization of the pumps in a broad range of different detergents was furthermore attempted as listed in section 2.12. Detergent-solubilized fractions were checked by Western Blot, which showed that solubilization was successful in all detergents tested, although at various degrees (Figure 4.19, A). However, in negative-stain EM analysis no improvement of the aggregation state was detected with any of the detergents (Figure 4.19, B). This might be partly explained by the fact that good solubilization does not necessarily correlate with the preservation of the assembled complex, but can also result in disassembly of the particles (as seemed to be the case for FC-12).

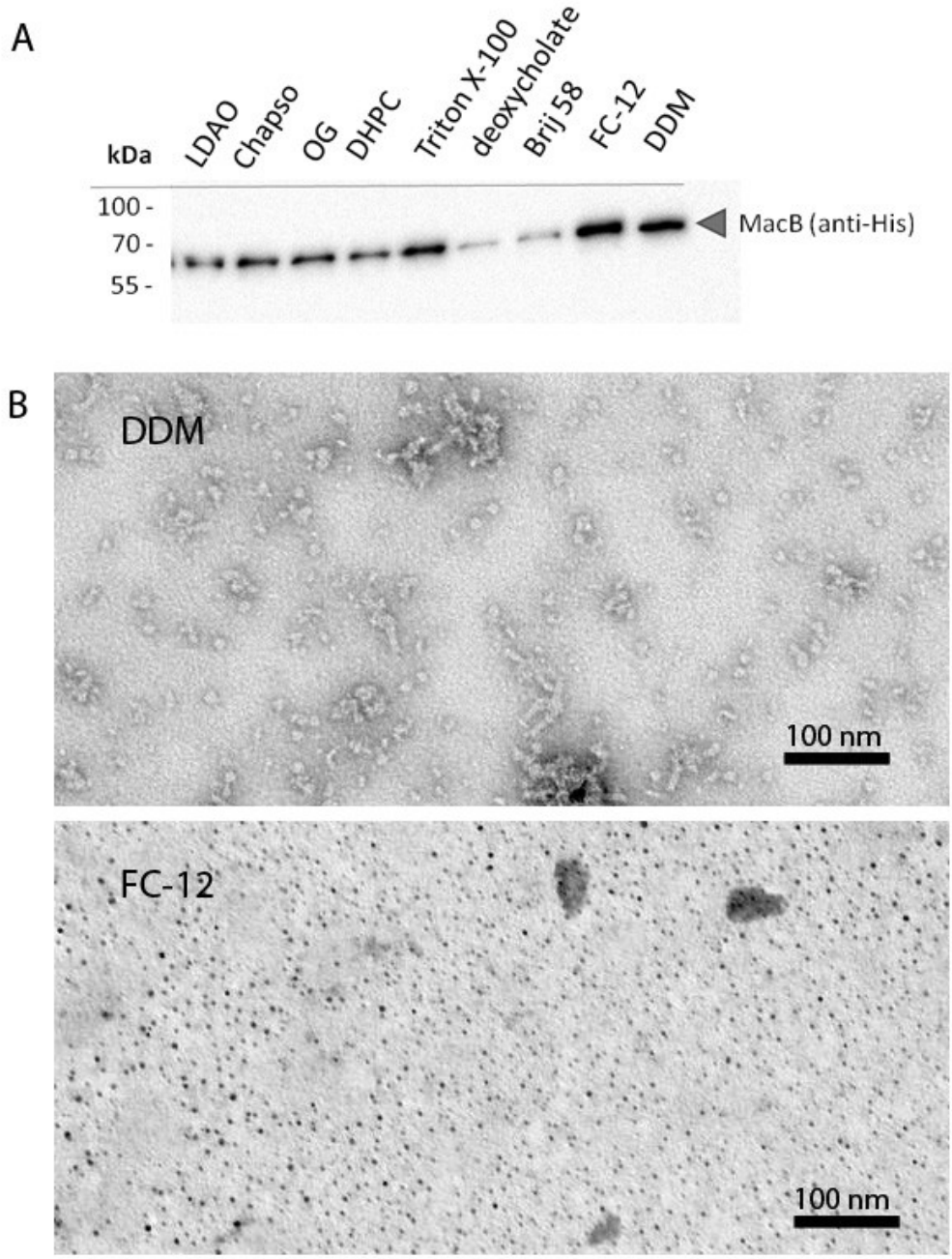

Figure 4.19: Detergent screening for MacAB-TolC solubilization

After pelleting of the CsCl gradient fractions, resuspension of the efflux pump was tested in different detergents. (A) MacB was detected on a Western Blot in representation of the whole MacAB-TolC pump and a stronger signal was interpreted as better solubilization of the particles. The detergents FC-12 and DDM appear to result in the best solubilization but did not prevent pump aggregation (DDM) or did not allow particle visualization (FC-12) when checked in negative stain EM (B).

4.9 Generation of *Salmonella* minicells to allow *in situ* visualization of efflux pumps

In order to study bacterial membrane protein complexes in an environment that is as close to native as possible, it can be beneficial to visualize them directly within the membrane. Because the cell body of *Salmonella* is too thick (~ 1 µm) to perform electron microscopy without too much undesired scattering, so called minicells have to be generated for *in situ* visualization of membrane proteins. These small bacterial cells arise when the proper placement of the cell division machinery and especially Z-ring positioning are disturbed, as happens when the regulatory Min system is blocked by deleting one or more of its components MinC, MinD and MinE[104]. Minicells contain all basic components of their parent cells except a chromosome, and as a result cannot divide or grow. Their size is variable but usually ranges around a diameter of 500 nm. Recently, they have been exploited for cryo-electron tomography studies of large molecular machines in a number of Gram-negative bacteria like *E. coli*, *Shigella flexneri* and *Salmonella enterica*[94,105,106].

As a first step towards *in situ* visualization of type I secretion systems, a *Salmonella* MinD knockout strain overexpressing AcrAB-TolC was generated. For this purpose*, S. enterica* serovar Typhimurium strain SB905 *ΔminD* (from lab collection) was transformed with a plasmid overexpressing the transcriptional activator *ramA*. Upon induction, expression of AcrAB and TolC was enhanced as shown on Figure 4.20 and the minicells were enriched from the culture using a protocol established by Nans et al.[95]. The presence of AcrAB-TolC in the minicell pellet was confirmed by Western Blot analysis (Figure 4.20) and the sample was stained with 2 % PTA and checked by transmission electron microscopy for successful minicell production and enrichment (Figure 4.21).

Unfortunately, the image quality of negative stain micrographs is usually not good enough to discern single membrane molecules, so the next step to *in situ* visualization of the efflux pump will require a switch to cryo-EM systems and ultimately cryo-electron tomography (cryo-ET).

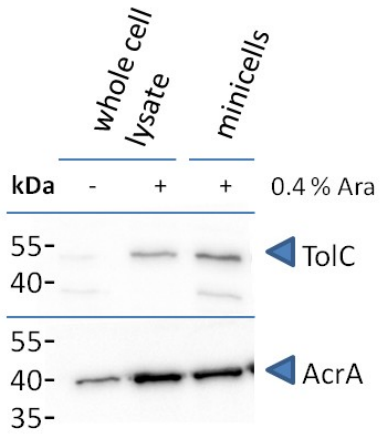

Figure 4.20: AcrAB-TolC overexpression in minicell-producing *Salmonella ΔminD* strain.
Western Blot analysis of TolC and AcrA expression in the strain SB905ΔminD_ramA before and after arabinose induction as well as after minicell enrichment (right lane). 0.02 OD units of whole cell lysates and 1 µl of the final minicell suspension were loaded.

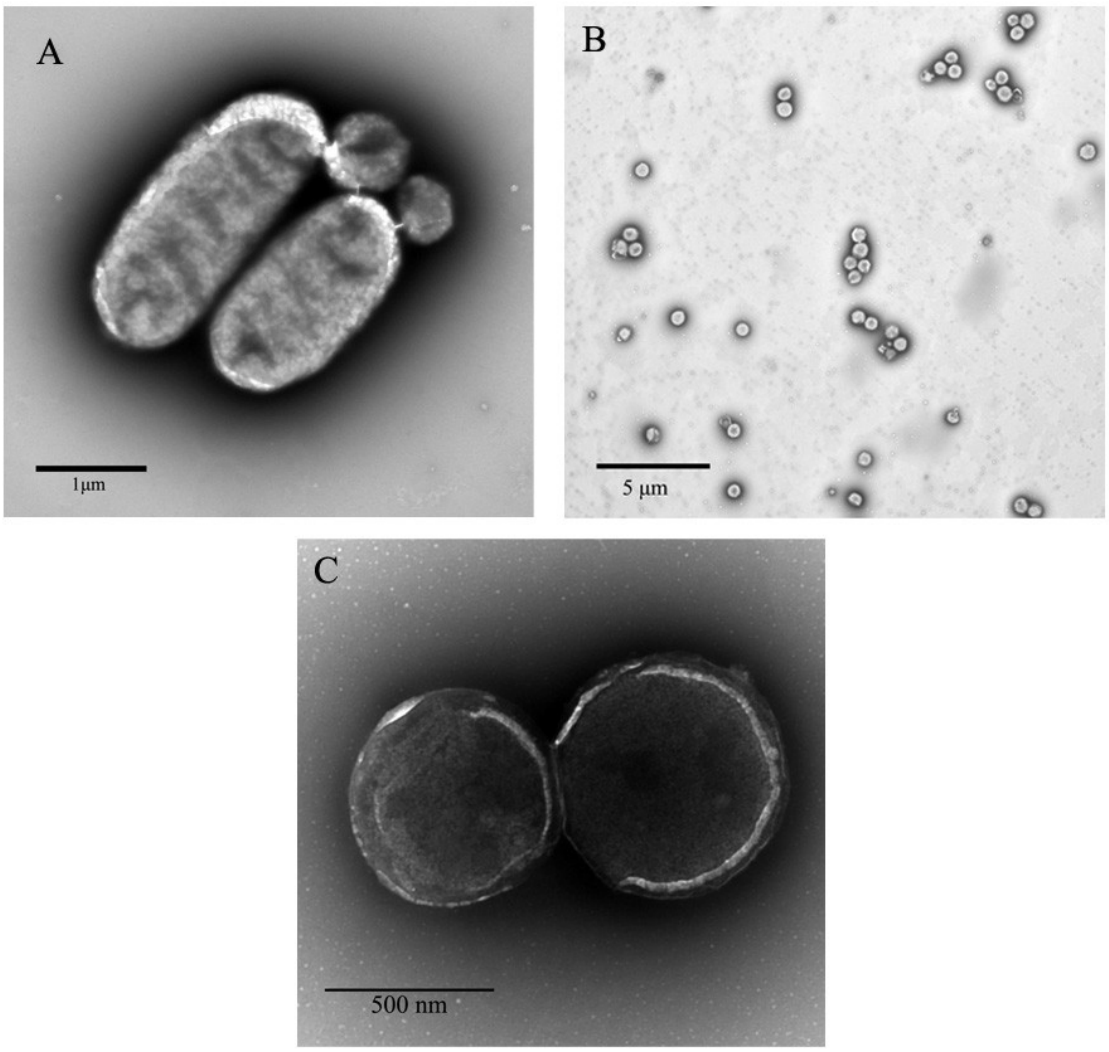

Figure 4.21: Imaging of *Salmonella* minicells by negative stain microscopy

Three micrographs showing normal-sized parent cells (*S. enterica* strain SB905*ΔminD*_ramA) next to growth deficient minicells (A), an overview over the enriched minicell fraction (B) and a close-up on two neighbouring minicells (C). In negative stain EM, individual features such as membrane complexes cannot be discerned; however, the generated minicells have the right size to make them amenable for future cryo-ET studies.

4.10 Visualization of AcrAB-TolC top and side views in cryo-electron microscopy (cryo-EM)

Negative-stain electron microscopy is inherently limited in resolution by the size of heavy salt microcrystals formed by the drying stain[107]. Thus, the use of cryo-electron microscopy for single particle analysis and 3D reconstruction is essential in attempting to achieve a high-resolution structure of the assembled complex. The isolated AcrAB-TolC complex from the *acrAB*-complemented *SB905ΔABΔDΔEF* triple knockout strain was used for first cryo-EM tests on a near-native assembled efflux pump. Visualization of the pump particles was possible and both ring-shaped top views as well as elongated stick-shaped side-views could be found (Figure 4.22). However, unspecific protein background was too high and sample homogeneity and concentration were not sufficient to start data collection on this sample.

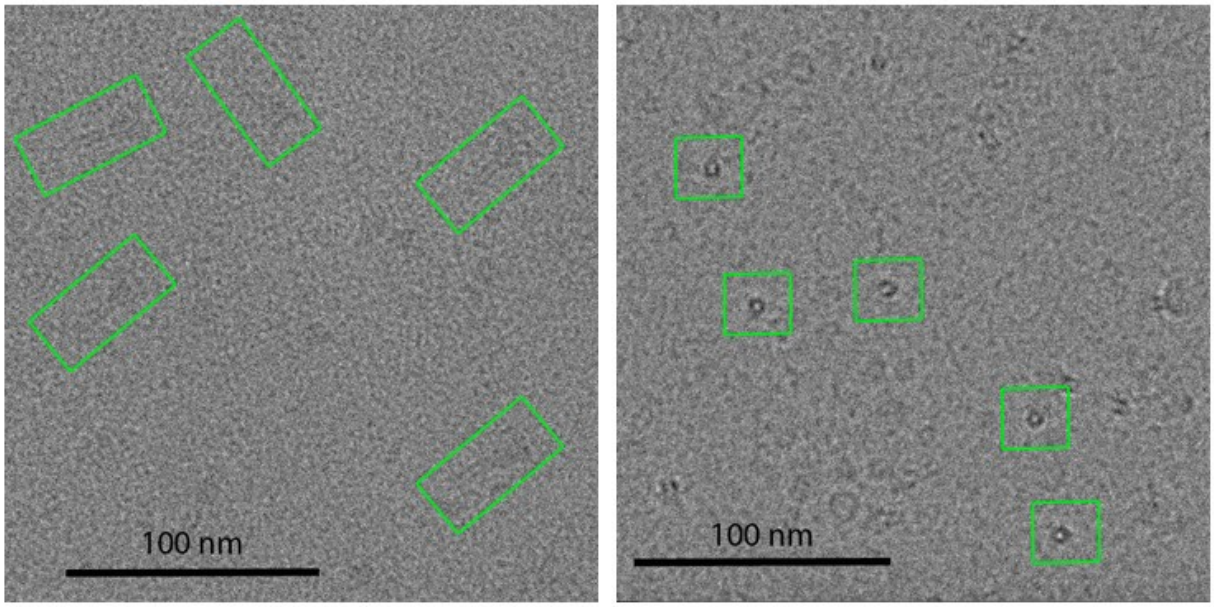

Figure 4.22: Visualization of isolated AcrAB-TolC in cryo-EM

Vitrified AcrAB-TolC sample isolated from *acrAB*-complemented *SB90ΔABΔDΔEF* strain was imaged at 39k magnification. Green boxes highlight electron density assumed to belong to the assembled efflux pump complexes. Both side-views (left) and top-views (right) of the pump particles could be found.

5 DISCUSSION

My Master thesis research focused on the structural and functional characterization of two multidrug efflux pumps belonging to two different transporter families in *Salmonella Typhimurium*. The RND-type pump AcrAB-TolC was chosen as it is the most clinical relevant and also the best characterized of any tripartite efflux pump known so far, and MacAB-TolC was chosen due to its role as the major representative of the ABC-type tripartite pumps.

5.1 MacAB-TolC and AcrAB-TolC are strongly conserved between *E. coli* and *Salmonella*, but their regulation is not

As has been shown by bioinformatic sequence analysis (see section 2.1), all the individual components of the two studied efflux pumps show strong homology between *E. coli* and *S. enterica,* both on the genomic as well as on the protein level. Consistent with this observation, 3D structure prediction of *Salmonella* MacA revealed an architecture which was very similar to the known crystal structure of MacA from *E. coli.* However, literature research shows that mechanisms regulating expression of the pumps are not conserved to the same degree. The *Salmonella macAB* operon was shown to be regulated by the PhoPQ system[86]. For *E. coli*, an effect of PhoPQ on *macAB* has not been reported so far, and a study comparing the PhoPQ regulons in both organisms found very limited overlap in PhoPQ dependent genes in general[108]. Similarly, the RamA-dependent regulation of AcrAB-TolC described in section 1.5 and utilized for pump overexpression in this study is present in *S. enterica* and some other Gram-negatives, but not in *E. coli*[82].

The conservation of the efflux pump genes is a strong indicator that their presence provides a substantial fitness advantage to both bacterial species, protecting them from a wide range of toxic substances. But even though *E. coli* and *Salmonella* are closely related, their natural environments and preferred host organisms as well as their epidemiology and even their infection sites are surprisingly diverse[109,110]. As a consequence, they usually encounter different environmental conditions including different small molecules; this might explain the need for divergent signaling systems for up- and downregulation of their respective efflux pumps.

5.2 Oligomerization state of native and heterologously expressed MacA

As discussed above, the *S. enterica macAB* operon shares a strong sequence homology with *macAB* from *E. coli*. Likewise, the MacA protein is predicted to have a very similar overall architecture both

to *E. coli* MacA and to other PAPs of Gram-negative bacteria (section 2.1). Considering this close similarity, it was interesting to explore whether the oligomerization state of MacA was also comparable between the two species. No structure of a fully assembled MacAB-TolC complex is available for either of the two species, so the actual association states of MacA and MacB remain uncertain; but knowing their oligomerization states in solution can help to make predictions about assembly and interplay of the components.

E. coli MacA lacking the N-terminal signal-like sequence has been reported to display a hexameric arrangement in the crystal lattice, but did not appear as a higher-order oligomer in solution[69]. Here, I could demonstrate that purified *Salmonella* MacA (also lacking its N-terminal signal-like sequence) elutes as a dimer in size exclusion chromatography after heterologous expression in *E. coli* (section 2.5). The formation of a MacA-dimer *in vitro* is not contradictive to a proposed hexameric state in the assembled complex, and the hypothetical association of three dimers to form a hexameric assembly *in vivo* is in good agreement with the suggested stoichiometry of 6:6:3 (MacB:MacA:TolC) for the active efflux pump. Additional support for this model is provided by recent reports on assembled AcrAB-TolC which generally also favor a hexameric structure for AcrA[37,45,50], whose major structural features are shared with MacA in both *E. coli* and *Salmonella*. It was further shown in our laboratory that purified AcrA presumably also forms a dimer *in vitro* (Master thesis of Tobias Thoeni).

Although investigation of the single efflux pump components can give hints about their interaction in the complex, only a high-resolution structure of the whole *in vivo* assembled complex will be able to reveal a complete picture of the assembled state and potentially facilitate the identification of new efflux pump inhibitors.

5.3 Knockout of AcrAB and its homologs allows background free overexpression of efflux pumps

The overall shape of the different tripartite efflux pumps in Gram-negative bacteria is believed to be largely similar, impeding visual distinction of the pumps on single electron microscopy images. Therefore, if isolation and visualization of one specific tripartite efflux pump is to be achieved, knocking out the other most abundant pumps helps to considerably reduce the background of visually similar but ontologically distinct pump-shaped particles.

In *Salmonella*, the most highly expressed efflux pump genes are *acrAB* and *tolC*, followed by the MFS-type pump operon *emrAB*, the here studied *macAB* and, lastly, *acrEF* and *acrD* (see section 1.5 and

reference[86]). A *Salmonella* strain lacking genomic *acrAB* already available in the laboratory was complemented with plasmid-born *acrAB* for a more controlled overexpression of the AcrAB-TolC pump. When MacAB-TolC was overexpressed in the *acrAB* deletion strain, there was still a relatively high abundance of AcrE and AcrF and lower abundance of AcrD in the final isolated fraction as revealed by mass spectrometry analysis (see section 4.8). Thus, the *Salmonella acrAB/acrD/acrEF* triple knockout strain was used for all further efflux pump isolation procedures to guarantee a low background of similar, but not identical pump particles.

Additional deletion of genomic *macAB* is not absolutely necessary, as its expression level under laboratory conditions is comparatively low (see section 1.5), but has the potential to further improve purity of the isolated efflux pump fractions. However, when an increasing number of efflux pumps are knocked out in *Salmonella,* the strain accumulates more growth problems and becomes increasingly difficult to handle (see section 2.2).

Even though EmrAB was previously shown to be rather abundant in a *S. enterica* wild type strain under laboratory conditions[86], it seems to be almost absent from the final isolated efflux pump sample: EmrA was only identified at very low levels in the mass spectrometry analysis and EmrB was not detected at all. Possible reasons for this are disassembly under the purification conditions or separation during the isolation process due to different biochemical characteristics of the molecule. Therefore, *emrAB* was not selected as a crucial knockout candidate in this study. An additional *emrAB* deletion might still be generated at a later time in efforts to improve purity, but this was not attempted so far due to the problems in strain fitness mentioned above.

5.4 Plasmid-born pump proteins can assemble into functional efflux pumps

MacAB and AcrAB were overexpressed from plasmids in *S. enterica* in order to allow a directed regulation of their expression and to increase protein levels. Also, a histidine tag was added to both plasmid-encoded MacB and AcrB, which could potentially interfere with the functionality of the proteins. As it is our major goal to isolate the efflux pumps in a state that is as close to native as possible, we needed to assess whether the plasmid-born pump components can still assemble with TolC and form pumps that are functional *in vivo*. For this purpose, the susceptibility to the macrolide-antibiotic Erythromycin was determined for the different strain variants used (see section 4.4). Erythromycin was chosen because macrolides have been reported to be substrates of both pumps investigated in this study[55,111].

Plasmid-born *acrAB* overexpression in the *acrAB/acrD/acrEF* knockout strain not only restored erythromycin resistance but in fact exceeded wild type resistance levels. This is most likely due to enhanced expression levels as compared to genomic, wild type *acrAB*. Hence, plasmid-born AcrAB not only complements the knockout strain on a biochemical, but also on a functional level. In contrast, plasmid-born *macAB* overexpression only gave a two-fold rise in resistance compared to the triple knockout strain. However, this small effect is reproducible and in good accordance with previously published drug sensitivity tests in *Salmonella* showing the same level of increased resistance[85,101]. It is important to note that the effects of *macAB* overexpression are too small to make a difference in the wild-type environment and are only unmasked when the basic resistance level is considerably lowered by *acrAB* deletion, as shown previously[101].

It can be concluded that the inner membrane and periplasmic components of both pumps are indeed functional when expressed from a plasmid and most probably interact with genomically encoded TolC to exert their function. This confirms the applicability of the chosen regulatory system to increase the appearance of certain drug efflux pumps.

5.5 Near-native AcrAB-TolC can be isolated from *Salmonella* and visualized in EM

Near-native AcrAB-TolC isolated from a wild type *Salmonella* SB905 strain has previously been used in our laboratory to reconstruct a 3D model of the complex from negative-stain EM data, reaching a relatively low resolution of 31 Å (Figure 5.1; see Master thesis of Tobias Thoeni). In terms of size and overall shape, this model is in good accordance with the structures published so far[44,50,72], providing further evidence for the adaptor bridging model. However, in order to proceed to cryo-EM analysis

and achieve a higher resolution structure, isolation of AcrAB-TolC from a triple efflux pump knockout strain is preferable (see section 5.4.).

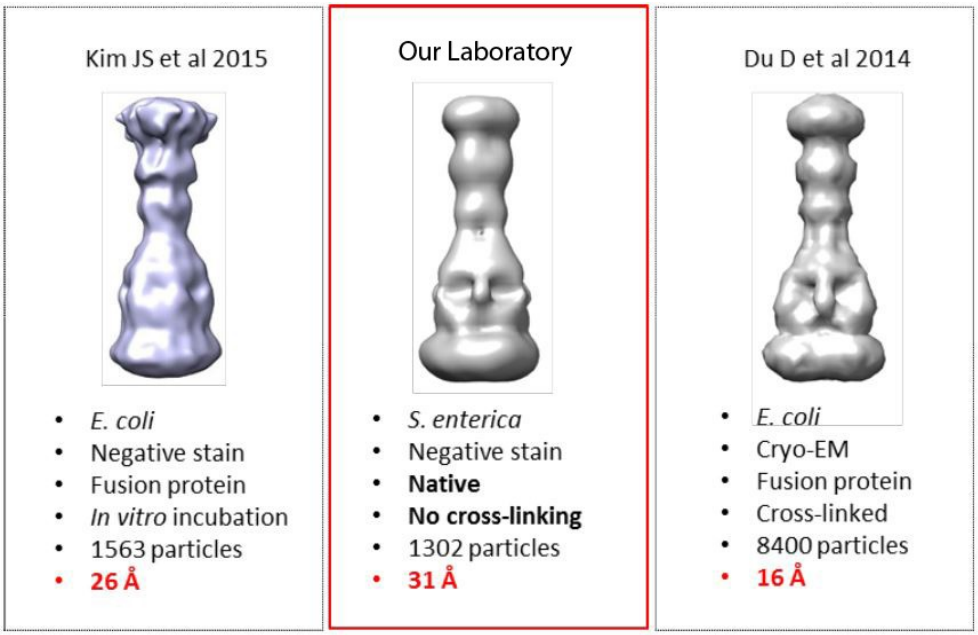

Figure 5.1: Comparison of available 3D models of AcrAB-TolC

Two of the models with the highest resolution known so far (left and right boxes) have both been derived from *in vitro* reconstructions of the *E. coli* AcrAB-TolC pump using fusion proteins In comparison, the 3D reconstruction generated in our laboratory (middle) is derived from natively assembled pump complexes. The overall shape and size are similar in all three models.

As has been shown in section 4.7., pump shaped particles can be isolated from the *acrAB*-complemented *acrAB/acrD/acrEF* triple knockout strain similar to those isolated from the wild-type strain. However, isolation of near-native AcrAB-TolC from the complemented strain resulted in a lower yield of pump complexes and, assumingly related to this, higher impurity and higher protein background. Because expression levels of AcrA and AcrB as detected on Western Blot are not lower in the complemented strain as compared to wild type, at this point we can only speculate about the underlying reasons for the poorer sample quality. One possible explanation is that a difference in the ratio of AcrAB:TolC forced by plasmid-born AcrAB overexpression may lead to a higher amount of unassembled pumps, contributing to the higher background of non-pump-shaped particles. A possible way to address this issue would be to include the *tolC* gene on the plasmid and overexpress it together with the other two components to reduce gene dosis effects.

Despite the not entirely satisfying sample quality, isolated AcrAB-TolC from the complemented *acrAB/acrD/acrEF* triple knockout strain has been used for first cryo-EM trials, where it was shown

that the pump particles can indeed be visualized distinctly after plunge freezing, with both top-views and side-views present. Thus, the efflux pump particles are in principle suitable for single particle cryo-EM analysis, yet the low concentration and the heterogeneity of the sample have so far prevented the start of large scale data collection. In order to increase final sample concentration, an increase in culture volume will be necessary, and additional or adapted purification steps could also prove useful.

The use of a HisTrap column to enrich for efflux pumps has already been tried but was not successful. It is likely that the pump particles disassemble as a consequence to the selective pull at the histidine-tagged AcrB. It might be possible to solve this issue by performing extended buffer screening to find more suitable buffer conditions; however, the low efflux pump yield is the biggest limiting factor for experiments of this kind. Additional purification steps could include a second gel filtration or an additional gradient centrifugation – here, a glycerol gradient might prove most suitable based on its size separation range.

5.6 Near-native MacAB-TolC has a strong tendency to aggregate upon isolation

When MacAB-TolC is overexpressed and isolated from *S. enterica* as described in section 4.8, following the same basic procedure as for AcrAB-TolC, the pump particles are observed to aggregate when visualized in negative stain EM after the CsCl gradient step. Aggregation patterns seem to be stochastic, with aggregates existing in all size ranges between two and several dozen pumps involved, and very few single pump particles. As visualization before the CsCl gradient step is not possible, it is unknown at exactly which step of the isolation procedure this aggregates form. Similarly unknown are the reasons for the aggregation itself. Possible explanations include the presence of self-attracting patches on the surface of the complex, the use of unsuitable detergents that do not sufficiently solubilize the pumps or the presence of membrane leftovers adhering to the pumps. It is further imaginable that the aggregated pumps are broken or partly disassembled, while only the few single pump particles present in the sample are still in their functional state.

Particle aggregation not only prevents single particle EM analysis, but also most further purification strategies such as gel filtration. Thus, I tried to identify sample and buffer conditions that might help to solubilize the pumps by screening for a range of different detergents, additives, pH-values and temperatures (see section 4.8). Unfortunately, this approach did not yield any success so far. Another conceivable approach is to separate the aggregated, possibly “broken” pumps from the functional, single pumps in a further gradient centrifugation step. However, as for the AcrAB-TolC sample, here

we are strongly limited by the low amount of sample material obtained from a relatively high amount of culture volume. To prevent extended hydrophobic patches during the purification process which could also cause aggregation, the search for suitable alternatives to detergents – such as amphipols – could be valuable.

5.7 The use of *Salmonella* minicells might allow *in situ* visualization of efflux pumps

While a near-native structure of a tripartite efflux pump would already be a big advance in the field, a structure of the pumps sitting directly in their native environment might provide a picture that is even closer to reality. Similar *in situ* structures have already been obtained for other nanomachines such as the type III secretion sorting platform in *Shigella*[106], bacterial chemoreceptor arrays in *Salmonella*[112] and bacteriophage P1 attached to the *E. coli* membrane[93]. For these experiments, bacterial strains deficient in certain cell division regulators are used that form so called "minicells", amenable to cryo-electron tomography due to their small size.

Following this rationale, AcrAB-TolC was overexpressed in a minicell-producing *Salmonella* strain. The minicells were visualized by negative stain EM, whose limited resolution, however, makes it close to impossible to individuate single small membrane embedded particles – particularly if they do not stick out of the membranes like the type III secretion system does. Therefore, cryo-ET will be necessary to determine whether *in situ* visualization of the tripartite efflux pumps is indeed possible.

5.8 Conclusion and Outlook

In this thesis I worked towards the structural characterization of two tripartite multidrug efflux pumps from two distinct mechanistic classes in *Salmonella enterica.* The drug/proton antiporter AcrAB-TolC and the ABC-type efflux pump MacAB-TolC are both major representatives of their families and as such they are of great importance for the understanding of multidrug efflux in general. In the course of my work, I constructed suitable strain variants for overexpression of the two pumps, verified the functionality of the overexpressed efflux pumps and isolated them from membrane fractions in order to visualize them in their near-native state. Visualization of single, spatially separated AcrAB-TolC particles was possible in both negative stain and cryo-EM, whereas visualization of isolated MacAB-TolC by negative stain EM showed mostly aggregated efflux-pumps.

Results from this study and from a previous master student (see Master thesis of Tobias Thoeni) confirm that the “adaptor bridging model” is likely to represent the native assembly state of both of the investigated pumps. However, high-resolution structures of the assembled complexes are still needed to provide detailed information about the architecture and assembly of the system. This could help answer both the remaining structural as well as the associated mechanistic questions:

- Which sites are important for interaction of the individual components?
- How is TolC channel opening regulated in the two pumps?
- What do the transmembrane and the cytoplasmic part of MacB look like, and can their structure provide information on the efflux mechanism?
- How are the substrates selected and what is the substrate path through MacAB-TolC?
- Is it possible to rationally design efflux pump inhibitors based on the structure?

In order to get the necessary structural information, cryo-electron microscopy and single particle reconstruction will be indispensable. Further improvement of the sample preparation process will be key to enable and facilitate cryo-EM data collection.

Residues important for the mechanistics of the efflux process as well as interactions sites could be identified by plasmid derived mutation and complementation experiments.

In conclusion, I hope that these experiments will help to better understand bacterial antibiotic resistance mechanisms and that this research will one day contribute to the development of new strategies to fight multidrug resistance.

6 ABSTRACT

The intracellular pathogen *Salmonella* infects both human and animal hosts and is a common cause of foodborne diseases, causing gastrointestinal illness or systemic infection depending on the serovar. While for light cases treatment is usually not necessary, patients with more severe forms of disease depend on antibiotic treatment. However, evolution of multidrug resistant strains is a recurring clinical problem for *Salmonella* as well as for other Gram-negative bacteria such as *E. coli* and *Pseudomonas aeruginosa.* This multidrug resistance includes not only antibiotics but also other toxic substances such as dyes, detergents and disinfectants and is often associated with increased ability of the bacterial cell to expel these substances via active membrane transporters. These multidrug efflux pumps in Gram-negative bacteria often span both membranes and are built up of three components in different copy numbers: i) an inner membrane transporter which provides the energy for substrate transport, ii) an outer membrane channel and iii) a periplasmic adaptor protein that acts as a connecting element between the two. Based on their mode of action, these tripartite efflux pumps are classified into primary-type pumps that use ATP as their primary energy source and secondary-type pumps which work as ion/drug antiporters and exploit the electrochemical potential gradient at the inner membrane. In this study, I investigated one member of each group: MacAB-TolC was chosen for its role as the major representative of the ABC-type tripartite pumps, while the proton/drug antiporter AcrAB-TolC was chosen as the most clinically relevant and best characterized of the tripartite efflux pumps. The detailed structure and assembly mode of the MacAB-TolC complex is largely unknown, while for AcrAB-TolC, some structural studies have been made, though none of them of the native protein. During my experimental work I managed to overexpress both efflux pumps directly in the organism they stem from (*S. enterica* serovar Typhimurium), therefore allowing assembly in native conditions. An established protocol allowed the isolation from membrane fractions and visualization of the near-native efflux pumps in negative-stain electron microscopy and for AcrAB-TolC also in cryo-EM. For individual expression of the two pumps, a mutant strain was constructed where presumably no other major tripartite efflux pumps are highly expressed, ensuring a more reliable identification and assignment of visualized pump-shaped particles. Furthermore, the periplasmic component of MacAB-TolC was purified and used for production of polyclonal antibodies, and the functionality of plasmid-expressed pump operons was assessed.

Ultimately, we hope that our efforts will lead to a better structural and mechanistic understanding of these tripartite efflux pumps and contribute to the development of new strategies to fight multidrug resistance.

7 ZUSAMMENFASSUNG

Der intrazelluläre Krankheitserreger Salmonella infiziert sowohl menschliche als auch tierische Wirte und ist eine häufige Ursache von Lebensmittelinfektionen. Abhängig von der Subspezies kann er entweder eine Magen-Darm-Infektion oder eine systemische Erkrankung verursachen. Während in leichten Fällen meist keine besondere Behandlung notwendig ist, werden schwerere Formen der Krankheit mit Antibiotika behandelt. Dabei ist die Evolution von multiresistenten Stämmen ein wiederkehrendes klinisches Problem bei *Salmonella* wie auch bei anderen Gram-negativen Bakterien, etwa *E. coli* oder *Pseudomonas aeruginosa*. Die Multiresistenz betrifft nicht nur Antibiotika, sondern auch andere toxische Substanzen wie Detergentien und Desinfektionslösungen und ist oft verbunden mit einer erhöhten Fähigkeit der Bakterien, diese Substanzen mit Hilfe von aktiven Membrantransportern zu exportieren. Diese sogenannten „multidrug efflux pumps“ reichen in Gram-negativen Bakterien oft durch beide Membranen und bestehen aus drei Komponenten in unterschiedlicher Kopienzahl: i) einem Transporter in der inneren Membran, der die Energie für den Substrattransport liefert, ii) einem Kanal in der äußeren Membran, und iii) einem periplasmatischen Adaptorprotein, welches als verbindendes Element zwischen den beiden dient. Basierend auf ihrer Funktionsweise werden diese Effluxpumpen eingeteilt in primäre Pumpen, die ATP als primäre Energiequelle verwenden, und sekundäre Pumpen, die als Ionen/Substrat Antiporter wirken und die elektrochemische Potentialdifferenz an der inneren Membran ausnutzen. Die vorliegende Studie untersucht je ein Mitglied beider Klassen: Ausgewählt wurden MacAB-TolC als der wichtigste Repräsentant der tripartiten Pumpen vom ABC-Typ sowie der Proton/Substrat Antiporter AcrAB-TolC, der die klinisch relevanteste und am besten untersuchte tripartite Effluxpumpe ist. Die detaillierte Struktur und der Assemblierungsmodus des MacAB-TolC Komplexes ist großteils unbekannt, während zur AcrAB-TolC Pumpe bereits einige strukturelle Studien durchgeführt wurden – allerdings keine davon mit dem nativen Proteinkomplex. Während meiner experimentellen Arbeit konnte ich beide Effluxpumpen direkt im Ursprungsorganismus (*S. enterica* serovar Typhimurium) überexprimieren, wodurch die Assemblierung unter nativen Bedingungen erfolgen kann. Ein etabliertes Protokoll ermöglichte die Isolierung aus Membranfraktionen und die Visualisierung von beinahe-nativen Effluxpumpen in „negative-stain“ Elektronenmikroskopie sowie im Falle von AcrAB-TolC auch in der Kryo-Elektronenmikroskopie. Für die individuelle Expression der zwei Pumpen wurde ein Deletionsstamm generiert, in dem keine anderen wichtigen tripartiten Effluxpumpen stark exprimiert werden, die die verlässliche Identifikation und Zuordnung der sichtbaren Partikel stören könnten. Weiters wurde die periplasmatische Komponente von MacAB-TolC aufgereinigt und für die Produktion polyklonaler Antikörper verwendet, und die Funktionalität der Plasmid-exprimierten Pumpen wurde bestätigt.

Wir hoffen, dass unsere Bemühungen zu einem besseren strukturellen und mechanistischem Verständnis der tripartiten Effluxpumpen führen und zur Entwicklung neuer Strategien zur Bekämpfung multiresistenter Keime beitragen können.

8 SUPPLEMENTARY MATERIAL

8.1 Amino acid sequences and secondary structure predictions of MacA and MacB from *Salmonella typhimurium*

8.1.1 MacA

- UniProt entry: A0A0F6AZ79
- Alternative gene name: ybjY
- Protein inferred by homology

MRAKGKKFKKRYLVIILILLVGGMAGWRMINAPLPTYQTLIVRPGDLEQSVLATGKLDALRKVDVGAQVSGQLKTLL
VSIGDNVKKDQLLGVIDPDQAENQIKEVEATLMELNAERQQAAAELKLARVTLARQQQLAKTQAVSQQDLDTAAT
EMAVKQARIGTIDAQIKRNRASLDTAKTNLEYTRIVAPMAGEVTQITTLQGQTVIAAQQAPNILTLADMSTMLVKA
QVSEADVIHLRAGQKAWFTIAGDPQTRYEGVLKDILPTPEKINDAIFYYARFEVPNPKRILRLDMTAQVYIQLMDVK
NVLIIPLAALGEPVGGNRYKVALLRNGEKREREVVIGERNDTDVEVVKGLEAGDEVIIGESRPGATP

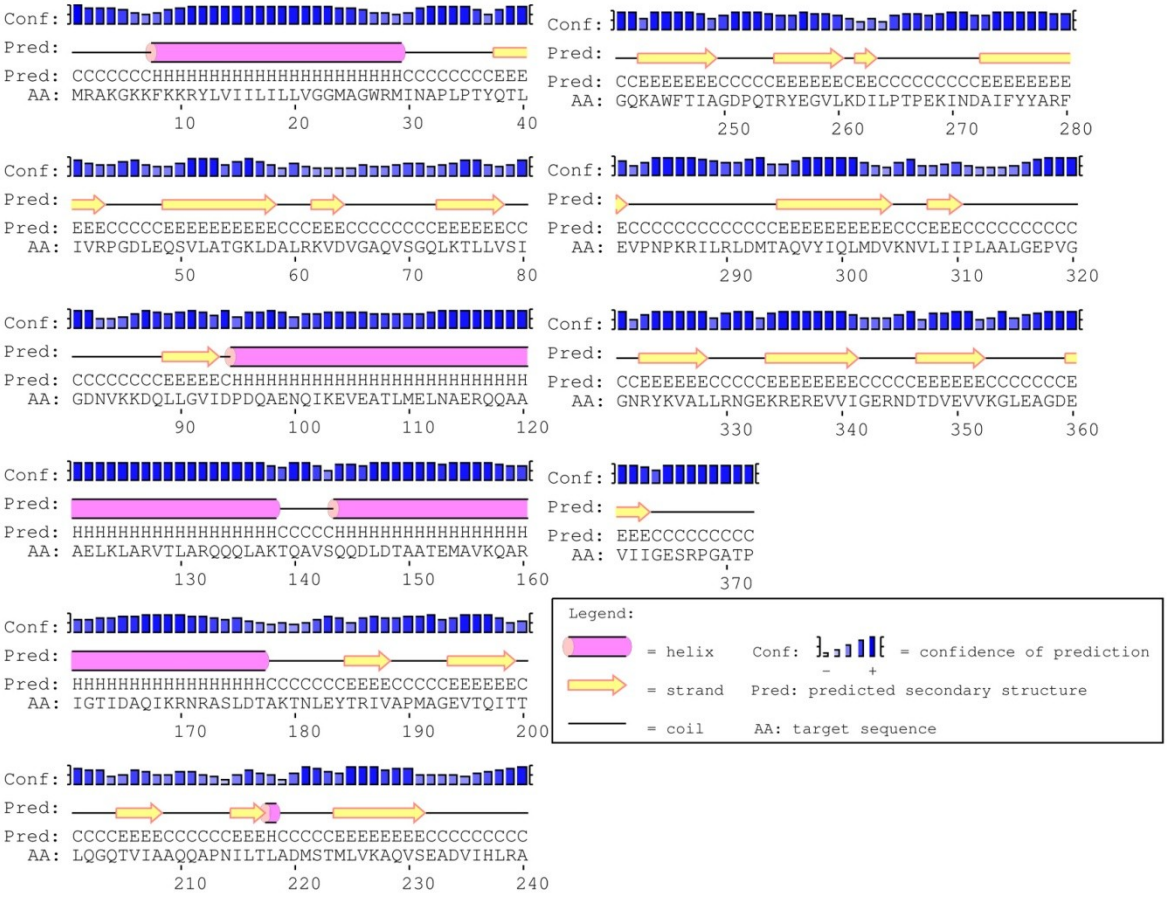

Secondary structure prediction was performed using the PSIPRED web server (http://bioinf.cs.ucl.ac.uk/psipred/) with the sequence listed above. The predicted trans-membrane helix is highlighted in green.

8.1.2 MacB

- UniProt entry: Q8ZQE4
- Alternative gene name: ybjZ
- Protein inferred by homology

MTALLELCNVSRSYPSGEEQVAVLKDISLQIHAGEMVAIVGVSGSGKSTLMNILGCLDKPTSGTYRVAGRDVSTLDP
DALAQLRREHFGFIFQRYHLLSHLTAAQNVEIPAVYAGIERKKRQARARELLLRLGLSDRVDYPPSQLSGGQQQRVSI
ARALMNGGQVILADEPTGALDSHSGEEVMAILRQLRDRGHTVIIVTHDPLIAAQAERIIEIHDGKIVHNPPAQEKKRE
QGVDAAVVNTAPGWRQFASSFREALSMAWLAMAANKMRTLLTMLGIIIGIASVVSIVVVGDAAKQMVLADIRA
MGTNTIDIHPGKDFGDDNPQYRQALKYDDLVAIQKQPWVNSATPSVSKSLRLRYGNIDIAVNANGVSGDYFNVYG
MSFREGNTFNAVQQQDRAQVVVLDANTRRQLFPNKANVVGEVVLAGNMPVIVIGVAEEKPSMYGNSNLLQVW
LPYSTMSDRIMGQSWLNSITVRVKDGVDSDQAEQQLTRLLTLRHGKKDFFTWNMDSVLKTAEKTTYTLQLFLTLVA
VISLVVGGIGVMNIMLVSVTERTREIGIRMAVGARASDVLQQFLIEAVLVCLVGGALGISLSMFIAFMLQLFLPGWEI
GFSLTALASAFLCSTFTGILFGWLPARNAARLDPVDALARE

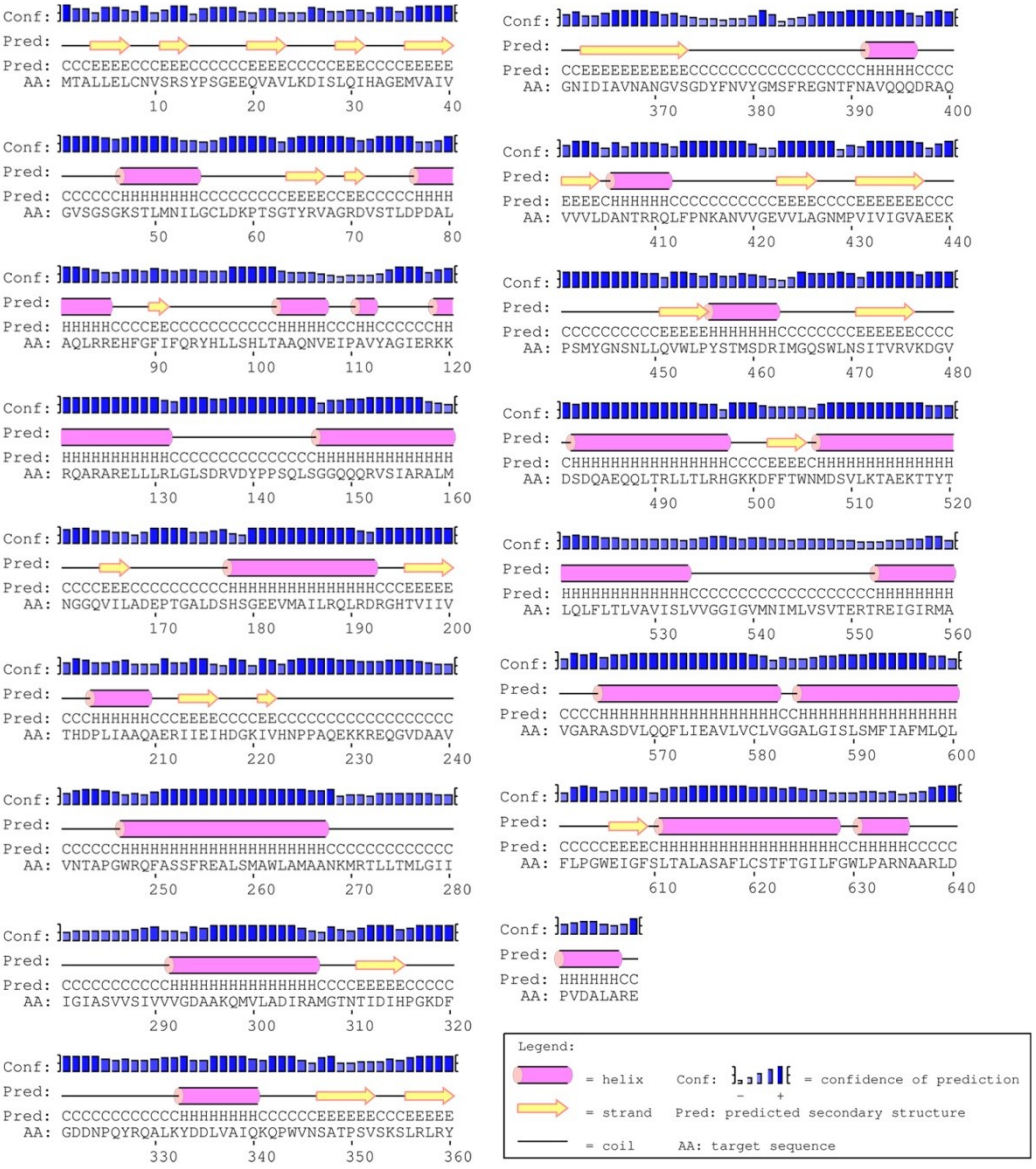

Secondary structure prediction was performed using the PSIPRED web server (http://bioinf.cs.ucl.ac.uk/psipred/) with the sequence listed above.

8.2 Size exclusion chromatography standard run

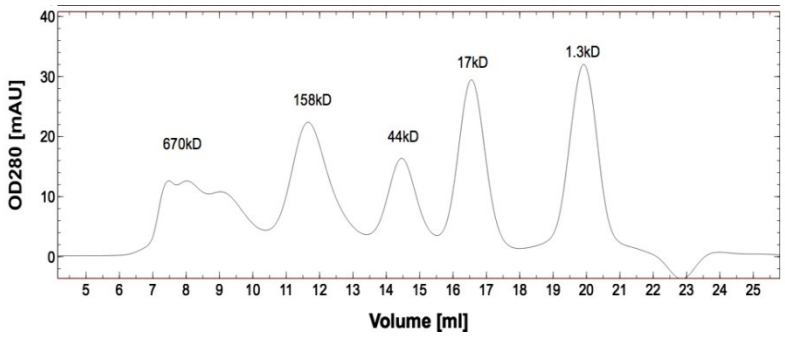

Figure S1 (left): Size exclusion chromatography profile (Superdex S200) of the "Gel Filtration Standard Lyophilized" from BioRad. For the standard run, the same buffer was used as in the elution of the MacAΔN sample (see Material and Methods).

column Superdex S200
void 7 ml

ml	Da	Log10 MW
8	670	2,8261
11,6	158	2,1987
14,5	44	1,6435
16,6	17	1,2304
19,9	1,3	0,1139

calculation	
slope	-0,2216
intercept	4,7309
correlation	-0,9869

calculation of specific molecular weight based on standard curve
y=kx+d
Mr=10^(y)

elution of unknown prot 13 ml
Mr of unknown protein 70,90 kD

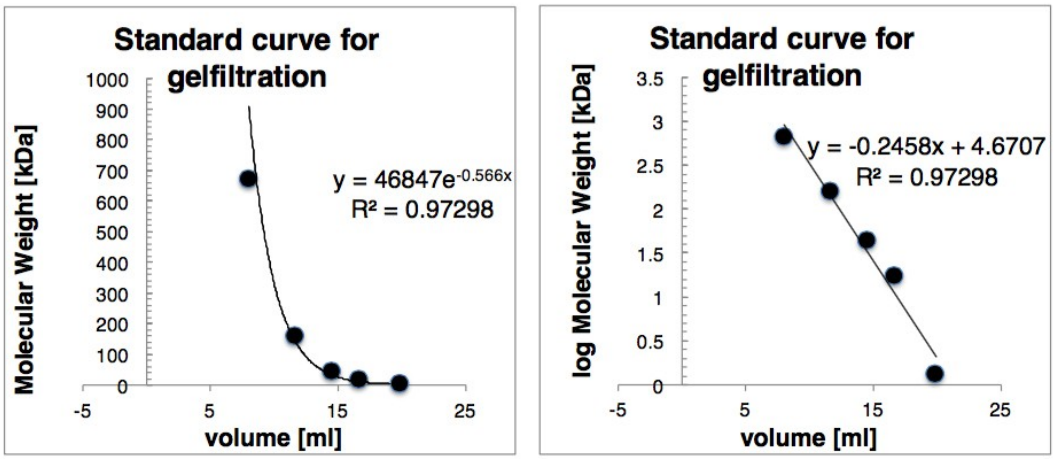

Figure S2: Based on the standard run, a calibration curve was established and used to calculate the specific molecular weight of the eluted sample.

8.3 Anti-MacA polyclonal antibody test

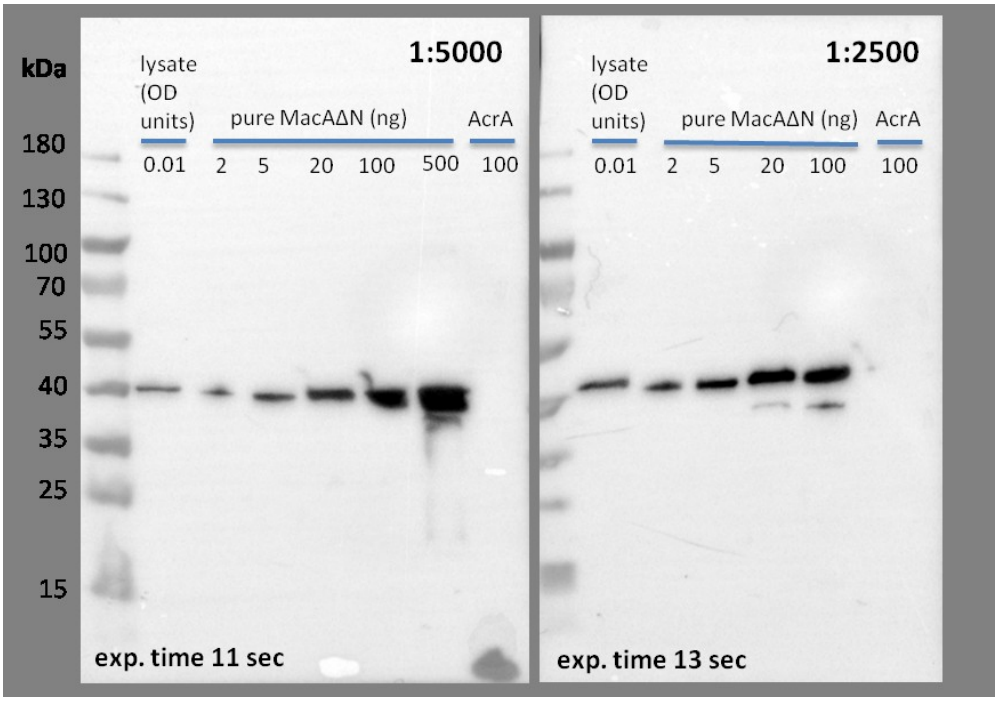

Figure S3: A polyclonal antibody was raised against *Salmonella* MacAΔN in rabbit and tested on purified MacAΔN and cell lysate from SB905ΔABΔDΔEF_ramA_MacAB (harvested 5 hours after induction). For the test, the Western Blots were incubated with the serum containing the antibody in the given dilutions for 1 hour, followed by incubation with secondary antibody (anti-rabbit HRP, 1:10000) for one hour. Exposure times are given for each blot separately.

8.4 Membrane isolation of non-efflux pump expressing control strain

As a negative control for MacAB-TolC and AcrAB-TolC isolation and visualization, the same protocol was carried out in the same *Salmonella* strain (see Materials and Methods) lacking the expression plasmid (pQE70). Fraction 2 after the CsCl gradient was visualized with negative-stain EM under the same conditions as for the actual isolation experiments (see Materials and Methods).

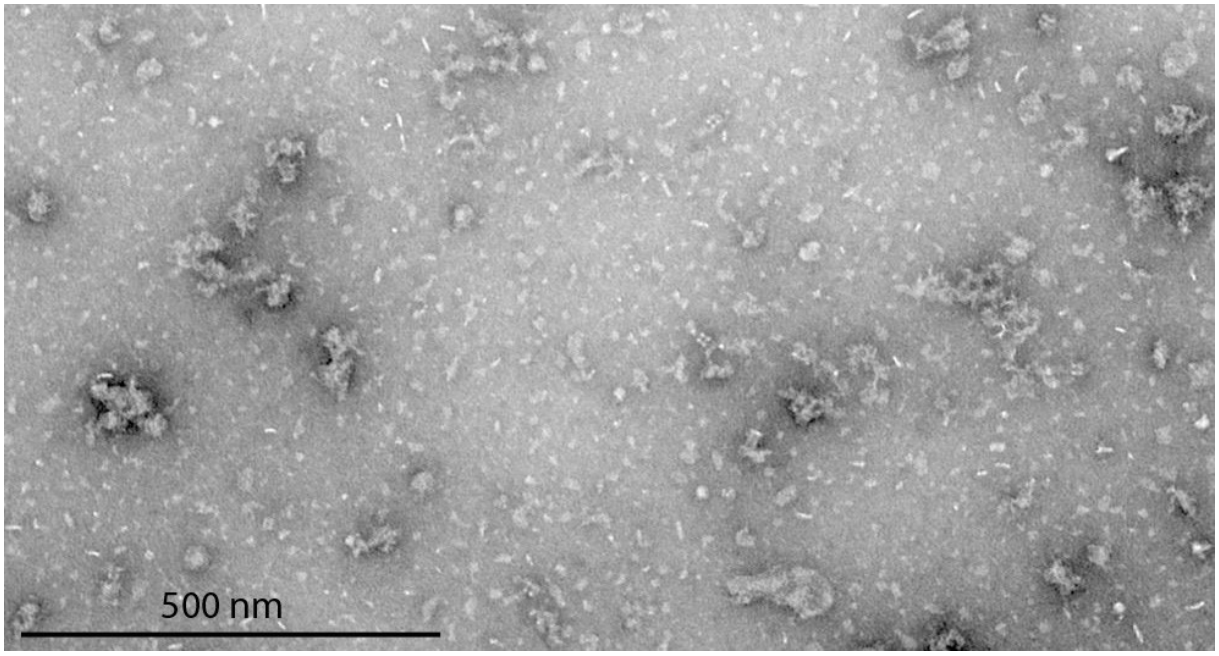

Figure S4: Representative negative-stain image of fraction 2 (dilution 1:25) after the CsCl-gradient (negative control experiment). No distinct pump-shaped particles as in the AcrAB-TolC and MacAB-TolC isolations are visible.

8.5 Plasmid maps

The schematic maps of the plasmids used in this study can be found here. More information regarding backbone origin, cloning strategy and used primers can be found in Section 3.2 (Lists and Tables).

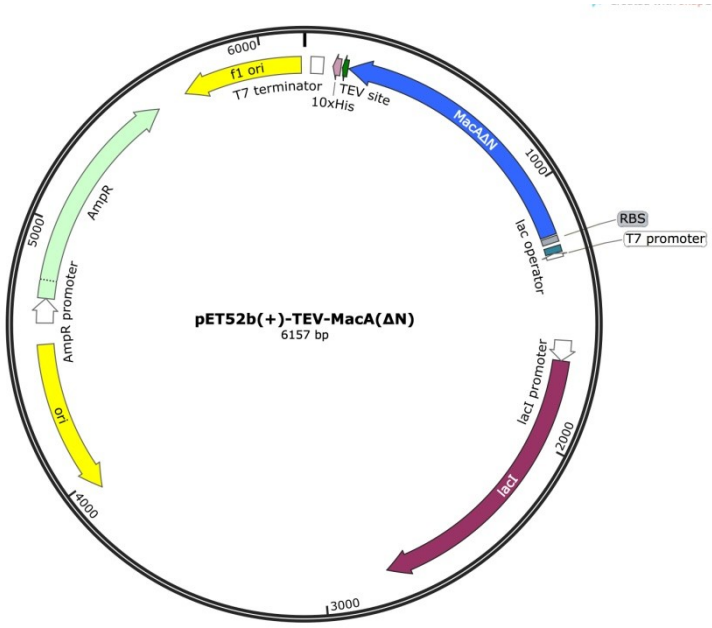

Figure S5: Plasmid map of pET52b(+)-TEV-MacAΔN

The coding sequence of *S. enterica* MacA (lacking amino acids 2-31) was cloned into pET52b(+) and the thrombin cleavage site was exchanged for a TEV cleavage site.

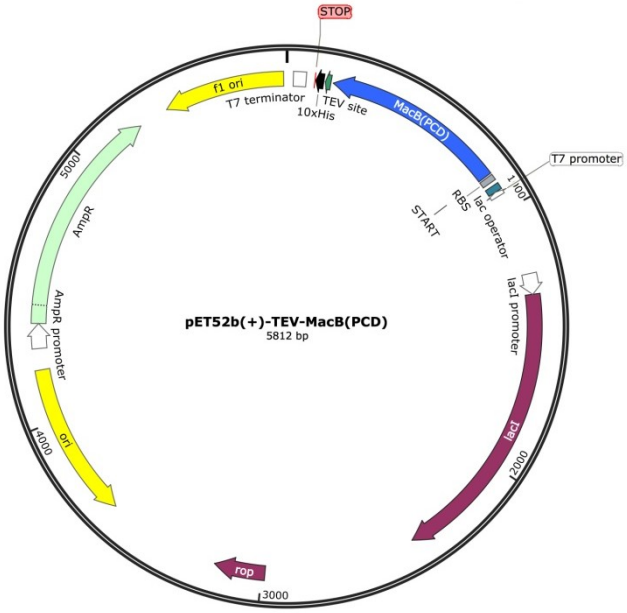

Figure S6: Plasmid map of pET52b(+)-TEV-MacB

The coding sequence of the periplasmic core domain of *S. enterica* MacB was cloned into pET52b(+) and the thrombin cleavage site was exchanged for a TEV cleavage site.

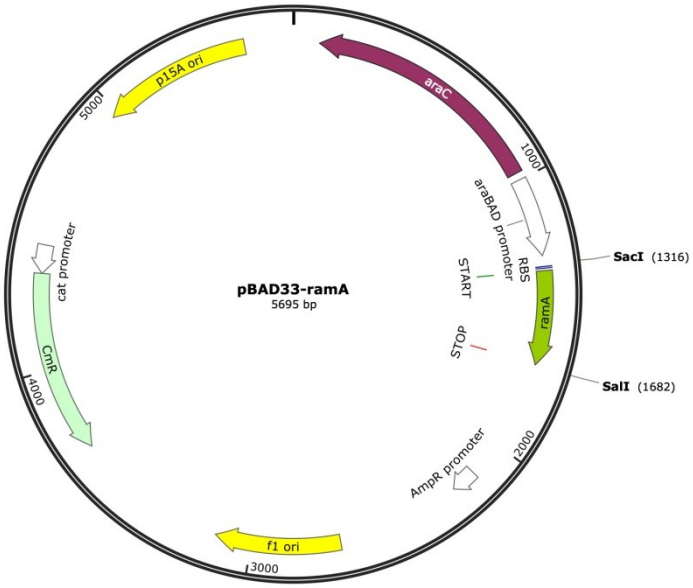

Figure S7: Plasmid map pBAD-ramA

The coding sequence of the *S.enterica* RamA protein was cloned into the pBAD33 vector under the control of an aribonose-inducible promoter.

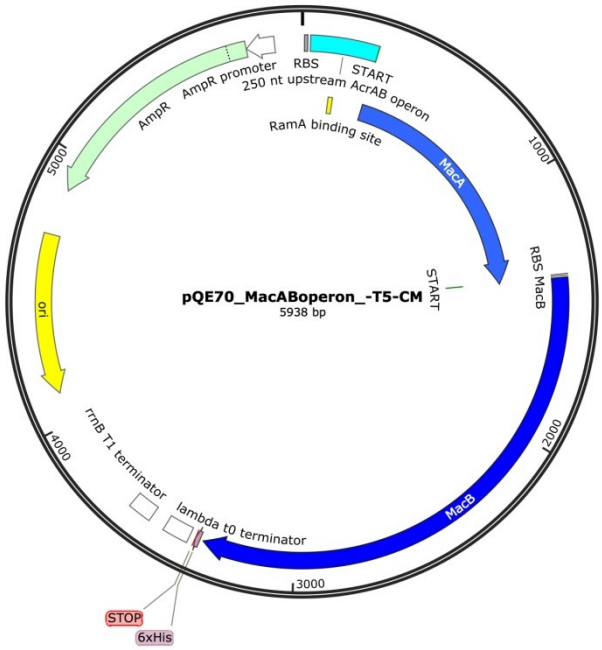

Figure S8: Plasmid map of pQE70-macAB_operon (--T5 –CAM)

The genetic sequence of the *S. enterica macAB* operon preceded by a RamA binding site was cloned into a pQE70 vector. The T5 promoter and a partial chloramphenicol resistance cassette (CAM) were deleted from the backbone.

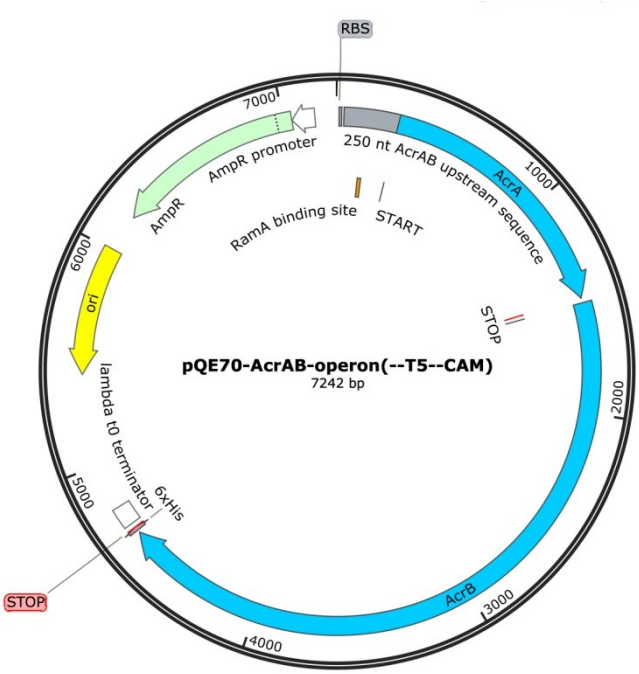

Figure S9: Plasmid map of pQE70-acrAB_operon (--T5 –CAM)

The genetic sequence of the *S. enterica acrB* operon preceded by its endogenous upstream region (250 nt) including a RamA binding site was cloned into a pQE70 vector. The T5 promoter and a partial chloramphenicol resistance cassette

8.6 Complete genomic sequences of all proteins used in this study:

MacA

>gi|16763390:**1018604-1019732** Salmonella enterica subsp. enterica serovar Typhimurium str. LT2 chromosome, complete genome (gene name: ybjY)

ATGCGTGCTAAGGGAAAGAAATTTAAAAAGCGTTATCTGGTCATTATTTTAATTCTTTTAGTGGGGGGGATGGCTGGCTGGCGAATGAT
AAATGCCCCGCTGCCAACTTATCAGACATTAATCGTGCGGCCAGGCGATCTTGAACAGAGTGTACTGGCGACTGGAAAACTGGACGCGT
TGCGTAAAGTGGATGTCGGCGCGCAGGTGAGCGGCCAGTTGAAAACGCTGCTGGTCTCCATTGGCGATAACGTTAAAAAAGATCAGCT
ACTCGGCGTGATTGACCCAGATCAGGCGGAGAACCAGATAAAAGAGGTCGAGGCCACCCTGATGGAGCTGAACGCGGAGCGTCAGCA
GGCAGCCGCTGAGTTAAAGCTGGCGCGGGTTACGCTGGCGCGCCAGCAGCAGTTAGCTAAGACTCAGGCGGTATCGCAACAGGATCTG
GATACCGCGGCGACGGAGATGGCGGTTAAACAGGCGCGTATTGGCACCATAGATGCCCAGATCAAACGTAATCGGGCCTCGTTGGACA
CCGCGAAAACCAACCTGGAATATACCCGTATTGTCGCCCCCATGGCGGGGGAAGTGACGCAAATCACTACCCTGCAAGGACAAACGGTG
ATTGCAGCTCAGCAGGCGCCCAATATTCTGACGCTGGCGGATATGAGCACCATGCTGGTAAAAGCGCAGGTCTCGGAAGCGGACGTGA
TCCATCTTCGGGCGGGGCAGAAAGCATGGTTCACCATTGCAGGCGATCCGCAAACGCGCTATGAAGGCGTTTTAAAAGATATTCTGCCG
ACGCCGGAAAAGATCAACGACGCTATTTTTTATTACGCCCGGTTTGAAGTGCCGAATCCCAAAAGAATCTTGCGTCTTGATATGACCGCA
CAGGTTTATATTCAACTCATGGATGTCAAAAATGTGCTGATTATTCCTCTCGCCGCGCTTGGCGAACCGGTGGGCGGCAATCGTTATAAA
GTGGCGCTGTTGCGTAACGGCGAAAAACGTGAGCGCGAAGTGGTCATTGGCGAGCGTAACGATACAGACGTGGAAGTGGTTAAAGGT
CTGGAAGCGGGCGATGAGGTGATCATCGGCGAAAGCAGGCCAGGAGCGACGCCATGA

The start and stop codon are highlighted in green and red, respectively. The sequence marked in yellow was deleted for protein purification purposes.

MacB

>gi|16763390:**1019729-1021675** Salmonella enterica subsp. enterica serovar Typhimurium str. LT2 chromosome, complete genome (gene name: ybjZ)

ATGACGGCATTGCTTGAACTGTGCAATGTGAGTCGTAGCTACCCCTCCGGAGAAGAGCAGGTGGCGGTGTTGAAAGATATCTCCCTGCA
AATCCACGCCGGGGAGATGGTGGCGATCGTCGGCGTTTCCGGTTCTGGAAAATCAACGCTGATGAATATCCTCGGGTGCCTGGATAAAC

CGACCAGCGGCACTTATCGGGTGGCGGGGCGGGACGTCTCGACGCTGGACCCGGACGCGCTGGCGCAGCTGCGGCGTGAGCATTTTGG
CTTTATCTTTCAGCGCTACCATCTGTTGTCGCATTTAACGGCAGCGCAAAATGTTGAAATCCCCGCCGTCTACGCCGGCATTGAACGCAAA
AAACGCCAGGCGCGCGCCAGAGAGTTGCTTTTGCGGCTGGGATTAAGCGATCGCGTCGATTACCCGCCTTCACAGCTTTCTGGCGGACA
GCAGCAGCGTGTCAGTATTGCCCGCGCTCTGATGAACGGCGGACAGGTGATTCTGGCAGATGAGCCGACCGGCGCGCTGGATAGCCAT
TCCGGCGAAGAGGTGATGGCGATTTTGCGCCAACTGCGCGATCGCGGACATACGGTGATCATTGTGACGCACGATCCGCTGATTGCCGC
CCAGGCGGAGCGGATTATTGAAATTCACGATGGCAAGATTGTCCATAATCCGCCCGCGCAGGAAAAGAAACGCGAACAGGGCGTTGAC
GCTGCCGTAGTTAATACGGCTCCCGGCTGGCGGCAATTTGCCAGCAGCTTTCGCGAAGCGCTGTCAATGGCGTGGTTAGCGATGGCCGC
TAACAAAATGCGTACTTTACTGACCATGCTGGGAATTATTATCGGTATTGCGTCGGTGGTGTCGATTGTGGTGGTCGGCGACGCCGCAAA
ACAGATGGTACTGGCGGATATCCGCGCTATGGGCACTAACACGATTGATATTCATCCAGGCAAAGATTTTGGCGACGACAACCCGCAGT
ATCGACAGGCGCTGAAATATGACGATCTGGTGGCTATTCAGAAACAGCCGTGGGTTAACTCTGCGACGCCCAGCGTTTCAAAGAGCTTA
CGTCTTCGCTATGGCAATATTGATATTGCCGTAAATGCTAATGGCGTCAGTGGCGATTATTTTAACGTTTACGGCATGTCCTTTAGGGAGG
GGAACACCTTCAATGCTGTACAGCAACAGGATCGCGCGCAGGTGGTGGTGCTGGATGCCAACACGCGACGCCAGCTATTTCCAAATAAA
GCGAATGTCGTAGGGGAAGTGGTGCTGGCGGGTAATATGCCGGTTATTGTTATTGGCGTGGCGGAAGAGAAACCGTCCATGTACGGCA
ATAGCAATCTGTTGCAAGTTTGGTTGCCCTATAGCACGATGTCAGATCGCATAATGGGTCAGTCATGGCTTAACTCGATCACCGTTCGTGT
GAAAGATGGCGTTGATAGCGATCAGGCTGAACAGCAGCTTACTCGCCTGCTCACCTTACGCCACGGTAAAAAAGACTTCTTCACCTGGAA
TATGGACAGCGTCCTGAAAACGGCTGAAAAAACCACCTATACTCTTCAGTTATTTCTGACGCTGGTGGCTGTCATTTCGCTGGTTGTCGGC
GGCATCGGCGTTATGAATATTATGCTGGTTTCCGTCACCGAGCGAACGCGTGAAATCGGCATCCGTATGGCGGTAGGCGCGCGCCAG
CGATGTGCTACAGCAGTTTCTTATTGAAGCGGTGCTGGTTTGCCTGGTTGGTGGAGCGCTGGGGATTAGCTTGTCGATGTTCATCGCATT
TATGCTACAGCTTTTCCTGCCCGGCTGGGAGATCGGTTTTTCACTGACTGCGCTGGCGAGCGCGTTTTTATGTTCGACGTTTACCGGGATA
CTGTTTGGCTGGCTACCGGCGAGAAACGCGGCGCGACTGGACCCGGTGGATGCGCTGGCAAGGGAGTAA

The start and stop codon are highlighted in green and red, respectively. The sequence marked in cyan corresponds to the periplasmic core domain and was cloned individually for protein expression purposes.

TolC

>gi|16763390:**3348573-3350042** Salmonella enterica subsp. enterica serovar Typhimurium str. LT2 chromosome, complete genome

ATGAAGAAATTGCTCCCCATCCTTATCGGCCTGAGCCTGTCGGGGTTCAGCACACTAAGCCAGGCAGAGAACCTGATGCAAGTTTATCAG
CAAGCACGCCTGAGCAACCCGGAATTGCGTAAATCCGCTGCCGATCGCGATGCTGCATTCGAAAAAATTAACGAAGCGCGTAGTCCTTTA
CTGCCGCAACTGGGTTTAGGTGCCGACTACACCTACAGCAACGGTTATCGCGATGCGAACGGTATCAACTCCAATGAAACCAGCGCTTCT
CTGCAATTAACGCAGACGCTATTTGATATGTCGAAATGGCGTGGGCTCACCCTGCAAGAAAAAGCAGCAGGCATTCAGGATGTCACCTA
TCAGACCGATCAGCAGACGCTGATCCTCAATACCGCGAACGCGTATTTTAAGGTATTGAACGCTATTGATGTGCTTTCCTATACCCAGGC
GCAAAAAGAGGCTATCTACCGTCAGTTAGATCAAACGACGCAACGTTTTAACGTGGGTCTGGTCGCCATTACCGACGTGCAAAACGCCC
GTGCGCAATATGATACCGTACTGGCGAATGAAGTGACCGCCCGCAACAACCTGGATAACGCGGTAGAAGAGCTGCGCCAGGTAACCGG
CAATTATTACCCGGAGCTGGCGTCGCTTAACGTCGAGCATTTTAAAACCGACAAACCCAAAGCTGTTAATGCGCTGTTGAAGGAAGCGG
AAAACCGTAACCTGTCGCTGTTGCAGGCGCGTTTAAGTCAGGATCTGGCGCGCGAGCAAATCCGTCAGGCGCAGGATGGTCACCTGCCG
ACGCTGAATTTAACGGCCTCAACCGGCATTTCTGATACCTCTTATAGCGGTTCTAAAACCAACTCCACCCAGTACGACGATAGCAACATGG
GGCAGAATAAAATCGGCCTTAACTTCTCCCTGCCGCTGTATCAAGGTGGGATGGTTAACTCGCAGGTAAAACAGGCGCAGTATAACTTC
GTCGGCGCAAGCGAACAGCTGGAAAGCGCGCACCGTAGCGTGGTGCAGACCGTACGTTCTTCCTTTAACAATATTAACGCCTCCATCAG
CAGCATCAACGCGTATAAACAGGCGGTCGTTTCCGCGCAAAGTTCTTTGGATGCCATGGAAGCCGGTTACTCGGTCGGTACACGTACCAT
TGTTGACGTACTGGATGCCACCACCACTCTGTATGATGCCAAGCAGCAACTGGCCAACGCGCGTTATACCTATTTGATTAATCAGTTAAAT
ATCAAATATGCGCTCGGTACGCTGAACGAGCAGGATCTGCTCGCGCTTAACAGTACGTTGGGTAAACCTATCCCGACGTCGCCGGAAAG
CGTAGCGCCGGAAACGCCAGATCAGGATGCTGCCGCAGACGGTTATAATGCTCATAGCGCCGCGCCAGCAGTACAGCCGACCGCCGCTC
GCGCCAACAGCAATAACGGCAATCCATTCCGGCATTGA

The start and stop codon are highlighted in green and red, respectively.

AcrAB operon

>gi|16763390:c**533862-529247** Salmonella enterica subsp. enterica serovar Typhimurium str. LT2 chromosome, complete genome

TCTCCGCCAGCGAGGTTGCCGATACGCCTTGCTGCGAGAACAAACGCAGGGCCACATCCAGGATGTGTTGTCGTGTCTCCAGCGCTTGTT
GTTTGGTTTTTCGTGCCATATGTCGGTGAATTTACAGGCGTTAGATTTACATACATTTATGGATGTATGTACCATAGCACGACGATAATAT
AAACGCAGCAATGGGTTTAAGGACCTTTGACCATTGACCAATTTGAAATCGGACACTCGAGGTTTACATATGAACAAAAACAGAGGGTT
AACGCCTCTGGCGGTCGTTCTGATGCTCTCAGGCAGCTTAGCGCTAACAGGATGTGACGACAAACAGGACCAGCAAGGCGGCCAGCAG

ATGCCAGAAGTTGGGGTTGTCACACTAAAAACGGAACCACTGCAAATCACAACTGAACTTCCGGGTCGTACCGTTGCTTACCGTATCGCC
GAAGTTCGCCCGCAGGTAAGCGGCATTATCCTGAAGCGTAATTTCGTTGAGGGAAGTGATATCGAAGCGGGAGTCTCTCTCTATCAGAT
TGATCCTGCGACCTACCAGGCGACTTACGACAGCGCTAAGGGCGATCTGGCAAAAGCGCAGGCCGCCGCGAATATCGCTGAACTGACG
GTGAAGCGTTATCAAAAGCTGCTGGGTACGCAGTACATCAGTAAGCAGGAATACGATCAGGCGCTGGCTGACGCACAACAAGCGACTG
CCGCTGTTGTCGCAGCAAAAGCCGCCGTTGAAACCGCACGTATCAACCTGGCGTATACCAAAGTCACCTCGCCGATTAGCGGTCGTATTG
GTAAGTCATCCGTAACGGAAGGCGCACTGGTACAGAACGGTCAGGCGTCGGCGCTGGCGACAGTGCAGCAGCTGGACCCTATTTATGT
CGATGTGACCCAGTCCAGCAATGACTTCCTGCGCCTGAAGCAGGAGCTGGCAAATGGTTCGCTGAAACAGGAAAACGGCAAAGCGAAG
GTCGACCTGGTGACCAGCGACGGTATCAAATTCCCGCAGTCCGGTACGCTTGAGTTCTCCGACGTGACCGTTGACCAAACCACCGGGTCT
ATTACTTTGCGCGCCATCTTCCCTAACCCGGATCACACCTTATTGCCAGGAATGTTCGTTCGCGCACGTCTGCAGGAAGGGACAAAACCG
ACGGCATTACTGGTTCCACAACAGGGCGTTACCCGTACTCCACGCGGCGATGCCACGGTGCTGGTGGTTGGCGCTGATAACAAAGTGGA
AACCCGCCAAATCGTCGCAAGCCAGGCGATCGGCGATAAGTGGCTGGTGACTGACGGATTGAAAGCGGGCGACCGCGTAGTCGTCAGC
GGGCTGCAAAAAGTACGTCCTGGCGCACAGGTTAAAGTACAGGAAATTACCGCGGATAACAAACAGCAAGCCGCAAGCGGTGATCAAC
CTGCTCAGCCCAGGTCTTAACTTAAACAGGAGCCGTTAAGACATGCCTAATTTCTTTATCGATCGCCCTATATTTGCGTGGGTGATCGCCA
TCATCATCATGTTGGCAGGGGGGCTCGCGATCCTCAAATTGCCGGTAGCGCAATATCCGACGATTGCGCCACCAGCAGTGACGATCTCC
GCAACCTACCCTGGCGCTGATGCGAAAACGGTACAGGATACCGTCACGCAGGTTATCGAACAGAATATGAACGGTATCGATAACCTGAT
GTATATGTCCTCCAACAGTGACTCCACGGGGACCGTGCAGATCACGCTGACCTTTGAATCCGGCACCGATGCGGATATCGCGCAGGTTCA
GGTTCAGAACAAGTTGCAACTGGCAATGCCGTTACTTCCCCAGGAAGTACAGCAACAGGGCGTGAGCGTTGAGAAGTCCTCAAGTAGCT
TCCTGATGGTAGTGGGCGTCATTAACACCGACGGCACCATGACCCAGGAGGATATTTCGGATTACGTTGCCGCCAATATGAAAGATCCG
ATCAGCCGTACCTCTGGGGTGGGCGACGTCCAGCTGTTTGGTTCGCAATATGCGATGCGTATCTGGATGAATCCGACAGAGCTGACCAA
ATACCAACTGACGCCGGTCGACGTGATTAACGCGATCAAAGCGCAGAACGCCCAGGTCGCGGCAGGTCAGCTCGGTGGTACGCCGCCG
GTTAAAGGCCAGCAGCTTAACGCATCGATTATTGCCCAAACGCGTCTGACCTCAACGGATGAGTTTGGCAAAATCCTGCTGAAAGTGAAT
CAGGATGGCTCCCAGGTTCGTCTGCGGGATGTAGCGAAAATTGAGCTTGGCGGCGAGAACTACGACGTCATTGCGAAATTTAACGGTCA
GCCAGCGTCAGGTCTTGGCATCAAACTGGCTACCGGCGCCAACGCGCTGGATACCGCTACCGCTATTCGTGCCGAACTGAAAAAAATGG
AACCGTTCTTCCCGCCAGGGATGAAAATCGTCTACCCGTATGACACCACGCCGTTCGTGAAGATCTCTATTCATGAAGTGGTAAAAACGC
TGGTCGAAGCGATTATCCTCGTGTTCCTGGTGATGTACCTGTTCCTGCAGAACTTCCGCGCGACGTTGATTCCGACTATTGCGGTTCCGGT
GGTGTTGTTGGGAACCTTTGCCGTGCTTGCGGCATTCGGTTTCTCGATAAACACGCTGACGATGTTCGGGATGGTGCTCGCCATCGGCTT
GCTGGTGGATGACGCCATCGTGGTGGTCGAGAACGTCGAACGTGTTATGACGGAAGAAGGCCTTCCGCCGAAGGAAGCGACGCGCAA
ATCCATGGGCCAGATTCAGGGCGCATTGGTGGGTATCGCGATGGTACTGTCGGCGGTATTTATTCCGATGGCCTTCTTTGGCGGCTCAAC
CGGGGCAATTTATCGTCAGTTCTCTATCACCATCGTATCGGCGATGGCGCTGTCGGTGCTGGTCGCGCTGATCCTGACGCCTGCGCTGTG
CGCGACGATGCTCAAACCCGTCGCCAAAGGCGATCATGGCGAAGGGAAAAAAGGCTTTTTCGGCTGGTTTAACCGCCTGTTTGATAAGA
GCACGCATCACTACACCGATAGCGTAGGCAATATTCTGCGCAGCACCGGGCGTTATCTGCTGCTCTATCTCATTATCGTCGTCGGTATGGC
TTATCTGTTCGTTCGTCTGCCAAGCTCTTTCTTGCCGGATGAAGACCAGGGCGTATTCCTGACAATGGTCCAGCTCCCCGCGGGCGCAAC
GCAAGAGCGCACGCAAAAAGTGCTGGATGAGGTCACGGATTACTATCTGAACAAAGAGAAAGCCAACGTTGAATCGGTATTCGCCGTC
AACGGCTTCGGTTTTGCAGGGCGCGGTCAGAATACCGGTATTGCATTCGTGTCGTTGAAAGACTGGGCCGATCGTCCAGGCGAAAAAAA
CAAGGTTGAAGCGATTACCCAGCGGGCAACCGCAGCGTTTTCACAAATTAAAGATGCGATGGTCTTCGCCTTTAACCTGCCGGCGATCGT
TGAGCTGGGCACCGCAACCGGCTTTGACTTCGAGTTGATTGACCAGGCGGGACTTGGTCATGAAAAACTCACCCAGGCACGTAATCAGT
TGTTCGGCGAGGTGGCGAAATATCCTGATCTGCTGGTCGGCGTTCGACCTAACGGTCTGGAAGATACGCCGCAGTTTAAAATCGATATC
GACCAGGAAAAAGCTCAGGCGCTGGGCGTATCTATTAGCGACATTAATACCACGCTGGGCGCAGCATGGGGCGGCAGCTATGTAAACG
ACTTTATCGATCGCGGTCGTGTGAAGAAAGTTTACGTGATGTCCGAAGCGAAATACCGCATGTTGCCGGATGATATTAACGACTGGTAC
GTTCGTGGTAGCGATGGTCAGATGGTGCCATTCTCCGCATTCTCCTCTTCCCGCTGGGAATATGGTTCGCCGCGTCTGGAACGCTATAAC
GGTCTGCCTTCGATGGAAATTCTGGGGCAGGCGGCGCCAGGCAAGAGTACCGGTGAAGCGATGGCGATGATGGAAGAACTGGCCAGC
AAGCTGCCGTCAGGCATTGGGTATGACTGGACCGGGATGTCCTACCAGGAGCGGTTGTCCGGCAACCAGGCCCCTGCCCTGTATGCTAT
ATCGCTGATCGTCGTCTTCCTGTGTCTGGCGGCATTGTATGAGAGCTGGTCTATCCCGTTCTCCGTAATGCTGGTTGTTCCGCTTGGGGTT
ATCGGCGCGCTGCTGGCTGCGACCTTCCGCGGACTGACTAACGACGTTTACTTCCAGGTGGGCCTGCTCACAACCATTGGGTTGTCGGCG
AAGAACGCGATACTTATCGTCGAATTCGCCAAAGACTTAATGGATAAAGAAGGGAAAGGTCTGGTAGAAGCGACGCTGGAGGCCGTCC
GGATGCGTTTGCGCCCGATTCTGATGACCTCGTTAGCGTTCATGCTGGGGGTTATGCCGCTGGTTATCAGTTCCGGCGCGGGTTCCGGCG
CGCAGAATGCGGTAGGTACTGGCGTACTGGGCGGGATGGTAACGGCAACCGTACTGGCTATTTTCTTCGTACCGGTCTTCTTCGTGGTG
GTACGCCGCCGCTTTAGCCGTAAAAGCGAAGATATTGAGCATAGTCATTCGACAGAACATCGCTGA

The upstream sequence of the *acrAB* operon (250 nucleotides) encoding the RamA binding site (highlighted in yellow) was included. The *acrA* and *acrB* genes are highlighted in cyan and grey, respectively. The start codon is highlighted in green and the stop codon is highlighted in red.

MacAB operon

>gi|16763390: **1018604-1021675** Salmonella enterica subsp. enterica serovar Typhimurium str. LT2 chromosome, complete genome

ATGCGTGCTAAGGGAAAGAAATTTAAAAAGCGTTATCTGGTCATTATTTTAATTCTTTTAGTGGGGGGGATGGCTGGCTGGCGAATGAT
AAATGCCCCGCTGCCAACTTATCAGACATTAATCGTGCGGCCAGGCGATCTTGAACAGAGTGTACTGGCGACTGGAAAACTGGACGCGT
TGCGTAAAGTGGATGTCGGCGCGCAGGTGAGCGGCCAGTTGAAAACGCTGCTGGTCTCCATTGGCGATAACGTTAAAAAAGATCAGCT
ACTCGGCGTGATTGACCCAGATCAGGCGGAGAACCAGATAAAAGAGGTCGAGGCCACCCTGATGGAGCTGAACGCGGAGCGTCAGCA

GGCAGCCGCTGAGTTAAAGCTGGCGCGGGTTACGCTGGCGCGCCAGCAGCAGTTAGCTAAGACTCAGGCGGTATCGCAACAGGATCTG
GATACCGCGGCGACGGAGATGGCGGTTAAACAGGCGCGTATTGGCACCATAGATGCCCAGATCAAACGTAATCGGGCCTCGTTGGACA
CCGCGAAAACCAACCTGGAATATACCCGTATTGTCGCCCCCATGGCGGGGGAAGTGACGCAAATCACTACCCTGCAAGGACAAACGGTG
ATTGCAGCTCAGCAGGCGCCCAATATTCTGACGCTGGCGGATATGAGCACCATGCTGGTAAAAGCGCAGGTCTCGGAAGCGGACGTGA
TCCATCTTCGGGCGGGGCAGAAAGCATGGTTCACCATTGCAGGCGATCCGCAAACGCGCTATGAAGGCGTTTTAAAAGATATTCTGCCG
ACGCCGGAAAAGATCAACGACGCTATTTTTTATTACGCCCGGTTTGAAGTGCCGAATCCCAAAAGAATCTTGCGTCTTGATATGACCGCA
CAGGTTTATATTCAACTCATGGATGTCAAAAATGTGCTGATTATTCCTCTCGCCGCGCTTGGCGAACCGGTGGGCGGCAATCGTTATAAA
GTGGCGCTGTTGCGTAACGGCGAAAAACGTGAGCGCGAAGTGGTCATTGGCGAGCGTAACGATACAGACGTGGAAGTGGTTAAAGGT
CTGGAAGCGGGCGATGAGGTGATCATCGGCGAAAGCAGGCCAGGAGCGACGCCATGACGGCATTGCTTGAACTGTGCAATGTGAGTC
GTAGCTACCCCTCCGGAGAAGAGCAGGTGGCGGTGTTGAAAGATATCTCCCTGCAAATCCACGCCGGGGAGATGGTGGCGATCGTCGG
CGTTTCCGGTTCTGGAAAATCAACGCTGATGAATATCCTCGGGTGCCTGGATAAACCGACCAGCGGCACTTATCGGGTGGCGGGGCGGG
ACGTCTCGACGCTGGACCCGGACGCGCTGGCGCAGCTGCGGCGTGAGCATTTTGGCTTTATCTTTCAGCGCTACCATCTGTTGTCGCATT
TAACGGCAGCGCAAAATGTTGAAATCCCCGCCGTCTACGCCGGCATTGAACGCAAAAAACGCCAGGCGCGCGCCAGAGAGTTGCTTTTG
CGGCTGGGATTAAGCGATCGCGTCGATTACCCGCCTTCACAGCTTTCTGGCGGACAGCAGCAGCGTGTCAGTATTGCCCGCGCTCTGATG
AACGGCGGACAGGTGATTCTGGCAGATGAGCCGACCGGCGCGCTGGATAGCCATTCCGGCGAAGAGGTGATGGCGATTTTGCGCCAAC
TGCGCGATCGCGGACATACGGTGATCATTGTGACGCACGATCCGCTGATTGCCGCCCAGGCGGAGCGGATTATTGAAATTCACGATGGC
AAGATTGTCCATAATCCGCCCGCGCAGGAAAAGAAACGCGAACAGGGCGTTGACGCTGCCGTAGTTAATACGGCTCCCGGCTGGCGGC
AATTTGCCAGCAGCTTTCGCGAAGCGCTGTCAATGGCGTGGTTAGCGATGGCCGCTAACAAAATGCGTACTTTACTGACCATGCTGGGA
ATTATTATCGGTATTGCGTCGGTGGTGTCGATTGTGGTGGTCGGCGACGCCGCAAAACAGATGGTACTGGCGGATATCCGCGCTATGGG
CACTAACACGATTGATATTCATCCAGGCAAAGATTTTGGCGACGACAACCCGCAGTATCGACAGGCGCTGAAATATGACGATCTGGTGG
CTATTCAGAAACAGCCGTGGGTTAACTCTGCGACGCCCAGCGTTTCAAAGAGCTTACGTCTTCGCTATGGCAATATTGATATTGCCGTAA
ATGCTAATGGCGTCAGTGGCGATTATTTTAACGTTTACGGCATGTCCTTTAGGGAGGGGAACACCTTCAATGCTGTACAGCAACAGGATC
GCGCGCAGGTGGTGGTGCTGGATGCCAACACGCGACGCCAGCTATTTCCAAATAAAGCGAATGTCGTAGGGGAAGTGGTGCTGGCGGG
TAATATGCCGGTTATTGTTATTGGCGTGGCGGAAGAGAAACCGTCCATGTACGGCAATAGCAATCTGTTGCAAGTTTGGTTGCCCTATAG
CACGATGTCAGATCGCATAATGGGTCAGTCATGGCTTAACTCGATCACCGTTCGTGTGAAAGATGGCGTTGATAGCGATCAGGCTGAAC
AGCAGCTTACTCGCCTGCTCACCTTACGCCACGGTAAAAAAGACTTCTTCACCTGGAATATGGACAGCGTCCTGAAAACGGCTGAAAAAA
CCACCTATACTCTTCAGTTATTTCTGACGCTGGTGGCTGTCATTTCGCTGGTTGTCGGCGGCATCGGCGTTATGAATATTATGCTGGTTTCC
GTCACCGAGCGAACGCGTGAAATCGGCATCCGTATGGCGGTAGGCGCGCGCCAGCGATGTGCTACAGCAGTTTCTTATTGAAGCGGT
GCTGGTTTGCCTGGTTGGTGGAGCGCTGGGGATTAGCTTGTCGATGTTCATCGCATTTATGCTACAGCTTTTCCTGCCCGGCTGGGAGAT
CGGTTTTTCACTGACTGCGCTGGCGAGCGCGTTTTTATGTTCGACGTTTACCGGGATACTGTTTGGCTGGCTACCGGCGAGAAACGCGGC
GCGACTGGACCCGGTGGATGCGCTGGCAAGGGAGTAA

MacA is highlighted in cyan and MacB is highlighted in grey. Start and stop codons are marked in green and red, respectively. The MacA and MacB genes are overlapping by four nucleotides, which contain the MacA stop codon and the MacB start codon and are highlighted in yellow.

RamA

>gb|AE006468.1|:**638994-639357** Salmonella enterica subsp. enterica serovar Typhimurium str. LT2, complete genome

GTTTGATAGAGGGGAGAGCACGATGACCATTTCCGCTCAGGTTATCGACACGATTGTCGAGTGGATTGATGATAATTTGAATCAGCCGTT
ACGTATTGATGATATTGCCCGTCATGCGGGGTATTCCAAGTGGCACCTGCAGCGCCTTTTTATGCAGTACAAAGGGGAGAGTCTGGGAC
GCTACGTGCGTGAACGGAAGCTAAAACTGGCGGCGCGCGACCTGCTCGACACCGACCAGAAGGTGTATGATATTTGTCTCAAGTATGGT
TTTGATTCGCAGCAAACCTTTACGCGCATTTTTACCCGCACGTTCAACCTGCCGCCAGGCGCTTATCGTAAAGAAAAGCATGGCCGTACGC
ATTGA

The upstream sequence of the gene (22 nucleotides) was included to provide the endogenous ribosomal binding site (in yellow). The start and stop codon are highlighted in red and green, respectively. The gene is not annotated in the strain LT2 but was inferred by homology (alignment analysis using nucleotide BLAST).

8.7 SDS-PAGE Coomassie Gels

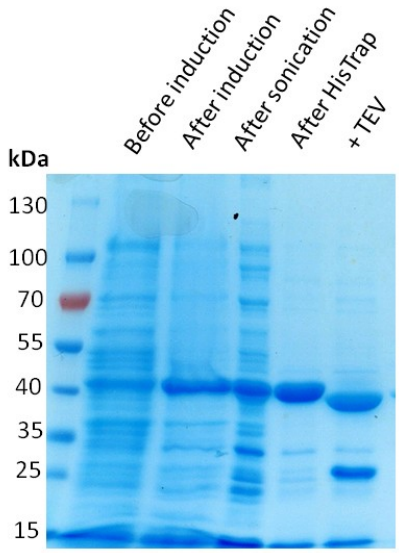

Figure S10: MacAΔN purification steps

Whole gel of SDS-PAGE after PAGE Blue staining. Sample of intermediate steps of MacAΔN purification were loaded as indicated.

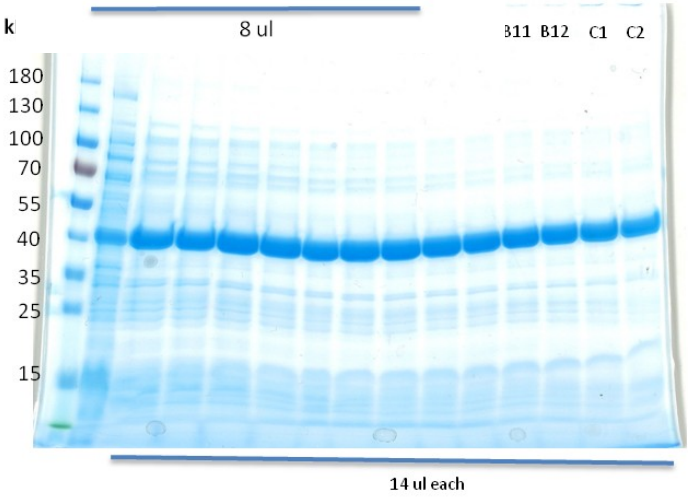

Figure S11: MacAΔN purification – HisTrap fractions

Whole gel of SDS-PAGE after PAGE Blue staining. The peak profile of HisTrap HP column was loaded as indicated. The original cell lysate sample was loaded on the left lane for comparison.

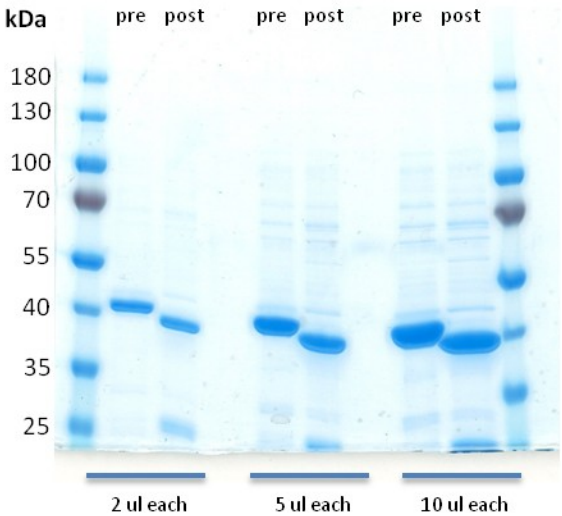

Figure S12: MacAΔN purification – sample before and after TEV cleavage

Whole gel of SDS-PAGE after PAGE Blue staining. The sample before and after TEV cleavage was loaded three times in three different amounts (as indicated).

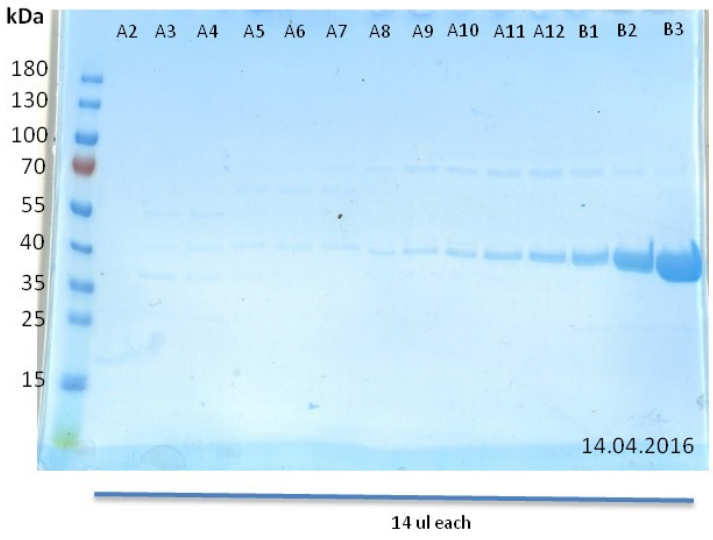

Figure S13: MacAΔN purification – Size exclusion fractions (1)

Whole gel of SDS-PAGE after PAGE Blue staining. The peak profile fractions of the size exclusion chromatography were loaded as indicated, starting on this gel and continuing on the next.

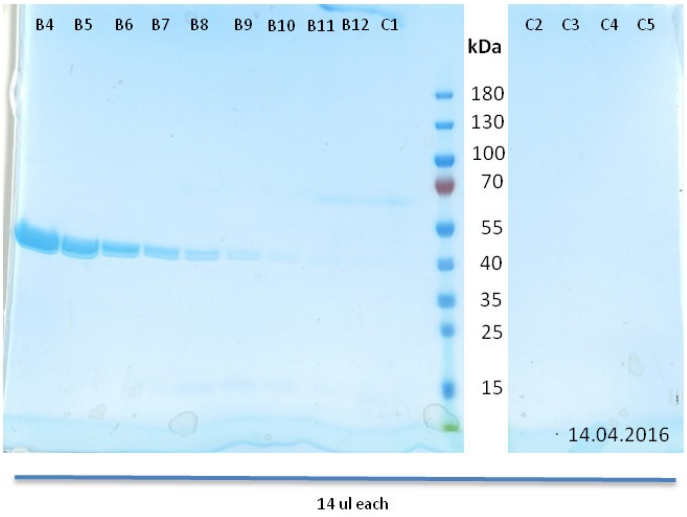

Figure S14: MacAΔN purification – Size exclusion fractions (2)

Whole gel of SDS-PAGE after PAGE Blue staining. The peak profile fractions of the size exclusion chromatography were loaded, starting on the previous gel and continuing on this one.

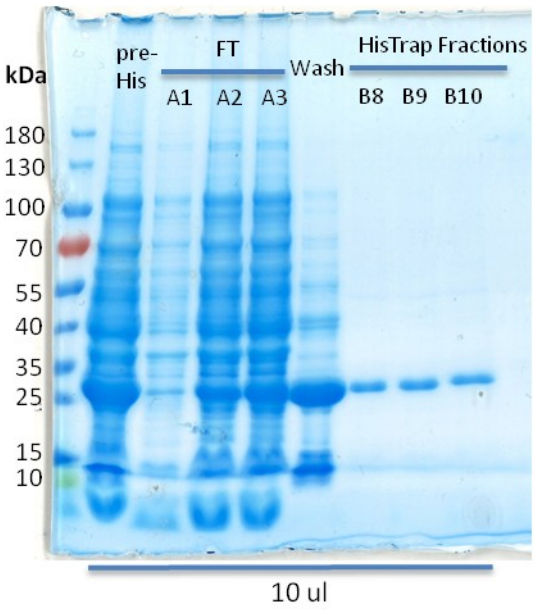

Figure S15: MacB-PCD purification – HisTrap fractions

Whole gel of SDS-PAGE after PAGE Blue staining. The sample applied to the HisTrap (left), the flowthrough (A1-A3) and wash fractions and the peak fractions were loaded as indicated.

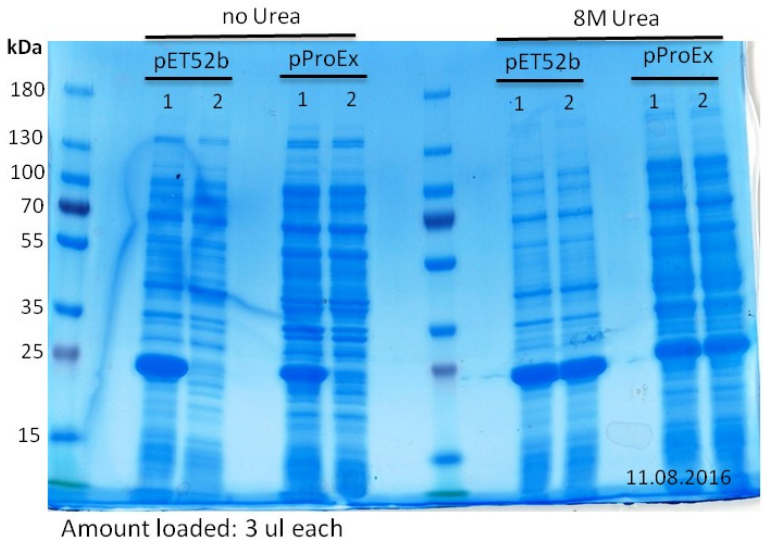

Figure S16: MacB-PCD overexpression

Whole gel of SDS-PAGE after PAGE Blue staining. Cell lysates from *E. coli* overexpressing MacB-PCD from two different vectors (pET52b and pProEx) dissolved in buffer with our without Urea are loaded as indicated.

1 … before centrifugation

2 … supernatant after centrifugation

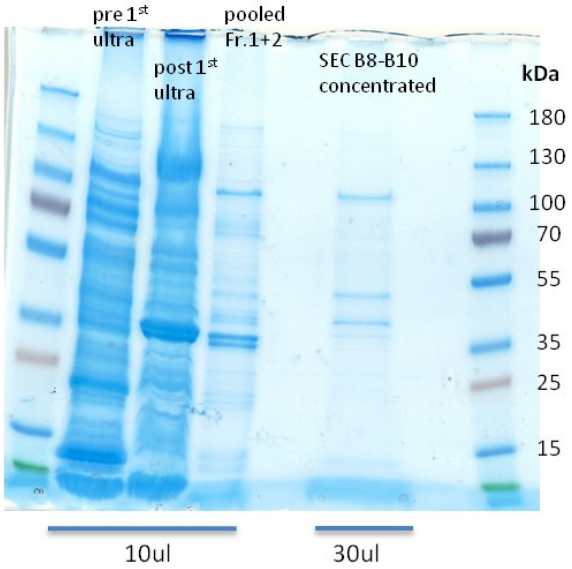

Figure S17: AcrAB-TolC isolation

Whole gel of SDS-PAGE after PAGE Blue staining. AcrAB-TolC was isolated from *SB905_ramA*. Intermediate steps from the isolation protocol as well as the final, pooled and concentrated size exclusion fractions were loaded as indicated.

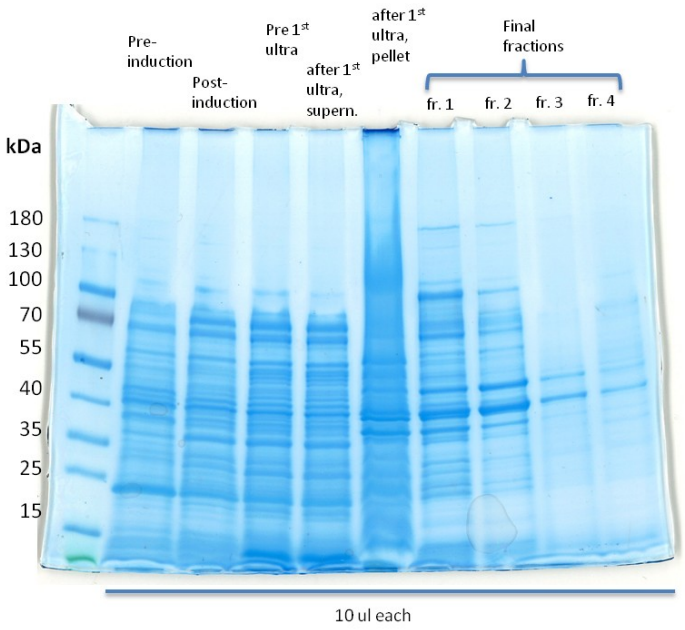

Figure S18: MacAB-TolC isolation

Whole gel of SDS-PAGE after PAGE Blue staining. MacAB-TolC was isolated from *SB905ΔABΔDΔEF_ramA_macAB*.

Intermediate steps from the isolation protocol as well as the final, pooled and concentrated size exclusion fractions were loaded as indicated.

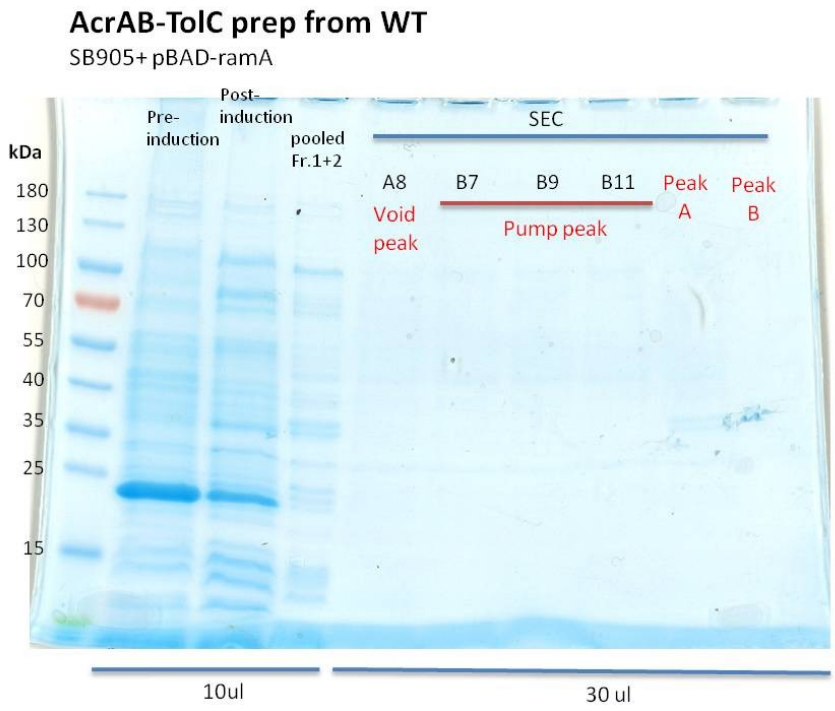

Figure S19: AcrAB-TolC isolation - SEC

Whole gel of SDS-PAGE after PAGE Blue staining. AcrAB-TolC was isolated from *SB905_ramA*. Cell lysate pre-induction and post-induction, pooled CsCl-fractions 1+2 as well as samples from all SEC peaks were applied. The protein concentration of individual fractions post-SEC is so small that it is close to the detection limit, if the sample is not concentrated before application to the gel.

8.8 Western Blots

TolC comparison in whole cell extracts

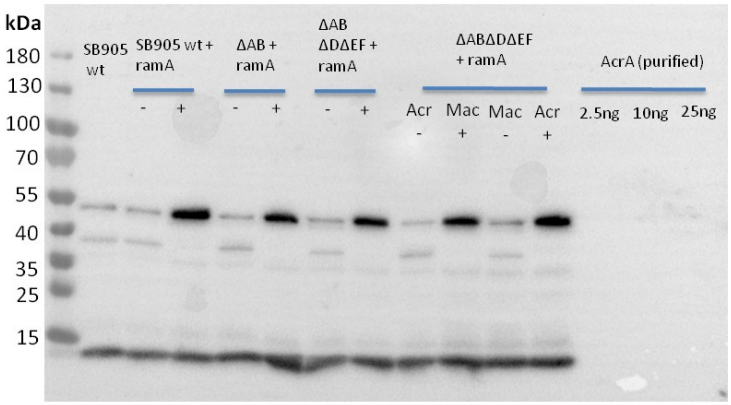

Amount loaded: 0.02 OD units each for whole cell extracts
anti-TolC (rabbit) 1:25 000 1h; anti-rabbit 1:10 000 1h

AcrA comparison in whole cell extracts

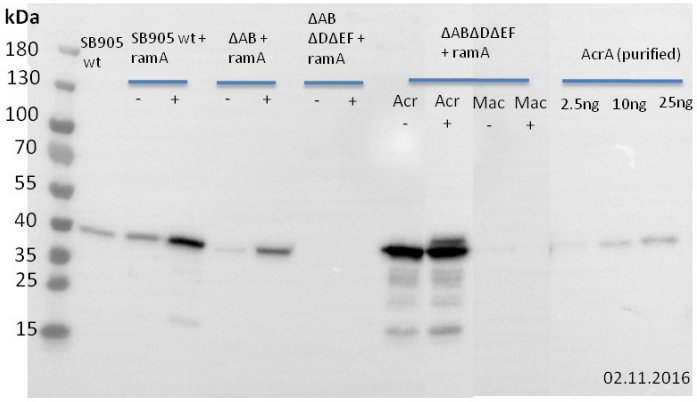

Amount loaded: 0.02 OD units each for whole cell extracts
anti-AcrA (rabbit) 1:50 000 1h; anti-rabbit 1:10 000 1h
- ... inuduced; + ... uninduced

Plasmid complementation

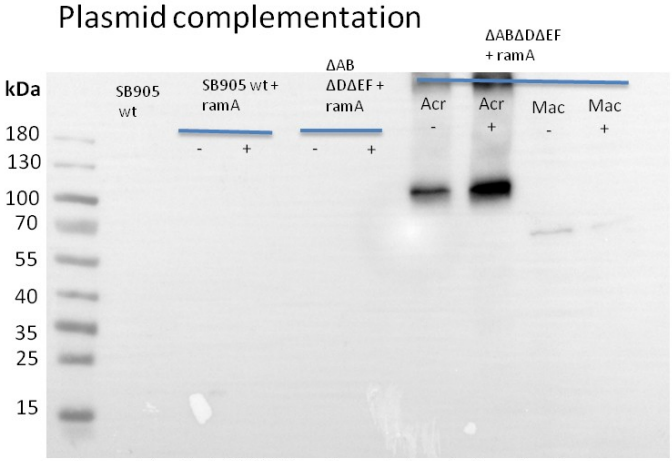

Amount loaded: 0.02 OD units each for whole cell extracts
anti-His (HRP coupled), 1:5000 overnight 4C

Plasmid complementation

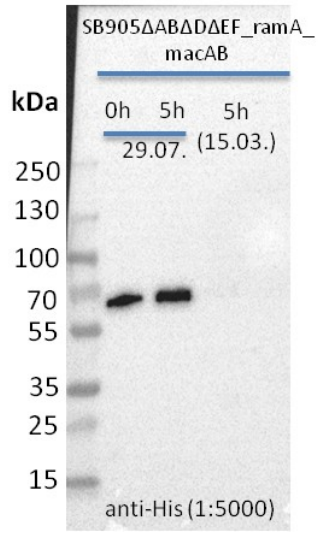

AcrAB-TolC prep from triple KO (CsCl gradient and SEC)

SB905ΔABΔDΔEF + pBAD-ramA + pQE70-AcrAB

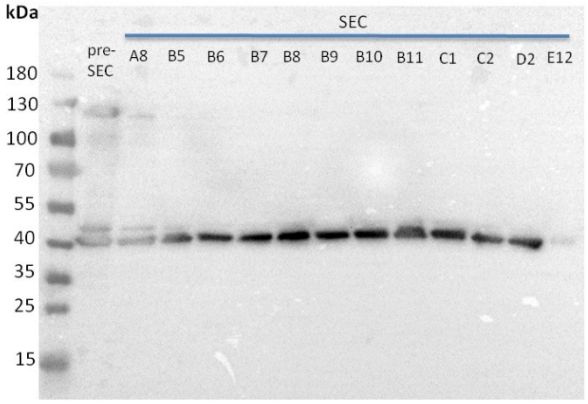

anti-AcrA 1h RT (1:50000)
anti-rabbit-HRP 1h RT (1:10000)
amount loaded: 1 ul each; except pre-SEC: 0.2 ul

AcrAB-TolC prep from triple KO (CsCl gradient and SEC)

SB905ΔABΔDΔEF + pBAD-ramA + pQE70-AcrAB

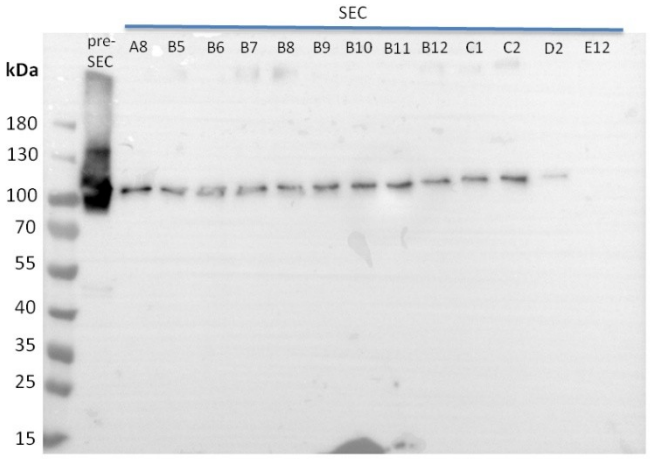

anti-His-HRP 1h RT (1:5000) --> recognizes AcrB-His
amount loaded: 1 ul each

AcrAB-TolC prep from triple KO (CsCl gradient and SEC)

SB905ΔABΔDΔEF + pBAD-ramA + pQE70-AcrAB

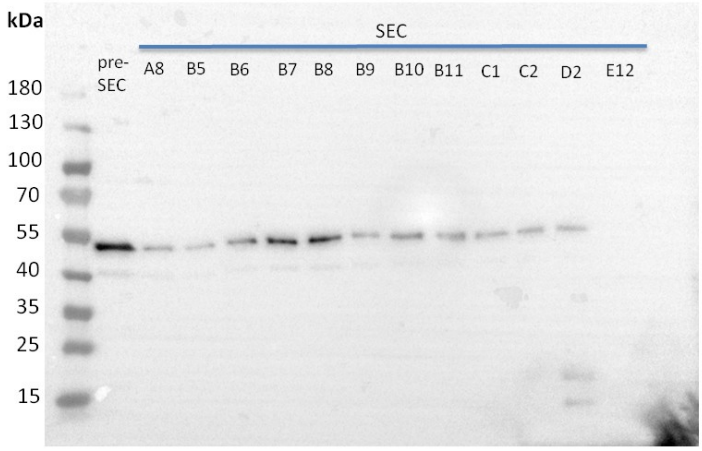

anti-TolC 1h RT (1:25000)
anti-rabbit-HRP 1h RT (1:10000)
amount loaded: 1 ul each; except pre-SEC: 0.2 ul

MacAB-TolC prep & detergent screen

SB905ΔABΔDΔEF + pBAD-ramA + pQE70-MacAB (--T5 --CAM)

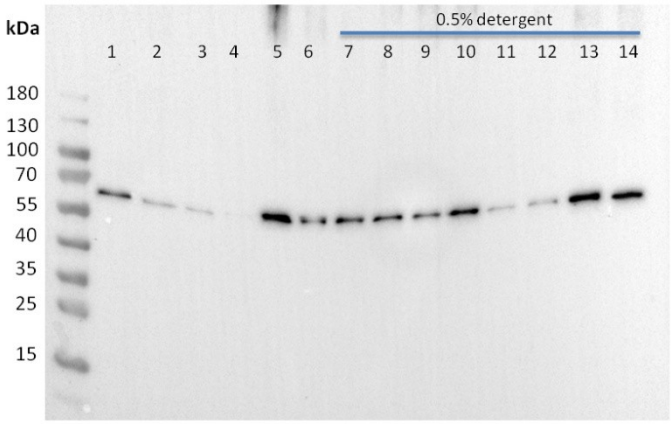

1) pre-induction
2) post-induction
3) before 1st ultra-centrifugation
4) after 1st ultra-centrifugation (supernatant)
5) after 1st ultra-centrifugation (redissolved pellet)
6) 0.1 % LDAO
7) Chapso
8) OG
9) DHPC
10) Triton X-100
11) deoxycholate
12) Brij 58
13) FC-12
14) DDM

anti-His-HRP 1h (1:5000)
amount loaded: 1 ul / 0.02 OD units each

Minicells

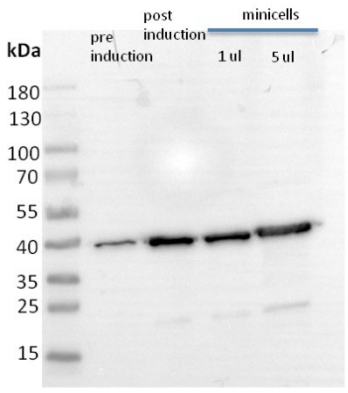

Amount loaded: 0.02 OD units each for whole cell extracts
anti-AcrA (rabbit) 1:50000 overnight, anti-rabbit 1:10000 1h

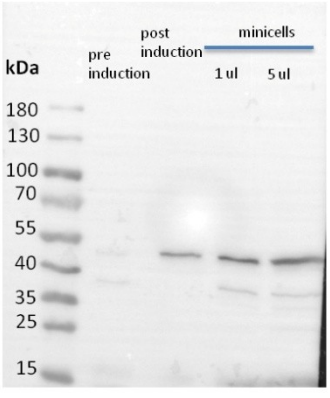

Amount loaded: 0.02 OD units each for whole cell extracts
anti-TolC(rabbit) 1:25000 overnight, anti-rabbit 1:10000 1h

MacAB-TolC prep from triple KO (gradient + SEC)

SB905ΔABΔD ΔEF + pBAD-ramA-MacABoperon

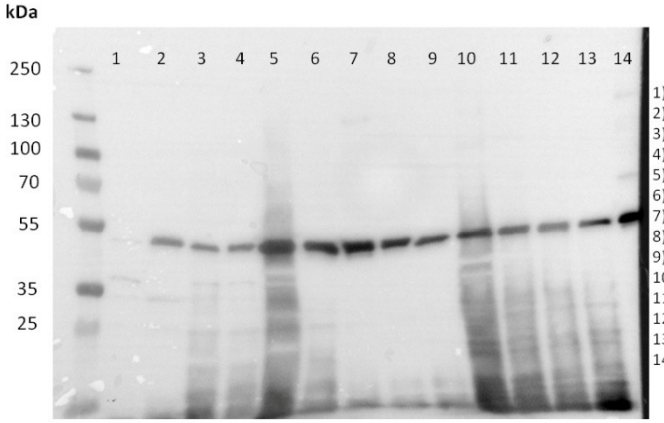

1) pre-induction
2) post-induction
3) before 1st ultra-centrifugation
4) after 1st ultra-centrifugation (supernatant)
5) after 1st ultra-centrifugation (redissolved pellet)
6) final fraction 1
7) final fraction 2
8) final fraction 3
9) final fraction 4
10) supernatant fraction 1
11) supernatant fraction 2
12) supernatant fraction 3
13) supernatant fraction 4
14) pooled fractions 1-4 before SEC

anti-TolC (rabbit) 1:25000, 1h; anti-rabbit 1: 10000, 1h
Amount loaded: 0.02 OD units / 1 ul each

MacAB-TolC prep

SB905ΔABΔDΔEF + pBAD-ramA + pQE70-MacAB (--T5 --CAM)

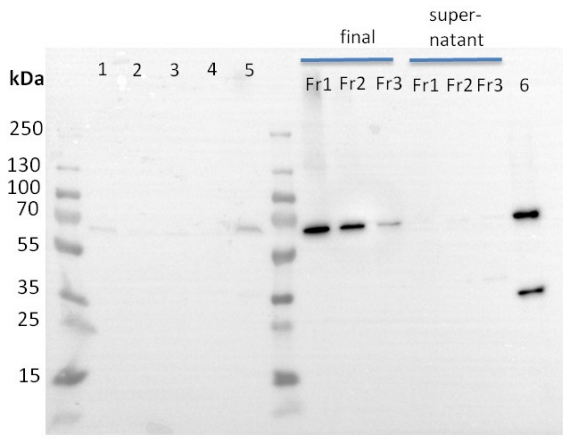

1) pre-induction (21.08.)
2) post-induction (21.08.)
3) before 1st ultra-centrifugation
4) after 1st ultra-centrifugation (supernatant)
5) after 1st ultra-centrifugation (redissolved pellet)
6) pre-SEC (pooled final Fractions 1-3)

anti-His-HRP 1h (1:5000)
amount loaded: 0.02 OD units each

MacAB-TolC prep

SB905ΔABΔDΔEF + pBAD-ramA + pQE70-MacAB (--T5 --CAM)

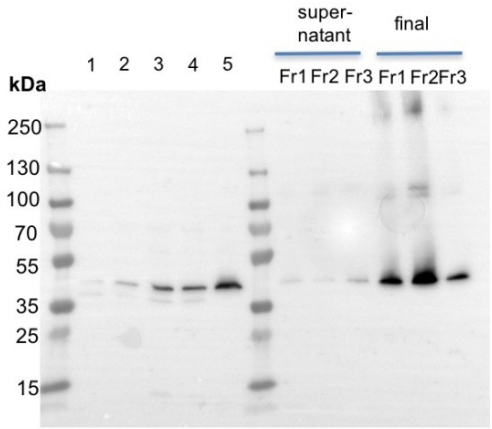

1) pre-induction
2) post-induction
3) before 1st ultra-centrifugation
4) after 1st ultra-centrifugation (supernatant)
5) after 1st ultra-centrifugation (redissolved pellet)

anti-MacA 1h (1:5000), anti-rabbit (HRP-coupled) 1:10000 1h
amount loaded: 0.02 OD units each

8.9 In solution Digestion - Mass Spectrometry: List of hits

The top hits of the mass spectrometry analysis are listed for the final MacAB-TolC sample expressed in SB905ΔAB_ramA_MacAB (see section 4.8), digested in solution. Efflux pump components are marked in grey.

NCBI Accession Number	Description	Area	Coverage [%]	# Peptides
444832925	macrolide transporter subunit MacA	1,70E+10	92,47	134
16421854	ATP-dependent zinc-metallo protease	1,30E+10	76,40	203
444824468	putative lipoprotein	6,30E+09	74,85	35
16767400	elongation factor Tu	4,10E+09	96,19	70
16421742	outer membrane channel	3,20E+09	88,19	130
267996694	FtsH protease regulator HflK	3,20E+09	90,21	125
444835813	FtsH protease regulator HflC	2,50E+09	79,04	74
16766723	30S ribosomal protein S3	2,20E+09	87,12	43
16419422	Fels-1 prophage protease subunits of ATP-dependent proteases	1,80E+09	5,22	3
378452741	DNA gyrase subunit B	1,70E+09	56,97	47
259452591	unnamed protein product	1,50E+09	64,32	103
16421202	phosphatidylserine synthase	1,40E+09	23,50	8
444824536	macrolide transporter ATP-binding /permease protein	1,20E+09	64,97	99
16421972	30S ribosomal subunit protein S4	1,20E+09	70,87	34
444831850	50S ribosomal protein L15	1,20E+09	68,06	19
444837885	glutamate synthase subunit alpha	1,10E+09	4,14	5
444836797	30S ribosomal protein S12	9,40E+08	66,13	16
444823294	phospho-2-dehydro-3-deoxyheptonate aldolase	9,30E+08	41,67	10
16767294	acetyltransferase	9,10E+08	13,98	3

267992111	putative thiol-alkyl hydroperoxide reductase	8,70E+08	85,00	37
267995502	50S ribosomal protein L21	8,00E+08	58,25	12
16421986	50S ribosomal subunit protein L14	7,90E+08	82,11	33
gi|42559186|sp|P60428.1|RL2_SALTY	50S ribosomal protein L2	7,80E+08	67,40	39
444836774	50S ribosomal protein L6	7,30E+08	83,05	29
378449539	putative phospholipase	6,90E+08	9,49	4
444836789	50S ribosomal protein L3	6,80E+08	66,99	26
16422707	50 S ribosomal subunit protein L11	6,80E+08	48,59	14
444835688	glycerol-3-phosphate acyltransferase	6,70E+08	49,88	50
gi|60412676|sp|P0A1X0.1|SLYB_SALTY	Outer membrane lipoprotein SlyB	6,70E+08	38,71	8
267993694	bifunctional acetaldehyde-CoA/alcohol dehydrogenase	6,60E+08	70,52	111
378453052	soluble pyridine nucleotide transhydrogenase	6,30E+08	82,62	60
267991834	pyruvate dehydrogenase subunit E1	6,00E+08	77,79	113
16421996	50S ribosomal subunit protein L4	6,00E+08	68,66	22
444823133	ribonuclease E	5,90E+08	69,45	124
444836851	osmolarity response regulator	5,80E+08	76,57	39
16766706	30S ribosomal protein S11	5,80E+08	84,50	23
444832054	dipeptide transporter ATP-binding subunit	5,70E+08	61,42	17
378452819	transcription termination factor Rho	5,40E+08	72,79	61
378449330	pyruvate formate lyase I	5,10E+08	70,26	82
444836777	50S ribosomal protein L5	5,00E+08	88,83	32

9 LITERATURE

1. Crump, J. A., Sjölund-Karlsson, M., Gordon, M. A. & Parry, C. M. Epidemiology, clinical presentation, laboratory diagnosis, antimicrobial resistance, and antimicrobial management of invasive Salmonella infections. *Clin. Microbiol. Rev.* **28,** 901–937 (2015).
2. Levy, S. B. & Marshall, B. Antibacterial resistance worldwide: causes, challenges and responses. *Nat.Med.* **10,** S122–S129 (2004).
3. Nikaido, H. Multidrug Resistance in Bacteria. *Annu Rev Biochem.* 119–146 (2010). doi:10.1146/annurev.biochem.78.082907.145923.Multidrug
4. Higgins, C. F. Multiple molecular mechanisms for multidrug resistance transporters. *Nature* **446,** 749–57 (2007).
5. Silhavy, T. J., Kahne, D. & Walker, S. The bacterial cell envelope. *Cold Spring Harb. Perspect. Biol.* **2,** 1–16 (2010).
6. Saier, M. H., Tran, C. V & Barabote, R. D. TCDB: the Transporter Classification Database for membrane transport protein analyses and information. *Nucleic Acids Res.* **34,** D181-6 (2006).
7. Li, X., Plésiat, P. & Nikaido, H. The Challenge of Efflux-Mediated Antibiotic Resistance in Gram-Negative Bacteria. *Clininacl Microbiol. Rev.* **28,** 337–418 (2015).
8. Paulsen, I. T. *et al.* The SMR family: A novel family of multidrug efflux proteins involved with the efflux of lipophilic drugs. *Mol. Microbiol.* **19,** 1167–1175 (1996).
9. Kuroda, T. & Tsuchiya, T. Multidrug efflux transporters in the MATE family. *Biochim. Biophys. Acta - Proteins Proteomics* **1794,** 763–768 (2009).
10. Yamaguchi, A., Nakashima, R. & Sakurai, K. Structural basis of RND-type multidrug exporters. *Front. Microbiol.* **6,** 1–19 (2015).
11. Elkins, C. a & Nikaido, H. Substrate Specifcity of the RND-Type Multidrug Efflux Pumps AcrB and AcrD of Escherichia coli Is Determined Predominantely by Two Large Periplasmatic Loops. *Society* **184,** 6490–6498 (2002).
12. Murakami, S., Nakashima, R., Yamashita, E. & Yamaguchi, A. Crystal structure of bacterial multidrug efflux transporter AcrB. *Nature* **419,** 587–593 (2002).
13. Murakami, S., Nakashima, R., Yamashita, E., Matsumoto, T. & Yamaguchi, A. Crystal structures of a multidrug transporter reveal a functionally rotating mechanism. *Nature* **443,** 173–179 (2006).
14. Seeger, M. A. Structural Asymmetry of AcrB Trimer Suggests a Peristaltic Pump Mechanism. *Science (80-.).* **313,** 1295–1298 (2006).
15. Sennhauser, G., Amstutz, P., Briand, C., Storchenegger, O. & Grütter, M. G. Drug export pathway of multidrug exporter AcrB revealed by DARPin inhibitors. *PLoS Biol.* **5,** 0106–0113 (2007).
16. Sjuts, H. *et al.* Molecular basis for inhibition of AcrB multidrug efflux pump by novel and powerful pyranopyridine derivatives. **I,** (2016).
17. Venter, H., Mowla, R., Ohene-Agyei, T. & Ma, S. RND-type drug efflux pumps from Gram-negative bacteria: Molecular mechanism and inhibition. *Front. Microbiol.* **6,** 1–11 (2015).
18. Hinchliffe, P., Symmons, M. F., Hughes, C. & Koronakis, V. Structure and operation of bacterial tripartite pumps. *Annu. Rev. Microbiol.* **67,** 221–42 (2013).
19. Mikolosko, J., Bobyk, K., Zgurskaya, H. I. & Ghosh, P. Conformational flexibility in the

multidrug efflux system protein AcrA. *Structure* **14,** 577–587 (2006).

20. Akama, H. *et al.* Crystal structure of the membrane fusion protein, MexA, of the multidrug transporter in Pseudomonas aeruginosa. *J. Biol. Chem.* **279,** 25939–25942 (2004).

21. Higgins, M. K., Bokma, E., Koronakis, E., Hughes, C. & Koronakis, V. Structure of the periplasmic component of a bacterial drug efflux pump. *Proc. Natl. Acad. Sci. U. S. A.* **101,** 9994–9 (2004).

22. Symmons, M. F., Marshall, R. L. & Bavro, V. N. Architecture and roles of periplasmic adaptor proteins in tripartite efflux assemblies. *Front. Microbiol.* **6,** 1–20 (2015).

23. Fralick, J. A. Evidence that TolC is required for functioning of the Mar/AcrAB efflux pump of Escherichia coli. *J. Bacteriol.* **178,** 5803–5805 (1996).

24. Koronakis, V. TolC - The bacterial exit duct for proteins and drugs. *FEBS Lett.* **555,** 66–71 (2003).

25. Horiyama, T., Yamaguchi, A. & Nishino, K. TolC dependency of multidrug efflux systems in Salmonella enterica serovar Typhimurium. *J. Antimicrob. Chemother.* **65,** 1372–1376 (2010).

26. Hancock, R. E. W. & Brinkman, F. S. L. Function of pseudomonas porins in uptake and efflux. *Annu. Rev. Microbiol.* **56,** 17–38 (2002).

27. Bunikis, I. *et al.* An RND-type efflux system in Borrelia burgdorferi is involved in virulence and resistance to antimicrobial compounds. *PLoS Pathog.* **4,** (2008).

28. Bina, J. E. & Mekalanos, J. J. Vibrio cholerae tolC is required for bile resistance and colonization. *Infect. Immun.* **69,** 4681–4685 (2001).

29. Giraud, E., Cloeckaert, a, Kerboeuf, D. & Chaslus-Dancla, E. Evidence for active efflux as the primary mechanism of resistance to ciprofloxacin in Salmonella enterica serovar typhimurium. *Antimicrob. Agents Chemother.* **44,** 1223–1228 (2000).

30. Blair, J. M. & Piddock, L. J. Structure, function and inhibition of RND efflux pumps in Gram-negative bacteria: an update. *Curr. Opin. Microbiol.* **12,** 512–519 (2009).

31. Piddock, L. J., White, D. G., Gensberg, K., Pumbwe, L. & Griggs, D. J. Evidence for an efflux pump mediating multiple antibiotic resistance in Salmonella enterica serovar Typhimurium. *Antimicrob. Agents Chemother.* **44,** 3118–21 (2000).

32. Masi, M., Duret, G., Delcour, A. H. & Misra, R. Folding and trimerization of signal sequence-less mature TolC in the cytoplasm of Escherichia coli. *Microbiology* **155,** 1847–1857 (2009).

33. Koronakis, V., Sharff, A., Koronakis, E., Luisi, B. & Hughes, C. Crystal structure of the bacterial membrane protein TolC central to multidrug efflux and protein export. *Nature* **405,** 914–9 (2000).

34. Andersen, C., Koronakis, E., Hughes, C. & Koronakis, V. An aspartate ring at the TolC tunnel entrance determines ion selectivity and presents a target for blocking by large cations. *Mol. Microbiol.* **44,** 1131–1139 (2002).

35. Pei, X.-Y. *et al.* Structures of sequential open states in a symmetrical opening transition of the TolC exit duct. *Proc. Natl. Acad. Sci. U. S. A.* **108,** 2112–2117 (2011).

36. Bavro, V. N. *et al.* Assembly and Channel Opening in a Bacterial Drug Efflux Machine. *Mol. Cell* **30,** 114–121 (2008).

37. Song, S., Kim, J. S., Lee, K. & Ha, N. C. Molecular architecture of the bacterial tripartite multidrug efflux pump focusing on the adaptor bridging model. *J Microbiol* **53,** 355–364 (2015).

38. Anes, J., McCusker, M. P., Fanning, S. & Martins, M. The ins and outs of RND efflux pumps in

Escherichia coli. *Front. Microbiol.* **6,** 1–14 (2015).

39. Lobedanz, S. *et al.* A periplasmic coiled-coil interface underlying TolC recruitment and the assembly of bacterial drug efflux pumps. *Proc Natl Acad Sci U S A* **104,** 4612–4617 (2007).

40. Symmons, M. F., Bokma, E., Koronakis, E., Hughes, C. & Koronakis, V. The assembled structure of a complete tripartite bacterial multidrug efflux pump. *Proc Natl Acad Sci U S A* **106,** 7173–7178 (2009).

41. Tamura, N., Murakami, S., Oyama, Y., Ishiguro, M. & Yamaguchi, A. Direct interaction of multidrug efflux transporter AcrB and outer membrane channel TolC detected via site-directed disulfide cross-linking. *Biochemistry* **44,** 11115–11121 (2005).

42. Xu, Y. *et al.* Funnel-like hexameric assembly of the periplasmic adapter protein in the tripartite multidrug efflux pump in gram-negative bacteria. *J. Biol. Chem.* **286,** 17910–17920 (2011).

43. Kim, H. M. *et al.* Functional relationships between the AcrA hairpin tip region and the TolC aperture tip region for the formation of the bacterial tripartite efflux pump AcrAB-TolC. *J. Bacteriol.* **192,** 4498–4503 (2010).

44. Kim, J.-S. *et al.* Structure of the Tripartite Multidrug Efflux Pump AcrAB-TolC Suggests an Alternative Assembly Mode. *Mol. Cells* **38,** 180–6 (2015).

45. Du, D. *et al.* Structure of the AcrAB-TolC multidrug efflux pump. *Nature* **509,** 512–515 (2014).

46. Touzé, T. *et al.* Interactions underlying assembly of the Escherichia coli AcrAB-TolC multidrug efflux system. *Mol. Microbiol.* **53,** 697–706 (2004).

47. Xu, Y. *et al.* Assembly and channel opening of outer membrane protein in tripartite drug efflux pumps of gram-negative bacteria. *J. Biol. Chem.* **287,** 11740–11750 (2012).

48. Janganan, T. K. *et al.* Evidence for the assembly of a bacterial tripartite multidrug pump with a stoichiometry of 3:6:3. *J. Biol. Chem.* **286,** 26900–26912 (2011).

49. Su, C. *et al.* Crystal structure of the CusBA-heavy metal efflux complex of Escherichia coli. *Nature* **470,** 558–562 (2011).

50. Jeong, H. *et al.* Pseudoatomic Structure of the Tripartite Multidrug Efflux Pump AcrAB-TolC Reveals the Intermeshing Cogwheel-like Interaction between AcrA and TolC. *Structure* **24,** 1–5 (2016).

51. Daury, L., Orange, F., Taveau, J. & Verchère, A. Tripartite assembly of RND multidrug efflux pumps. *Nat. Commun.* 1–30 (2016). doi:10.1038/ncomms10731

52. Yamasaki, S., Nagasawa, S., Hayashi-Nishino, M., Yamaguchi, A. & Nishino, K. AcrA dependency of the AcrD efflux pump in Salmonella enterica serovar Typhimurium. *J. Antibiot. (Tokyo).* **64,** 433–7 (2011).

53. Rensch, U., Nishino, K., Klein, G. & Kehrenberg, C. Salmonella enterica serovar Typhimurium multidrug efflux pumps EmrAB and AcrEF support the major efflux system AcrAB in decreased susceptibility to triclosan. *Int. J. Antimicrob. Agents* **44,** 179–180 (2014).

54. Olliver, A., Vallé, M., Chaslus-Dancla, E. & Cloeckaert, A. Overexpression of the multidrug efflux operon acrEF by insertional activation with IS1 or IS10 elements in Salmonella enterica serovar typhimurium DT204 acrB mutants selected with fluoroquinolones. *Antimicrob. Agents Chemother.* **49,** 289–301 (2005).

55. Kobayashi, N., Nishino, K. & Yamaguchi, A. Novel Macrolide-Specific ABC-Type Efflux Transporter in Escherichia coli. *J. Bacteriol.* **183,** 5639–5644 (2001).

56. Turlin, E. *et al.* Protoporphyrin (PPIX) efflux by the MacAB-TolC pump in Escherichia coli. *Microbiologyopen* **3,** 849–859 (2014).

57. Bogomolnaya, L. M. *et al.* The ABC-type efflux pump MacAB protects Salmonella enterica serovar typhimurium from oxidative stress. *MBio* **4,** 1–11 (2013).

58. Yamanaka, H., Kobayashi, H., Takahashi, E. & Okamoto, K. MacAB is involved in the secretion of Escherichia coli heat-stable enterotoxin II. *J. Bacteriol.* **190,** 7693–7698 (2008).

59. Lu, S. & Zgurskaya, H. I. MacA, a periplasmic membrane fusion protein of the macrolide transporter MacAB-TolC, binds lipopolysaccharide core specifically and with high affinity. *J. Bacteriol.* **195,** 4865–4872 (2013).

60. Zhang, C., Chen, X., Stephanopoulos, G. & Too, H.-P. Efflux transporter engineering markedly improves amorphadiene production in Escherichia coli. *Biotechnol. Bioeng.* **9999,** n/a-n/a (2016).

61. Kobayashi, N., Nishino, K., Hirata, T. & Yamaguchi, A. Membrane topology of ABC-type macrolide antibiotic exporter MacB in Escherichia coli. *FEBS Lett.* **546,** 241–246 (2003).

62. Lin, H. T. *et al.* MacB ABC transporter is a dimer whose ATPase activity and macrolide-binding capacity are regulated by the membrane fusion protein MacA. *J. Biol. Chem.* **284,** 1145–1154 (2009).

63. Xu, Y. *et al.* Crystal structure of the periplasmic region of MacB, a noncanonic ABC transporter. *Biochemistry* **48,** 5218–5225 (2009).

64. Oldham, M. L., Davidson, A. L. & Chen, J. Structural insights into ABC transporter mechanism. *Curr. Opin. Struct. Biol.* **18,** 726–733 (2008).

65. Higgins, C. F. & Linton, K. J. The ATP switch model for ABC transporters. *Nat. Struct. Mol. Biol.* **11,** 918–926 (2004).

66. Modali, S. D. & Zgurskaya, H. I. The periplasmic membrane proximal domain of MacA acts as a switch in stimulation of ATP hydrolysis by MacB transporter. *Mol. Microbiol.* **81,** 937–951 (2011).

67. Tikhonova, E. B., Devroy, V. K., Lau, S. Y. & Zgurskaya, H. I. Reconstitution of the Escherichia coli macrolide transporter: The periplasmic membrane fusion protein MacA stimulates the ATPase activity of MacB. *Mol. Microbiol.* **63,** 895–910 (2007).

68. Zgurskaya, H. I., Yamada, Y., Tikhonova, E. B., Ge, Q. & Krishnamoorthy, G. Structural and functional diversity of bacterial membrane fusion proteins. *Biochim. Biophys. Acta - Proteins Proteomics* **1794,** 794–807 (2009).

69. Yum, S. *et al.* Crystal Structure of the Periplasmic Component of a Tripartite Macrolide-Specific Efflux Pump. *J. Mol. Biol.* **387,** 1286–1297 (2009).

70. Piao, S., Xu, Y. & Ha, N. C. Crystallization and preliminary X-ray crystallographic analysis of MacA from Actinobacillus actinomycetemcomitans. *Acta Crystallogr. Sect. F Struct. Biol. Cryst. Commun.* **64,** 391–393 (2008).

71. Angelis, F. De, Lee, J. K., Connell, J. D. O., Miercke, L. J. W. & Verschueren, K. H. Metal-induced conformational changes in ZneB suggest an active role of membrane fusion proteins in ef fl ux resistance systems. *PNAS* **107,** 11038–11043 (2010).

72. Du, D., van Veen, H. W. & Luisi, B. F. Assembly and operation of bacterial tripartite multidrug efflux pumps. *Trends Microbiol.* **23,** 311–319 (2015).

73. Xu, Y. *et al.* The tip region of the MacA α-hairpin is important for the binding to TolC to the Escherichia coli MacAB-TolC pump. *Biochem. Biophys. Res. Commun.* **394,** 962–965 (2010).

74. Xu, Y. *et al.* Functional implications of an intermeshing cogwheel-like interaction between TolC and MacA in the action of macrolide-specific efflux pump MacAB-TolC. *J. Biol. Chem.* **286,** 13541–13549 (2011).

75. Mcmurry, L. M., Oethinger ', M. & Levy, S. B. Overexpression of marA, soxS, or acrAB produces resistance to triclosan in laboratory and clinical strains of Escherichia coli. *Microbiol. Lett. FEMS Microbiol. Lett.* **166,** 305–309 (1998).

76. Gu, M. & Imlay, J. A. The SoxRS response of Escherichia coli is directly activated by redox-cycling drugs rather than by superoxide. *Mol. Microbiol.* **79,** 1136–1150 (2011).

77. Ricci, V., Busby, S. J. W. & Piddock, L. J. V. Regulation of RamA by RamR in Salmonella enterica serovar Typhimurium: Isolation of a RamR superrepressor. *Antimicrob. Agents Chemother.* **56,** 6037–6040 (2012).

78. Chollet, R., Chevalier, J., Bollet, C., Pages, J. & Davin-regli, A. RamA Is an Alternate Activator of the Multidrug Resistance Cascade in Enterobacter aerogenes RamA Is an Alternate Activator of the Multidrug Resistance Cascade in Enterobacter aerogenes. *Antimicrob. Agents Chemother.* **48,** 2518–2523 (2004).

79. Baucheron, S. *et al.* Binding of the RamR repressor to wild-type and mutated promoters of the ramA gene involved in efflux-mediated multidrug resistance in Salmonella enterica serovar typhimurium. *Antimicrob. Agents Chemother.* **56,** 942–948 (2012).

80. Abouzeed, Y. M., Baucheron, S. & Cloeckaert, A. ramR mutations involved in efflux-mediated multidrug resistance in Salmonella enterica serovar Typhimurium. *Antimicrob. Agents Chemother.* **52,** 2428–2434 (2008).

81. Yamasaki, S. *et al.* The crystal structure of multidrug-resistance regulator RamR with multiple drugs. *Nat. Commun.* **4,** 2078 (2013).

82. Ricci, V., Blair, J. M. A. & Piddock, L. J. V. RamA, which controls expression of the MDR efflux pump AcrAB-Tolc, is regulated by the lon protease. *J. Antimicrob. Chemother.* **69,** 643–650 (2014).

83. Nikaido, E., Yamaguchi, A. & Nishino, K. AcrAB multidrug efflux pump regulation in Salmonella enterica serovar Typhimurium by RamA in response to environmental signals. *J. Biol. Chem.* **283,** 24245–53 (2008).

84. Groisman, E. A. The Pleiotropic Two-Component Regulatory System PhoP-PhoQ. *J. Bacteriol.* **183,** 1835–1842 (2001).

85. Nishino, K., Latifi, T. & Groisman, E. A. Virulence and drug resistance roles of multidrug efflux systems of Salmonella enterica serovar Typhimurium. *Mol. Microbiol.* **59,** 126–141 (2006).

86. Nishino, K., Nikaido, E. & Yamaguchi, A. Regulation and physiological function of multidrug efflux pumps in Escherichia coli and Salmonella. *Biochim. Biophys. Acta* **1794,** 834–43 (2009).

87. Kunkel, T. a. Rapid and efficient site-specific mutagenesis without phenotypic selection. *Proc. Natl. Acad. Sci. U. S. A.* **82,** 488–492 (1985).

88. Datsenko, K. A. & Wanner, B. L. One-step inactivation of chromosomal genes in Escherichia coli K-12 using PCR products. *Proc. Natl. Acad. Sci. U. S. A.* **97,** 6640–5 (2000).

89. Khlebnikov, A., Skaug, T. & Keasling, J. D. Modulation of gene expression from the arabinose-inducible araBAD promoter. *J. Ind. Microbiol. Biotechnol.* **29,** 34–37 (2002).

90. Wiegand, I., Hilpert, K. & Hancock, R. E. W. Agar and broth dilution methods to determine the minimal inhibitory concentration (MIC) of antimicrobial substances. *Nat. Protoc.* **3,** 163–75 (2008).

91. Marlovits, T. C. *et al.* Structural Insights into the Assembly of the Type III Secretion Needle Complex. *Science (80-.).* **306,** 1040–1042 (2004).

92. Alonso, H. & Roujeinikova, A. Characterization and two-dimensional crystallization of membrane component AlkB of the medium-chain alkane hydroxylase system from

Pseudomonas putida GPo1. *Appl. Environ. Microbiol.* **78,** 7946–7953 (2012).

93. Liu, J., Chen, C. Y., Shiomi, D., Niki, H. & Margolin, W. Visualization of bacteriophage P1 infection by cryo-electron tomography of tiny Escherichia coli. *Virology* **417,** 304–311 (2011).

94. Kawamoto, A. *et al.* Common and distinct structural features of *Salmonella* injectisome and flagellar basal body. *Sci. Rep.* **3,** 3369 (2013).

95. Nans, A., Kudryashev, M., Saibil, H. R. & Hayward, R. D. Structure of a bacterial type III secretion system in contact with a host membrane in situ. *Nat. Commun.* **6,** 10114 (2015).

96. Sukhan, A., Kubori, T., Wilson, J. & Galan, J. E. Genetic Analysis of Assembly of the Salmonella enterica Serovar Typhimurium Type III Secretion-Associated Needle Complex. *J. Bacteriol.* **183,** 1159–1167 (2001).

97. Guzman, L. M., Belin, D., Carson, M. J. & Beckwith, J. Tight regulation , modulation , and high-level expression by vectors containing the arabinose These include : Tight Regulation , Modulation , and High-Level Expression by Vectors Containing the Arabinose P BAD Promoter. *J. Bacteriol.* **177,** 4121–4130 (1995).

98. Cherepanov, P. P. & Wackernagel, W. Gene disruption in Escherichia coli: TcR and KmR cassettes with the option of Flp-catalyzed excision of the antibiotic-resistance determinant. *Gene* **158,** 9–14 (1995).

99. Zhang, Y. I-TASSER server for protein 3D structure prediction. *BMC Bioinformatics* **9,** 40 (2008).

100. Yang, J. *et al.* The I-TASSER Suite: Protein structure and function prediction. *Nat. Methods* **12,** 7–8 (2015).

101. Yamasaki, S. *et al.* Phenotype microarray analysis of the drug efflux systems in Salmonella enterica serovar Typhimurium. *J. Infect. Chemother.* 1–5 (2016). doi:10.1016/j.jiac.2016.03.015

102. Yachdav, G. *et al.* PredictProtein - An open resource for online prediction of protein structural and functional features. *Nucleic Acids Res.* **42,** 337–343 (2014).

103. Kim, J. S. *et al.* Crystal Structure of a Soluble Fragment of the Membrane Fusion Protein HlyD in a Type i Secretion System of Gram-Negative Bacteria. *Structure* **24,** 477–485 (2016).

104. Rowlett, V. W. & Margolin, W. The Min system and other nucleoid-independent regulators of Z ring positioning. *Front. Microbiol.* **6,** 1–10 (2015).

105. Farley, M. M., Hu, B. & Margolin, W. Minicells , Back in Fashion. **198,** 1186–1195 (2016).

106. Hu, B. *et al.* Visualization of the type III secretion sorting platform of Shigella flexneri. *Proc. Natl. Acad. Sci. U. S. A.* **112,** 1047–52 (2015).

107. Ohi, M., Li, Y., Cheng, Y. & Walz, T. Negative Staining and Image Classification - Powerful Tools in Modern Electron Microscopy. *Biol. Proced. Online* **6,** 23–34 (2004).

108. Monsieurs, P. *et al.* Comparison of the PhoPQ regulon in Escherichia coli and Salmonella typhimurium. *J. Mol. Evol.* **60,** 462–474 (2005).

109. Lavigne, J.-P. & Blanc-Potard, A.-B. Molecular evolution of Salmonella enterica serovar Typhimurium and pathogenic Escherichia coli: from pathogenesis to therapeutics. *Infect. Genet. Evol.* **8,** 217–26 (2008).

110. Madigan, M., Martinko, J., Stahl, D. & Clark, D. *Brock – Biology of Microorganisms.* (Pearson Education Inc., 2012).

111. Schuster, S., Vavra, M. & Kern, W. V. Evidence of a substrate discriminating entrance channel in the lower porter domain of the multidrug resistance efflux pump AcrB. *Antimicrob. Agents*

Chemother. **60,** AAC.00314-16- (2016).

112. Briegel, a. *et al.* Bacterial chemoreceptor arrays are hexagonally packed trimers of receptor dimers networked by rings of kinase and coupling proteins. *Proc. Natl. Acad. Sci.* **109,** 3766–3771 (2012).